

$J/\psi$  as a function of  $p_T$ ,  $y$  and centrality  
in small systems with  
Yue Hang Leung's Correlated Background:  
Run15pp and  
Run15pAu, Run15pAl, Run14<sup>3</sup>HeAu Centrality

[AN 1354](#) and [AN 1391](#) precede this analysis note

Matt Durham<sup>1</sup>, Anthony Frawley<sup>2</sup>, Sanghoon Lim<sup>3</sup> and Krista Smith<sup>2</sup>

<sup>1</sup>Los Alamos National Lab

<sup>2</sup>Florida State University

<sup>3</sup>University of Colorado Boulder

August 15, 2019

# Contents

<b>Correction to Preliminary Plots</b>	<b>5</b>
<b>1 Introduction</b>	<b>6</b>
<b>2 Yue Hang Leung's Correlated Background</b>	<b>6</b>
2.1 Motivation . . . . .	6
2.2 Unlike-sign Background Estimation . . . . .	6
2.3 Fit Function . . . . .	7
<b>3 Run15pp Correlated Background</b>	<b>8</b>
3.1 Initial Fits . . . . .	8
3.2 Parameters as a function of $p_T$ . . . . .	8
3.3 Checks on Run15pp Correlated Background . . . . .	10
3.3.1 Rescaled Fits . . . . .	10
3.3.2 Parameter Ratio plots . . . . .	11
3.3.3 Ratio of Rescaled Fit/Initial Fit . . . . .	12
3.4 Final $p_T$ binning . . . . .	14
<b>4 Run15pAu Correlated Background</b>	<b>14</b>
4.1 Initial Fits . . . . .	14
4.2 Parameters as a function of $p_T$ . . . . .	15
4.3 Checks on Run15pAu Correlated Background . . . . .	17
4.3.1 Rescaled Fits . . . . .	17
4.3.2 Parameter Ratio plots . . . . .	17
4.3.3 Ratio of Rescaled Fit/Initial Fit . . . . .	18
4.4 Final $p_T$ binning . . . . .	18
<b>5 Run15pAl and Run14HeAu Correlated Backgrounds</b>	<b>19</b>
5.1 Final $p_T$ binning, Run15pAl . . . . .	19
5.2 Final $p_T$ binning, Run14HeAu . . . . .	20
<b>6 Correlated Background Systematic Uncertainty</b>	<b>20</b>
6.1 Sanghoon's Method . . . . .	20
6.2 Combinatorial Background Contribution . . . . .	21
6.3 Systematic Study Conclusion . . . . .	24
6.4 Check on CaseFGH . . . . .	24
6.5 Systematic Study Results . . . . .	25
6.5.1 Run14HeAu Systematic Uncertainty . . . . .	30
<b>7 Run15pp Checks on <math>J/\psi</math> Counts</b>	<b>33</b>
7.1 Sum Over $p_T$ . . . . .	33
7.2 Sum Over Rapidity . . . . .	34

<b>8</b>	<b>Run15pAu Checks on <math>J/\psi</math> Counts</b>	<b>35</b>
8.1	Sum Over $p_T$	35
8.2	Sum Over Rapidity	35
8.3	Sum Over Centrality	35
8.4	$\sigma$ vs $p_T$	38
<b>9</b>	<b>Run15pAl Checks on <math>J/\psi</math> Counts</b>	<b>39</b>
9.1	Sum over $p_T$	39
9.2	Sum over Rapidity	39
9.3	Sum over Centrality	39
9.4	$\sigma$ vs. $p_T$	39
<b>10</b>	<b>Run14HeAu Checks on <math>J/\psi</math> Counts</b>	<b>41</b>
10.1	Sum over $p_T$	41
10.2	Sum over Rapidity	41
10.3	Sum over Centrality	41
10.4	$\sigma$ vs. $p_T$	41
	10.4.1 Fixing the $J/\psi$ Width	44
	10.4.2 Fixing the Center of the $J/\psi$ Peak	44
<b>11</b>	<b>Bias Correction Factor</b>	<b>44</b>
<b>12</b>	<b>Centralities</b>	<b>45</b>
<b>13</b>	<b>NEW: 0-5-10-20% pAu Analysis</b>	<b>46</b>
13.1	Checks	46
13.2	Summary of Analysis Method	46
<b>14</b>	<b>Binshift Corrections</b>	<b>47</b>
<b>15</b>	<b>Uncertainties: Type A, B and C</b>	<b>56</b>
15.1	Type A: Statistical Uncertainty	56
15.2	Type B: Systematic Uncertainty	56
	15.2.1 Run14HeAu: Fixing the $J/\psi$ Width and Center of the Peak	56
15.3	Type C: Global Uncertainty	56
<b>16</b>	<b>Trigger and Acceptance Reconstruction Efficiencies</b>	<b>59</b>
<b>17</b>	<b>Run15pp Results</b>	<b>60</b>
17.1	GEANT3/GEANT4 Discrepancy	60
	17.1.1 Sanghoon's HI PWG Presentation	60
<b>18</b>	<b>Run15pAu Results</b>	<b>62</b>
18.1	Fraction of Events per Centrality Range	62

<b>19 Run15pAl Results</b>	<b>68</b>
19.1 Fraction of Events per Centrality Range	68
19.1.1 Sanghoon's High Luminosity Study of Run15pAl	68
19.2 Rebinning Centralities	68
<b>20 Run14HeAu Results</b>	<b>70</b>
20.1 Fraction of Events per Centrality Range	70
20.2 Rebinning Centralities	70
20.2.1 Combining TH2D Histograms	71
20.3 $p_T$ Integrated $N_{coll}$	72
<b>21 <math>\langle p_T^2 \rangle</math> vs. <math>N_{coll}</math></b>	<b>72</b>
<b>22 Sum Over Centrality vs. Centrality Integrated</b>	<b>72</b>
<b>23 <math>R_{AB}</math> vs. <math>y</math></b>	<b>77</b>
<b>24 Rapidity with Centrality Dependence</b>	<b>78</b>
24.1 Checks	78
24.2 Corrbg Systematic Uncertainty	84
24.3 Example Fits	85
24.4 Results	86
<b>A Raw J/<math>\psi</math> Counts:</b>	
$p_T$ /Rapidity/Centrality Integrated	<b>87</b>
<b>B Raw J/<math>\psi</math> Counts:</b>	
$p_T$ Dependent (Rapidity/Centrality Integrated)	<b>88</b>
<b>C Raw J/<math>\psi</math> Counts:</b>	
$p_T$ /Centrality Dependent (Rapidity Integrated)	<b>90</b>
<b>D Preliminary Plot Data Arrays</b>	<b>92</b>
<b>Corrected Preliminary Plot Data Arrays</b>	<b>92</b>



## Correction to Preliminary Plots

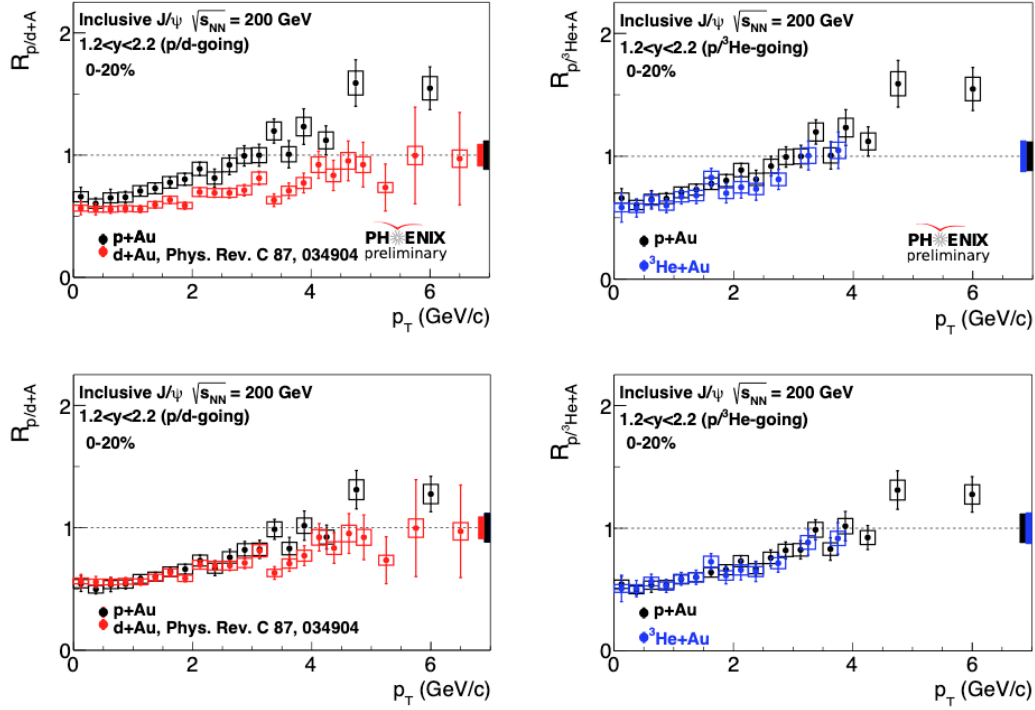


Figure 1: Top: Preliminary Plots. Bottom: Corrected Preliminary Plots. Left: Run15  $R_{pAu}$  vs. Run08  $R_{dAu}$  in the North arm for 0-20% Centrality. Right: Run15  $R_{pAu}$  vs. Run14  $R_{HeAu}$  in the North arm for the same centrality.

Preliminary was granted for  $R_{pAu}$  and  $R_{HeAu}$  on May 10, 2019. At this time, pAu and HeAu North 0-20% centrality agreed with each other, but pAu and dAu North 0-20% did not. These results were surprising to the analyzers, but many cross checks were performed and it was not apparent a mistake had been made during the analysis process.

Preliminary was requested for Tony Frawley to present at the 13th International Heavy Quarkonium Workshop on May 14, 2019. But Tony had doubts the North arm results were correct, and a bug in the nuclear modification calculation code was suspected. This code was then rewritten, although the same results were observed.

**Sanghoon Lim then offered to look at the rewritten nuclear modification code. He found that the fraction of events per centrality range used in the denominator of the invariant yield calculations were incorrect for both systems (pAu and HeAu). This mistake was a conceptual error in the way the events in each centrality bin were counted.**

Sanghoon then determined the correct fraction of events per centrality, the plots were updated, and the HI PWG was notified. Please see sections 15.1 and 17.1 for more details on how Sanghoon determined the correct fraction of events per centrality.

# 1 Introduction

This analysis note is an extension of AN 1391. The topic of both this analysis note and AN 1391 is  $J/\psi$  as a function of  $p_T$  and centrality in small systems. But the important distinction between the two is that the analysis presented in this note has used Yue Hang Leung's correlated background results from [AN 1306](#) (Run15pp) and [AN 1369](#) (Run15pAu).

Another important distinction is that the method for determining the systematic uncertainty due to the correlated background shape has been revised. Lastly, this current analysis note presents centrality results for pAu, pAl and  $^3\text{HeAu}$ , where AN 1391 presents centrality for only one system: pAu. Otherwise, the current analysis has continued as outlined in AN 1391.

**UPDATE:** Sanghoon Lim requested additional measurements for this analysis note that were not included in AN 1354. The measurements he requested are  $J/\psi$  as a function of  $y$  with centrality dependence. Please see section 22 for details.

## 2 Yue Hang Leung's Correlated Background

### 2.1 Motivation

In AN 1391 we describe the difference in  $J/\psi$  counts that was observed when the shape of the correlated background changed. The actual shape of the correlated background is not fully known. Due to this uncertainty, it was suggested by **Xioachun He** during an FVTX meeting that we use Yue Hang Leung's results from his analysis of the correlated background in Run15pp (AN 1306) and Run15pAu (AN 1369).

### 2.2 Unlike-sign Background Estimation

The total background is the sum of the combinatorial and correlated backgrounds. The background is composed of unlike-sign muon pairs, such that

$$BG(UL) = c\bar{c}(UL) + b\bar{b}(UL) + corr\_had(UL) + dy(UL) + comb(UL). \quad (1)$$

AN 1306 showed the following:

$$\begin{aligned} b\bar{b}(UL) &\approx b\bar{b}(LS) \\ corr\_had(UL) &\approx corr\_had(LS) \\ comb(UL) &\approx comb(LS). \end{aligned}$$

In this analysis, we have estimated the unlike-sign background using like-sign pairs:

$$BG(UL) = LS\_pairs + c\bar{c}(UL) + dy(UL), \quad (2)$$

where LS pairs include  $b\bar{b}$  and correlated hadron pairs in addition to combinatorial pairs:

$$LS\_pairs = b\bar{b}(LS) + corr\_had(LS) + comb(LS). \quad (3)$$

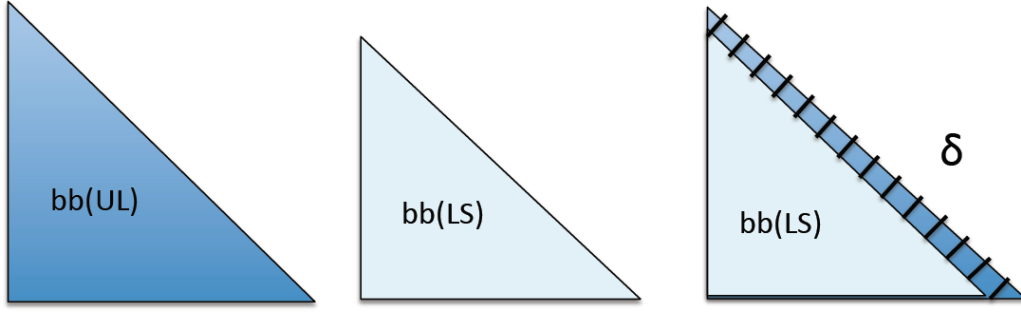


Figure 2: Schematic of the  $\delta_{b\bar{b}}$  contribution for estimating the unlike-sign background using like-sign pairs.

But for the most precise results, we have used

$$BG(UL) = LS\_pairs + c\bar{c}(UL) + dy(UL) + \delta_{b\bar{b}}(UL) + \delta_{corr\_had}(UL), \quad (4)$$

where

$$\delta_{b\bar{b}}(UL) = b\bar{b}(UL) - b\bar{b}(LS) \quad (5)$$

$$\delta_{corr\_had}(UL) = corr\_had(UL) - corr\_had(LS). \quad (6)$$

A schematic of  $\delta$  is included in Figure 1. Therefore, in our reconstruction of Yue Hang's correlated background, we have used all of the following components directly from his studies except for the comb(LS):

$$BG(UL) = c\bar{c}(UL) + b\bar{b}(UL) + corr\_had(UL) + dy(UL) + comb(LS) - b\bar{b}(LS) - corr\_had(LS). \quad (7)$$

## 2.3 Fit Function

The function used to fit Yue Hang's correlated background is the same function used in AN 1391 and AN 1354. It contains five parameters, with 'c' being the normalization. It will be used in various ways throughout the analysis, with some parameters fixed and others free, depending on the purpose of the fit.

$$y = \frac{c}{(e^{-ax-bx^2} + x/d)^e}$$

Figure 3: The correlated background fit function (AN 1354 Eq. 2, AN 1391 Section 1).

### 3 Run15pp Correlated Background

#### 3.1 Initial Fits

We began with reconstructing the correlated background for Run15pp. Figure 3 shows the mass distribution for 500 MeV/c  $p_T$  slices over the range 0 – 7 GeV/c, where we have fit the background using the function described above. For the initial fits, all parameters are free. We also fit well beyond the lower mass limit of 2.0 GeV/c<sup>2</sup>.

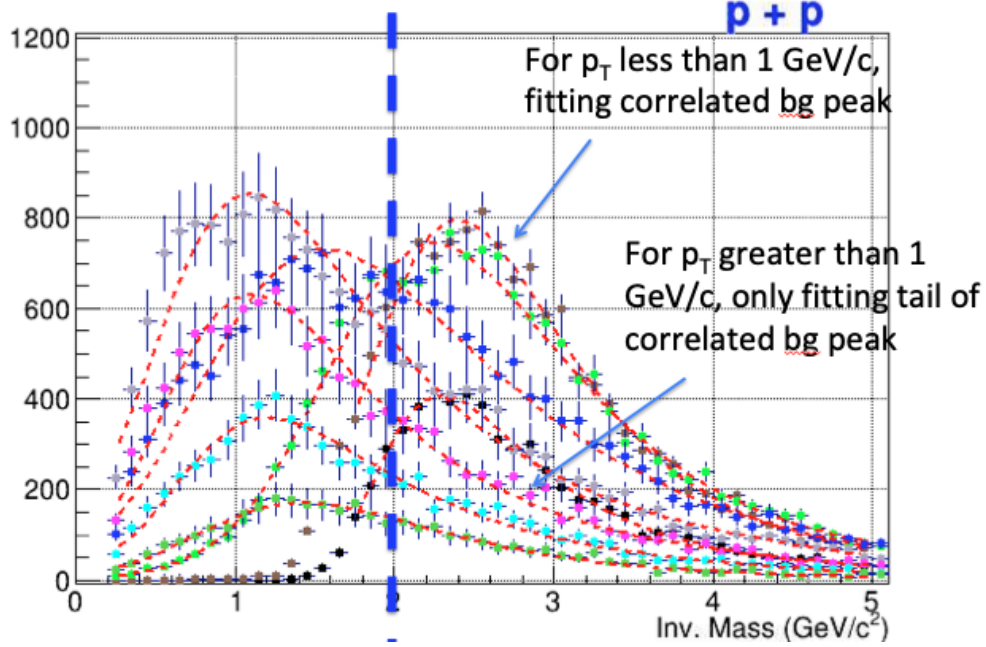


Figure 4: Yue Hang's Run15pp correlated background in 500 MeV/c binwidths in the North Arm. All parameters are free.

Immediately we can see that the distribution is divided around 2 GeV/c<sup>2</sup>. At low  $p_T$ , which is approximately 0-1 GeV/c, the correlated background peaks to the right of 2 GeV/c<sup>2</sup>. But for  $p_T$  greater than 1 GeV/c, the peak begins shifting to the left of 2 GeV/c<sup>2</sup>. For this analysis, we are fitting the data in the window 2-5 GeV/c<sup>2</sup>. These results suggest the correlated background could be  $p_T$  dependent. We therefore took the resulting bestfit parameters for a, b, d, e and plotted them as a function of  $p_T$ .

#### 3.2 Parameters as a function of $p_T$

The parameters over the range 1-7 GeV/c were similar enough to fit with polynomial functions. The results are shown in Figure 4. These polynomial functions were then input into the Crystal Ball fitter, and the initial parameter values individually calculated for each  $p_T$  value.

However, the parameters over the range 0-1 GeV/c changed too rapidly to find functions that could accurately describe their behavior. In particular, the parameter 'd' had the most rapid change,

as shown in Figure 5. Instead, the bestfit results for parameters a, b, d, e were directly used as the initial parameters in the Crystal Ball fitter.

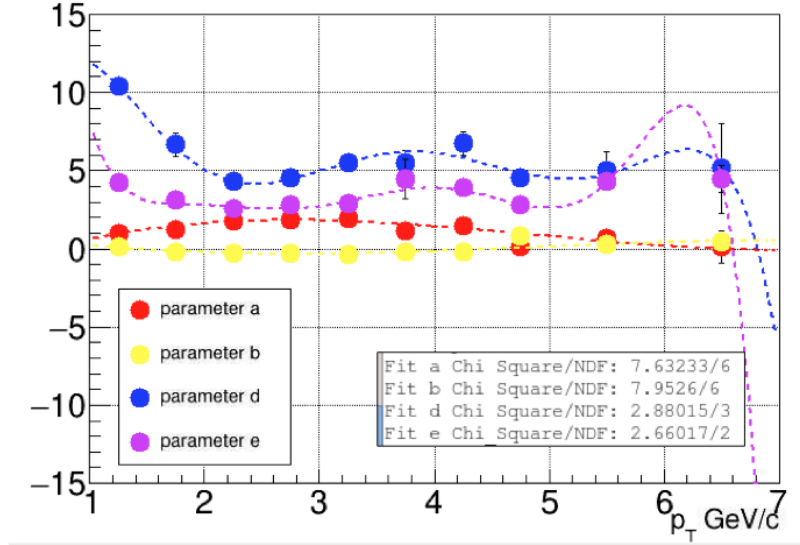
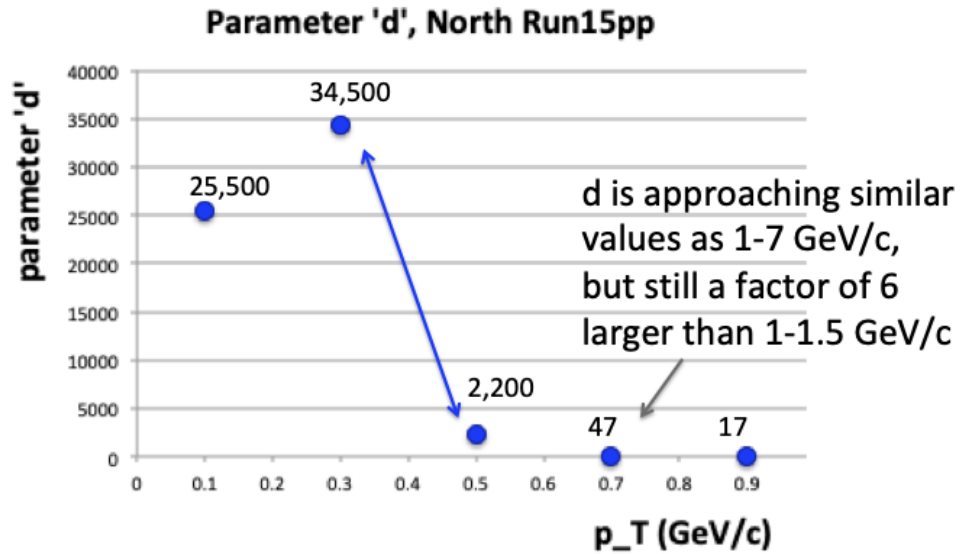


Figure 5: 1-7 GeV/c: Bestfit parameters of the correlated background fit function plotted vs.  $p_T$  for Run15pp North arm. The parameters are fit with polynomials of varying degrees.



Changes very rapidly between 300 MeV/c and 500 MeV/c

Figure 6: 0-1 GeV/c: Bestfit parameter 'd' of the correlated background fit function plotted vs.  $p_T$  for Run15pp North arm. We could not find functions that accurately describe the parameters over this range.

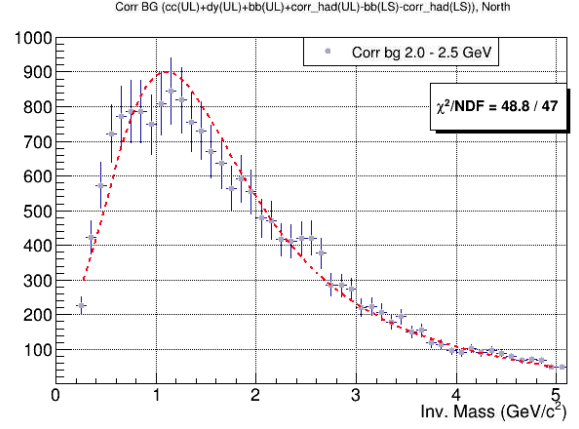
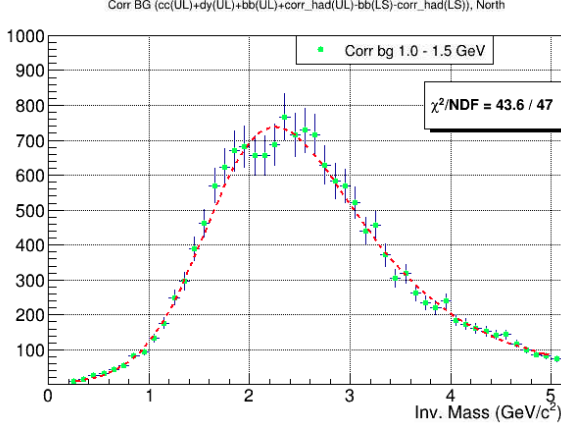


Figure 7: Run15pp North arm rescaled fits for  $1.0 < p_T < 1.5$  GeV/c, left, and  $2.0 < p_T < 2.5$  GeV/c. Only parameter ‘c’ is free.

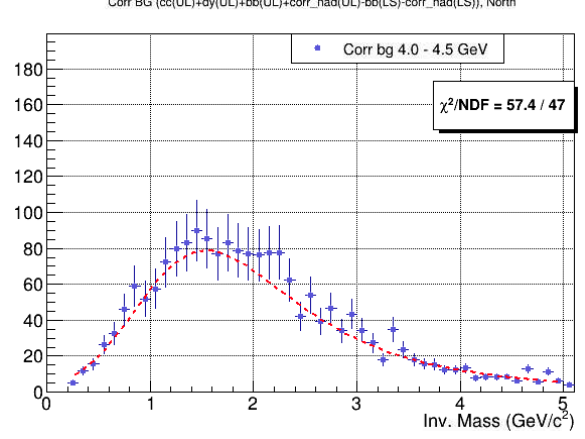
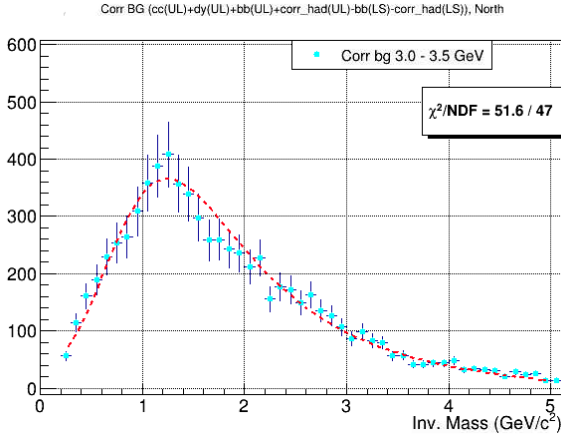


Figure 8: Run15pp North arm rescaled fits for  $3.0 < p_T < 3.5$  GeV/c, left, and  $4.0 < p_T < 4.5$  GeV/c. Only parameter ‘c’ is free.

### 3.3 Checks on Run15pp Correlated Background

We performed several checks to verify the accuracy of the parameter functions in fitting Yue Hang’s initial correlated background shape.

#### 3.3.1 Rescaled Fits

We refit each correlated background mass distribution using the polynomial functions to calculate the bestfit parameter for the given  $p_T$  value. For this purpose, we fixed all parameters aside from the normalization, and the rescaled fit is taken over the same mass range as the initial fit. Examples of these results are shown in Figures 6 and 7.

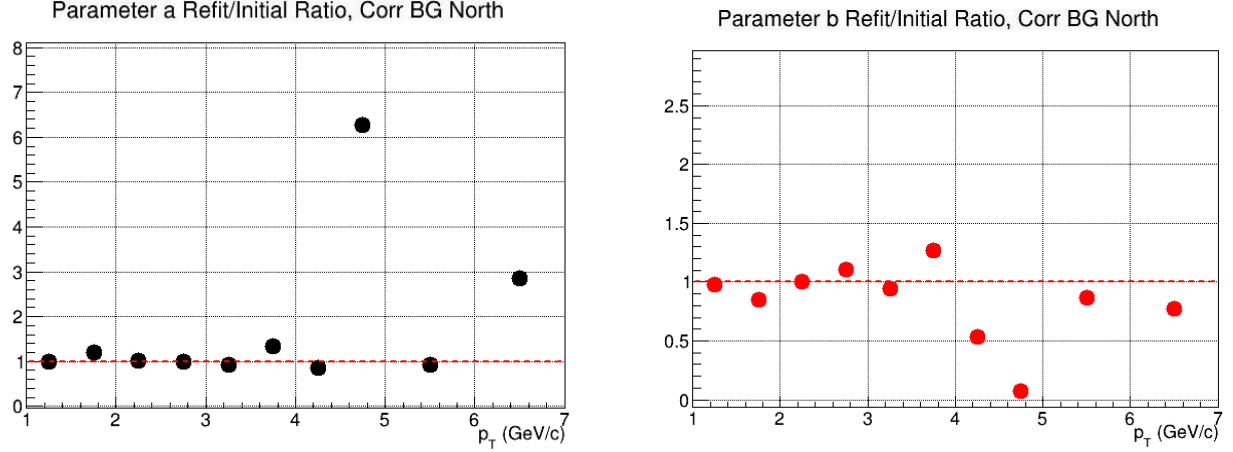


Figure 9: Run15pp North arm parameter ‘a’, left, and parameter ‘b’ ratios of rescaled fit value to initial fit value. We take a closer look at  $4.5 < p_T < 5.0$  GeV/c below.

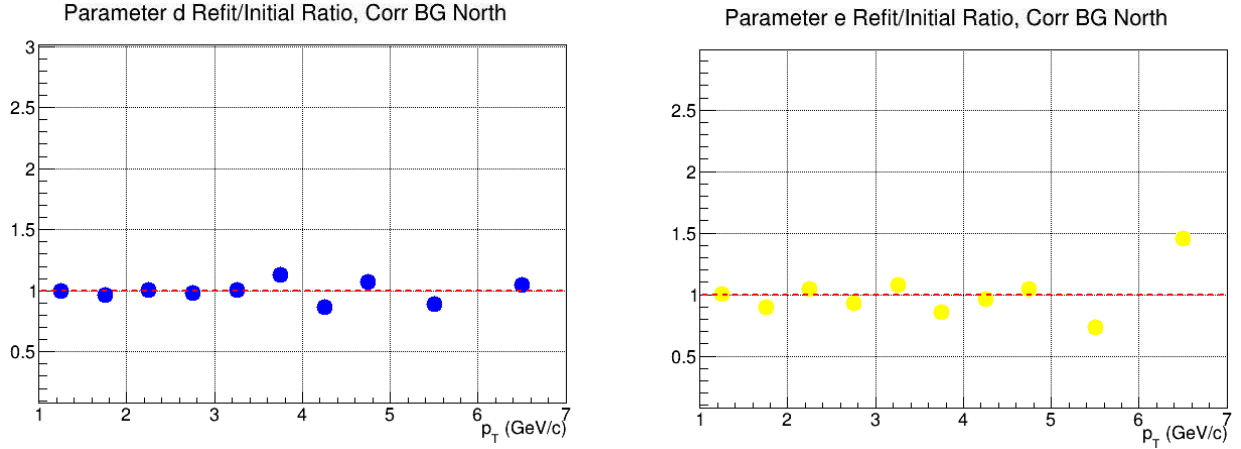


Figure 10: Run15pp North arm parameter ‘d’, left, and parameter ‘e’ ratios of rescaled fit value to initial fit value.

### 3.3.2 Parameter Ratio plots

Additionally, we took the ratio of the parameter value in the rescaled fit compared to the parameter value in the initial fit. The plots for parameters a, b, d, and e are shown in Figures 8 and 9.

Based on the parameter ‘a’ and ‘b’ plot results for  $4.0 < p_T < 4.5$  GeV/c, we take a closer look at the rescaled fit. As previously mentioned, the initial fits, as well as the rescaled fits, are over a broader mass range than the range we are using in the Crystal Ball fitter. Figure 10 shows the rescaled fit over the broader mass range compared with the rescaled fit over the Crystal Ball mass range. We see that the main reason for the poor fit is due to the peak. But at higher  $p_T$ , the peak does not fall within the mass range used in the Crystal ball fitter. And the fit over the actual data range is quite good, with  $\chi^2/NDF = 1.28$ .

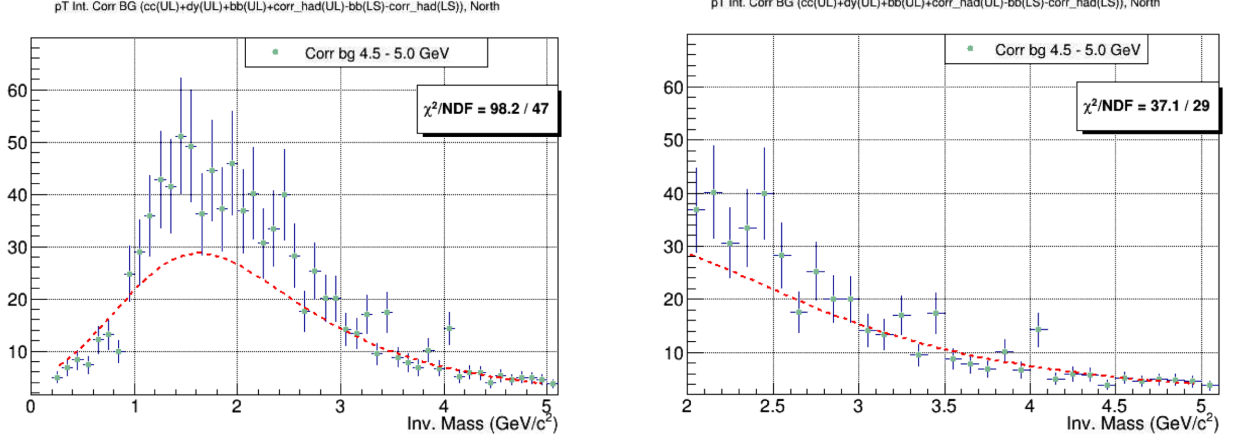


Figure 11: Left: The rescaled correlated background fit for  $4.5 < p_T < 5.0$  GeV/c over the same mass range as the initial fit. Right: The same rescaled correlated background fit over the mass range used in the Crystal Ball fitter.

### 3.3.3 Ratio of Rescaled Fit/Initial Fit

The final check we made on the parameter functions is the  $p_T$  integrated comparison between the rescaled fits and Yue Hang's raw correlated background. The raw correlated background is the sum of all correlated background mass distributions over the  $p_T$  range 0-7 GeV/c, and is then fit *once*, after all the components have been summed over.

The rescaled  $p_T$  integrated background, on the other hand, is the sum of all *individual* fits over the same  $p_T$  range. Since the area under the curve of each distribution varies, we used a weighted average to determine  $p_T$  integrated for the rescaled fits:

$$y(x) = \frac{\sum_i x_i w_i}{\sum_i w_i}. \quad (8)$$

Here, the weight  $w_i$  is the area under each correlated background curve, and  $x_i$  is the rescaled fit evaluated at each mass bin. Then the weighted average can be written as

$$y(m) = \frac{\sum_{p_T} A_{p_T} f(m|p_T)}{\sum_{p_T} A_{p_T}}, \quad (9)$$

where the area is taken as the area under the curve of the initial fit,  $f_0(m|p_T)$

$$A_{p_T} = \int_2^5 f_0(m|p_T) dm. \quad (10)$$

See Figures 11 and 12 for the rescaled  $p_T$  integrated correlated background shape and for the ratio with the raw  $p_T$  integrated shape.



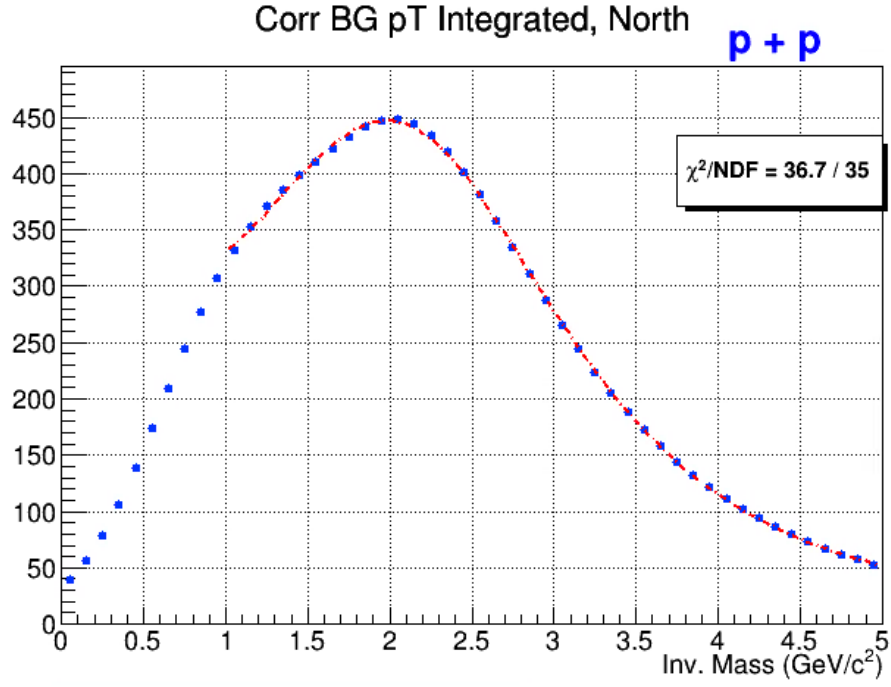


Figure 12: The rescaled  $p_T$  integrated correlated background.

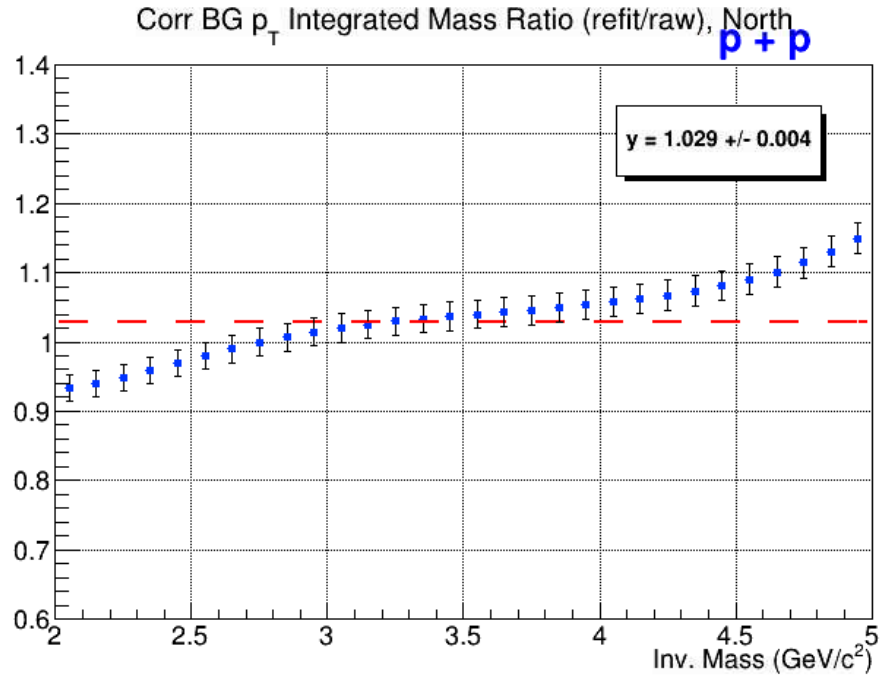


Figure 13: The mass ratio of the rescaled  $p_T$  integrated correlated background to the Yue Hang's raw  $p_T$  integrated correlated background over the mass range 2-5  $\text{GeV}/c^2$ .

### 3.4 Final $p_T$ binning

The final  $p_T$  binning used for the Run15pp correlated background is:

- 0 - 1 GeV/c: 200 MeV/c binwidths (omitted 400 - 600 MeV/c)
- 1 - 5 GeV/c: 500 MeV/c binwidths
- 5 - 7 GeV/c: 1 GeV/c binwidths

The final  $p_T$  binning used for the Run15pp data is:

- 0 - 6 GeV/c: 250 MeV/c binwidths
- 6 - 7 GeV/c: 500 MeV/c binwidths

## 4 Run15pAu Correlated Background

The Run15pAu correlated background consists of the same components as Run15pp, since we are again estimating the unlike-sign background using like-sign pairs, such that

$$BG(UL) = c\bar{c}(UL) + b\bar{b}(UL) + corr\_had(UL) + dy(UL) + comb(LS) - b\bar{b}(LS) - corr\_had(LS). \quad (11)$$

The Run15pAu correlated background was constructed by modifying the Run15pp correlated background. Aside from the comb(LS), all components listed above were modified except the contributions from dy(UL), since these modifications are not known.

For all other components, the Run15pp contributions were multiplied by a scaled modification factor determined by PYTHIA simulations, based on the Run08dAu nuclear modification results. Please see Yue Hang's AN 1369 for more detailed and precise information regarding the scaled modification factors.

### 4.1 Initial Fits

We proceed now in the same manner as Run15pp. We began with the same  $p_T$  binwidths as Run15pp, which were 500 MeV/c  $p_T$  slices. Figures 13 and 14 show the Run15pAu mass distribution for 500 MeV/c  $p_T$  slices over the range 0 – 7 GeV/c, where we have fit the background using the same function as Run15pp (defined in section 2.3). For the initial fits, all parameters are free. We also fit well beyond the lower mass limit of 2.0 GeV/c<sup>2</sup>. The Run15pAu fits in the North and South arm are directly compared with the Run15pp fits.

But the rescaled fits had poor chisquare values, even over the same range as the Crystal Ball fitter. It became clear that the correlated background must change more rapidly in Run15pAu than in Run15pp, and that finer  $p_T$  binning would be needed. Therefore, we switched to 300 MeV/c binwidths in  $p_T$  for the Run15pAu correlated background.

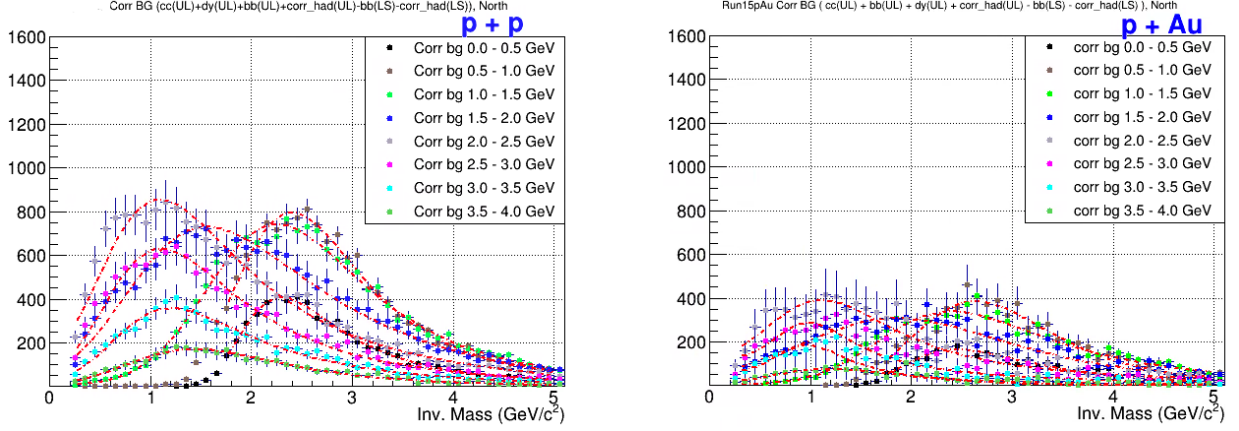


Figure 14: North Arm: Run15pp correlated background mass distribution, left, compared with Run15pAu. All parameters are free.

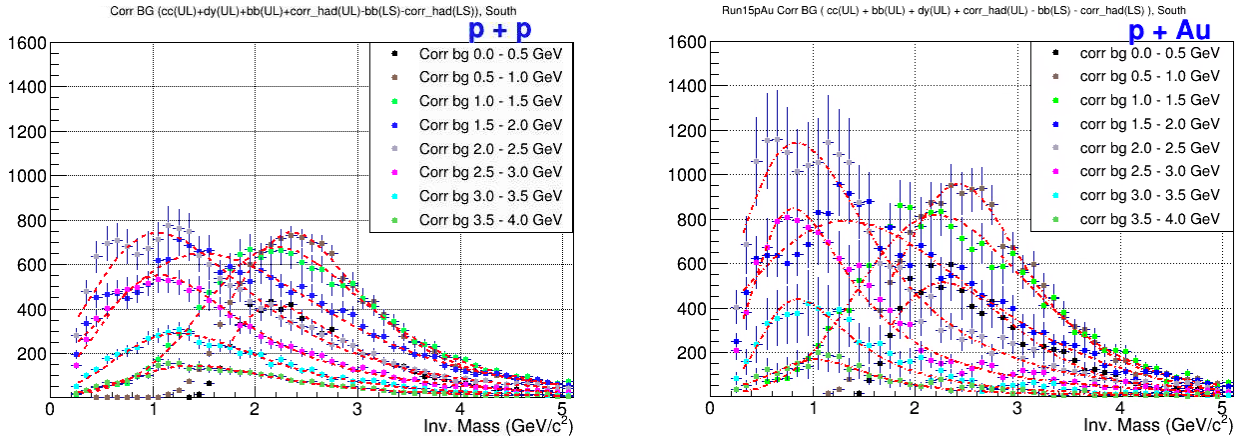


Figure 15: South Arm: Run15pp correlated background mass distribution, left, compared with Run15pAu. All parameters are free.

## 4.2 Parameters as a function of $p_T$

The parameters over the range 1-7 GeV/c were similar enough to fit with polynomial functions, as was the case for Run15pp. The results are shown in Figure 15. These polynomial functions were then input into the Crystal Ball fitter, and the initial parameter values individually calculated for each  $p_T$  value.

However, the parameters over the range 0-1 GeV/c changed too rapidly to find functions that could accurately describe their behavior, which was also the case in Run15pp. The same method was followed here as well, with the bestfit results for parameters a, b, d, e directly used as the initial parameters in the Crystal Ball fitter.

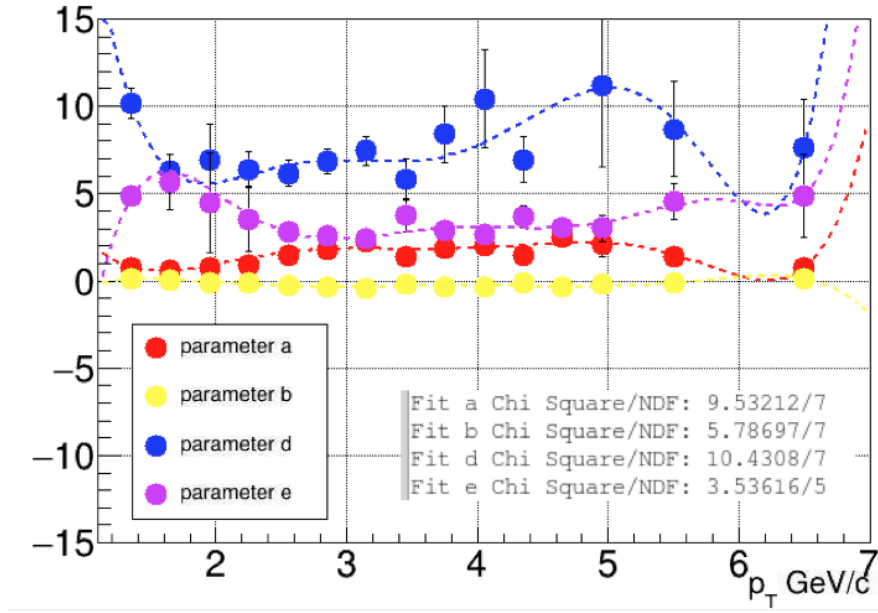


Figure 16: 1-7 GeV/c: Bestfit parameters of the correlated background fit function plotted vs.  $p_T$  for Run15pAu North arm. The parameters are fit with polynomials of varying degrees.

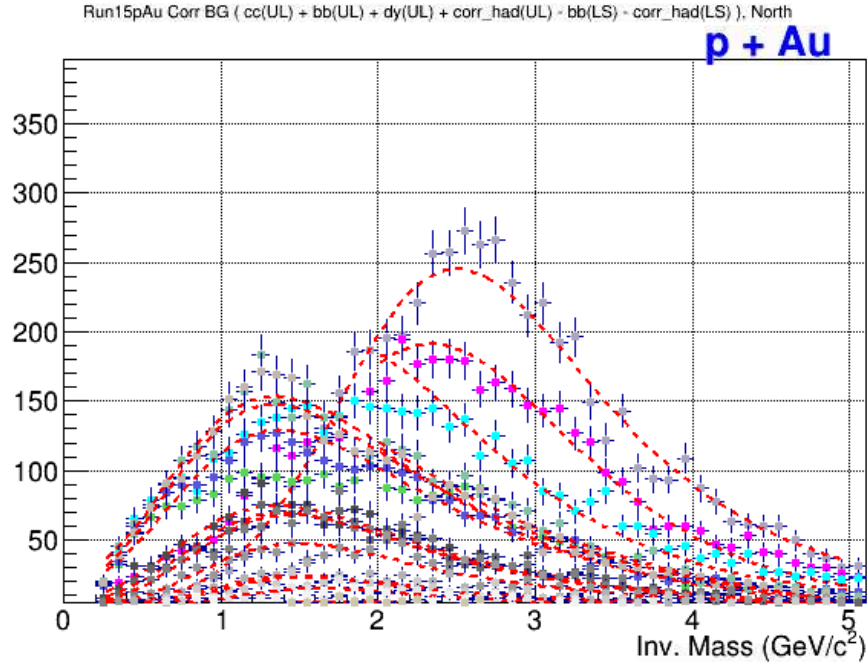


Figure 17: Rescaled fits for Run15pAu in the North Arm with 300 MeV/c binning. The initial parameter values were calculated from the polynomial functions shown in the above plot. Only the normalization parameter 'c' is free.

### 4.3 Checks on Run15pAu Correlated Background

The same checks were performed on the correlated background for Run15pAu as Run15pp.

#### 4.3.1 Rescaled Fits

We refit each correlated background mass distribution using the polynomial functions to calculate the bestfit parameter for the given  $p_T$  value. For this purpose, we fixed all parameters aside from the normalization. These fits are shown in Figure 16.

#### 4.3.2 Parameter Ratio plots

We also took the ratio of the parameter value in the rescaled fit compared to the parameter value in the initial fit. The plots for parameters a, b, d, and e are shown in Figures 17 and 18.

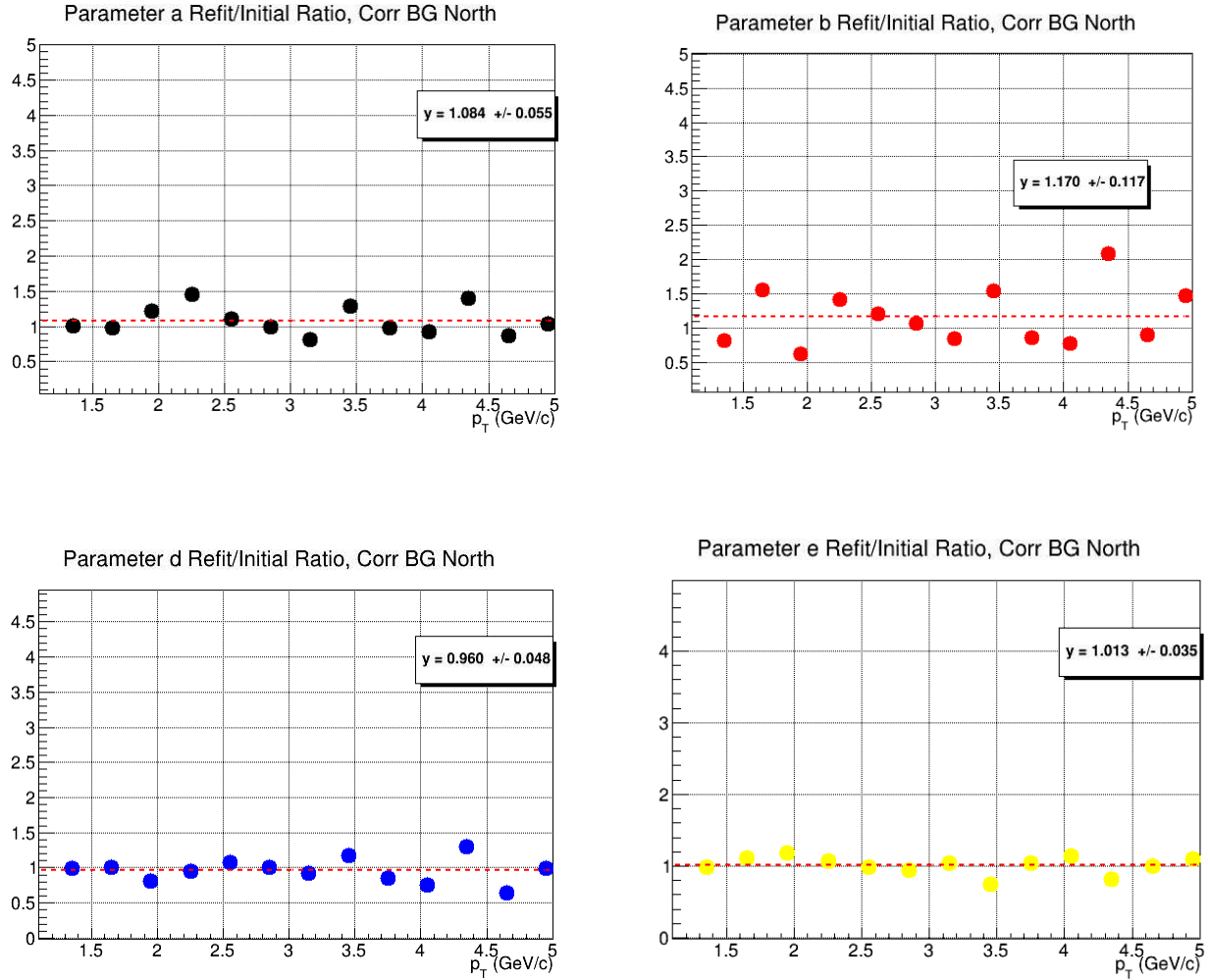


Figure 19: Top: Run15pAu North arm parameter 'a', left, and parameter 'b' ratios of rescaled fit value to initial fit value. Bottom: Run15pAu North Arm parameter 'd' and parameter 'e' ratios.

### 4.3.3 Ratio of Rescaled Fit/Initial Fit

The final check we made on the parameter functions is the  $p_T$  integrated comparison between the rescaled fits and Yue Hang's raw correlated background, as shown in Figures 19 and 20. See Section 3.3.3 for details of the method.

## 4.4 Final $p_T$ binning

The final  $p_T$  binning used for the Run15pAu correlated background is:

- 0 - 1 GeV/c: 200 MeV/c binwidths (omitted 400 - 600 MeV/c)
- 1 - 5 GeV/c: 300 MeV/c binwidths
- 5 - 7 GeV/c: 1 GeV/c binwidths

The final  $p_T$  binning used for the Run15pAu Centrality data is:

- 0 - 4 GeV/c: 250 MeV/c binwidths
- 4 - 5 GeV/c: 500 MeV/c binwidths
- 5 - 7 GeV/c: 2 GeV/c binwidth

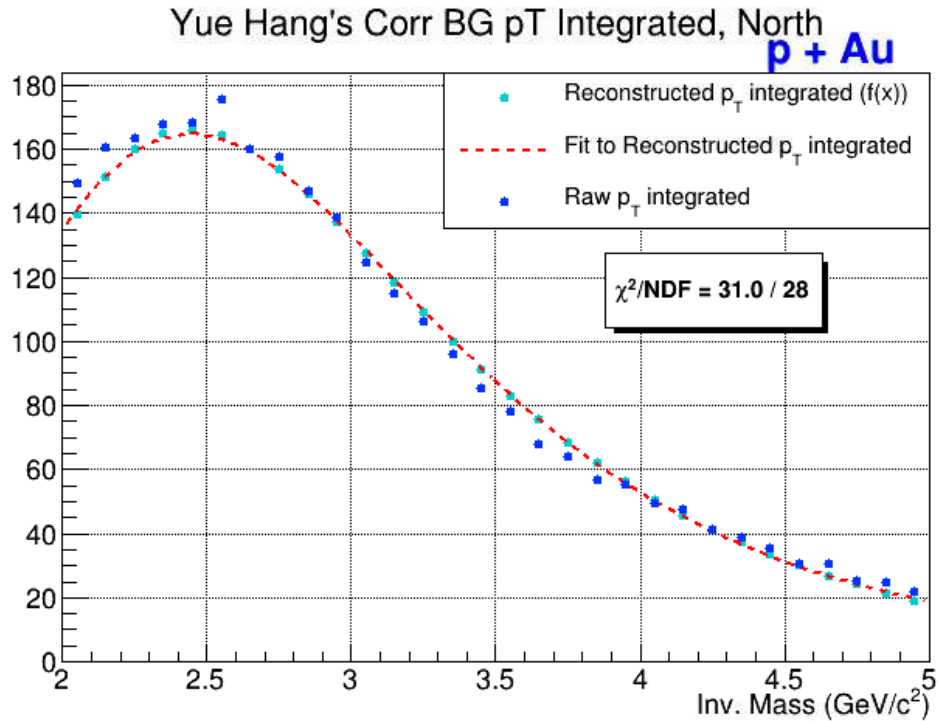


Figure 20: Run15pAu North Arm: The rescaled  $p_T$  integrated correlated background shown together with Yue Hang's raw  $p_T$  integrated correlated background over the mass range 2-5  $\text{GeV}/c^2$ .

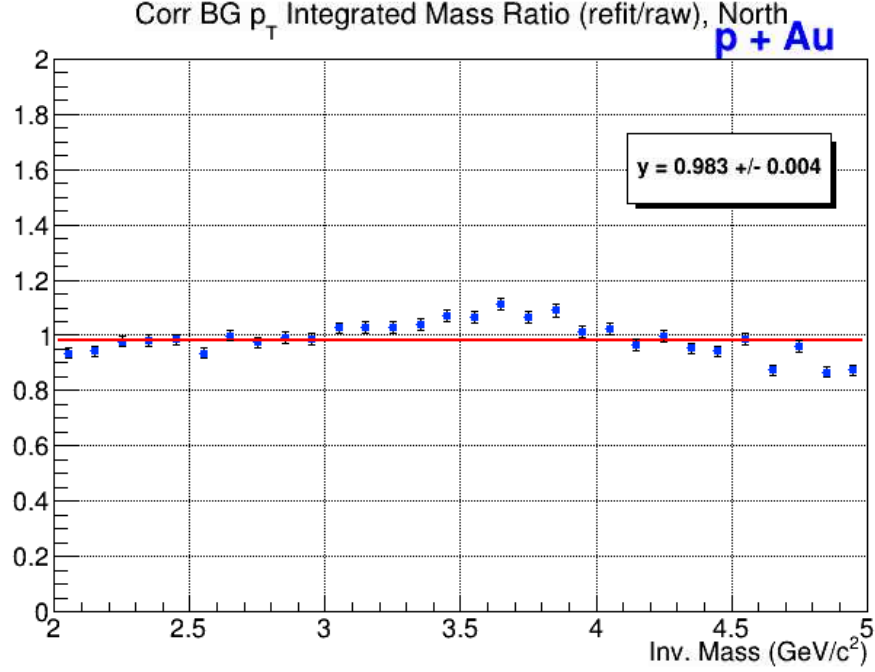


Figure 21: Run15pAu North Arm: The mass ratio of the rescaled  $p_T$  integrated correlated background to the Yue Hang's raw  $p_T$  integrated correlated background over the mass range 2-5  $\text{GeV}/c^2$ .

## 5 Run15pAl and Run14HeAu Correlated Backgrounds

Yue Hang did not study the correlated backgrounds for Run15pAl or Run14HeAu. Therefore, to maintain uniformity in the analysis, we used the Run15pp correlated background results to fit Run15pAl, and we used the Run15pAu correlated background results to fit Run14HeAu.

We initially tried using the  $p_T$  dependent correlated background parameter functions, but the uncertainties in the fits were large and the fits themselves were less stable than what was observed in Run15pp and Run15pAu. Therefore, we decided to use the  $p_T$  integrated fit results for the initial parameters in both systems.

### 5.1 Final $p_T$ binning, Run15pAl

The final  $p_T$  binning used for the Run15pAl correlated background is the Run15pp binning:

- 0 - 1  $\text{GeV}/c$ : 200  $\text{MeV}/c$  binwidths (omitted 400 - 600  $\text{MeV}/c$ )
- 1 - 5  $\text{GeV}/c$ : 500  $\text{MeV}/c$  binwidths
- 5 - 7  $\text{GeV}/c$ : 1  $\text{GeV}/c$  binwidths

## 5.2 Final $p_T$ binning, Run14HeAu

The final  $p_T$  binning used for the Run14HeAu correlated background is the Run15pAu binning:

- 0 - 1 GeV/c: 200 MeV/c binwidths (omitted 400 - 600 MeV/c)
- 1 - 5 GeV/c: 300 MeV/c binwidths
- 5 - 7 GeV/c: 1 GeV/c binwidths

The final  $p_T$  binning used for the Run14HeAu Centrality data is:

- 0 - 2.5 GeV/c: 250 MeV/c binwidths
- 2.5 - 4 GeV/c: 500 MeV/c binwidths

## 6 Correlated Background Systematic Uncertainty

The systematic uncertainties associated with each system are detailed in AN 1391, Table 11. These systematic uncertainties were applied in the same manner for the results presented in this note except for the correlated background systematic uncertainties.

### 6.1 Sanghoon's Method

One of the important differences between this analysis note and AN 1391 is the new method proposed by Sanghoon Lim to calculate the systematic uncertainty arising from the uncertainty in the correlated background shape. Here we present the logic for the study:

1.  $J/\psi$  fit with unmodified correlated background shape from Yue Hang's results is not good.
2. This is understandable because we're using different cuts and different mass calculation. In addition, his shape is also from simulation.
3. In order to handle that, we can free some parameters in the fit function for Yue Hang's correlated background shape.
4. Since we don't know how many free parameters are best, we tested two cases: one free except for normalization (case A) and two free except for normalization (Case FGH).

We have included an example of this method using a high statistics bin from Run15pp: bin 7, which corresponds to the  $p_T$  range 1.50 – 1.75 GeV/c. See Figures 21 - 24.

This same method was applied to extract the counts for all  $p_T$  in both the North and South arms. We then calculated the systematic uncertainty between the Case A  $J/\psi$  counts and the average of the Case F, Case G, and Case H  $J/\psi$  counts, using the following formula:

$$\sigma_{corrbg} = \frac{|J/\psi^{CaseA} - J/\psi^{CaseFGH}|}{J/\psi^{CaseA}} \pm \frac{\sigma^{CaseA}}{J/\psi^{CaseA}}. \quad (12)$$



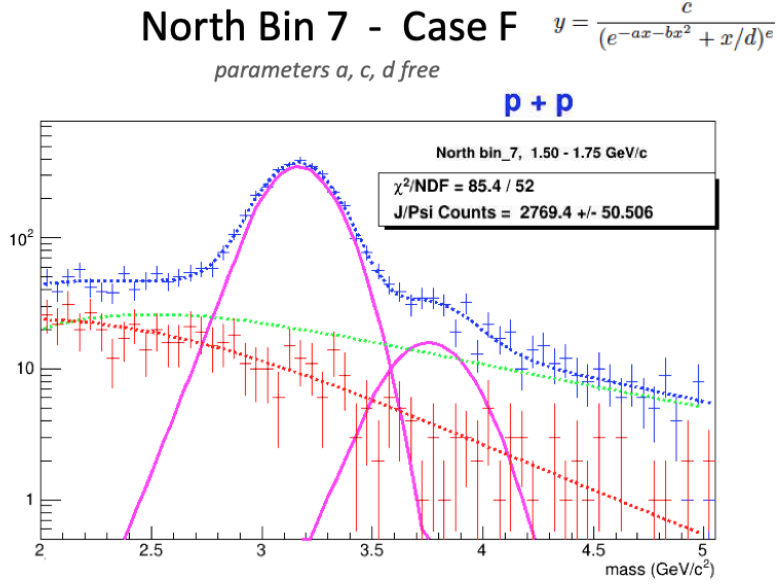


Figure 22: Example: Run15pp North Arm bin 7 ( $1.5 < p_T < 1.75$  GeV/c) data fit using Case F, which has parameters  $a, c, d$  free.

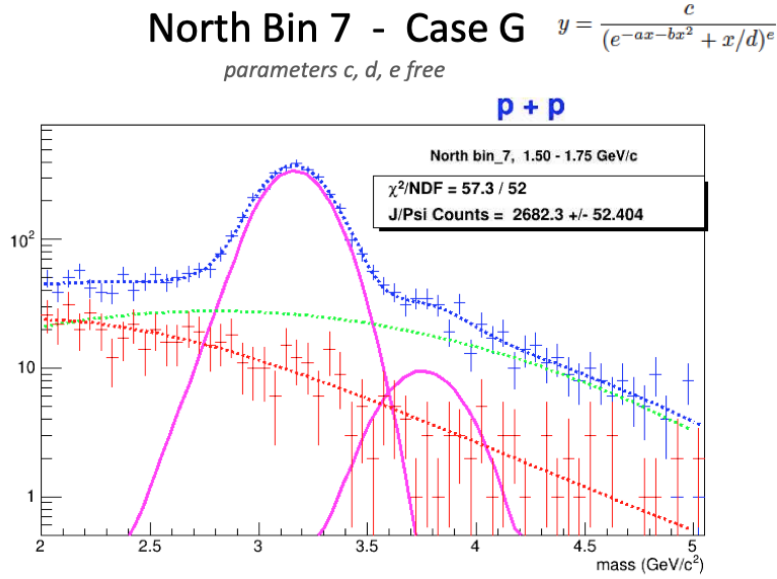


Figure 23: Example: Run15pp North Arm bin 7 ( $1.5 < p_T < 1.75$  GeV/c) data fit using Case G, which has parameters  $c, d, e$  free.

## 6.2 Combinatorial Background Contribution

The resulting distribution was plotted as a function of  $p_T$  in Figure 25. The systematic uncertainty distribution shows differences between the counts that are larger than the statistical uncertainty. The contribution from the slope of the fit to the combinatorial background is enough to cause a

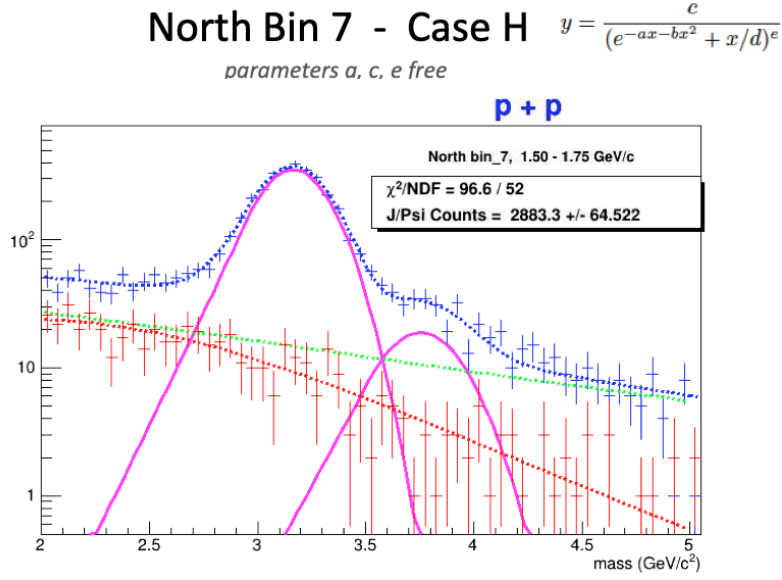


Figure 24: Example: Run15pp North Arm bin 7 ( $1.5 < p_T < 1.75$  GeV/c) data fit using Case H, which has parameters  $a, c, e$  free.

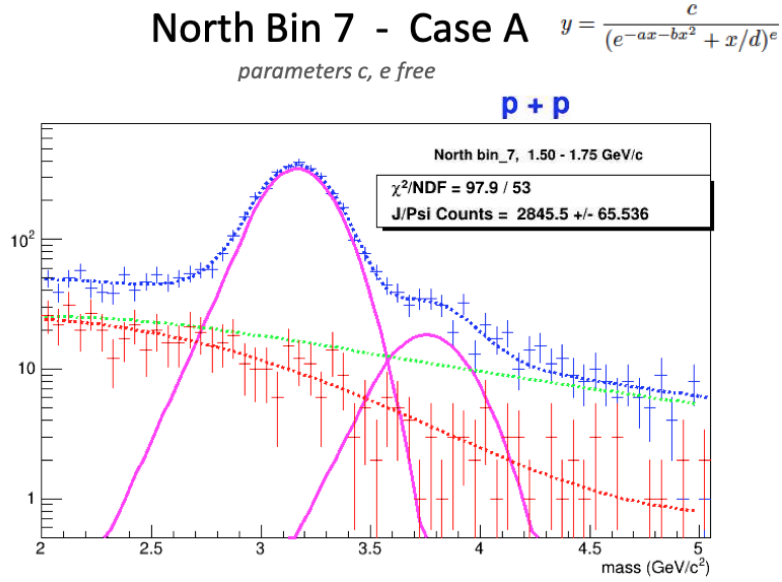


Figure 25: Example: Run15pp North Arm bin 7 ( $1.5 < p_T < 1.75$  GeV/c) data fit using Case A, which has parameters  $c, e$  free.

discrepancy between the Case A and the Case FGH counts.

For the fitting of Cases F, G and H, the same initial parameters for the combinatorial background were used in all three cases for the aforementioned reason. We went back and fit Case A using the same set of initial parameters used for the Cases F, G and H. If the Case A fit failed,

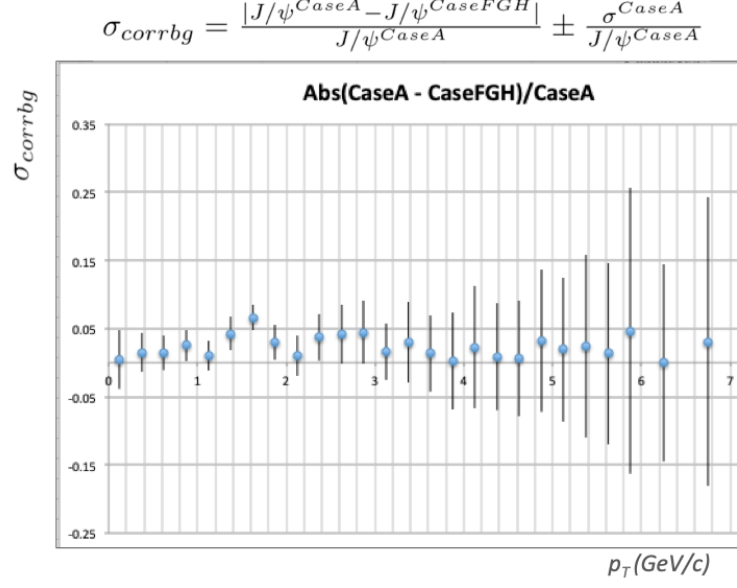


Figure 26: Run15pp North systematic uncertainty distribution as a function of  $p_T$ . There are discrepancies between the two cases larger than statistical uncertainty due to the combinatorial background.

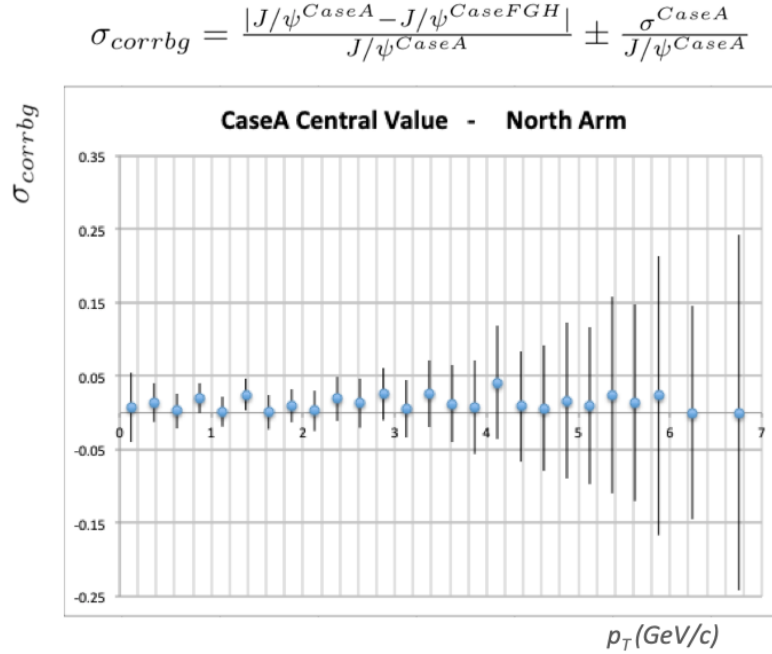


Figure 27: Run15pp North systematic uncertainty distribution as a function of  $p_T$  with the same combinatorial background initial parameters used in all four cases.

then A, F, G and H were refit with a new set of combinatorial initial parameters. This resolved the discrepancy between the counts. See Figure 26 for the final results.

### 6.3 Systematic Study Conclusion

From these four different cases of fixing and freeing the five parameters of the correlated background fit function, we can see the variation in  $J/\psi$  counts due to the uncertainty in the correlated background shape. In Table 1, we have summarized the resulting  $J/\psi$  counts from the four different cases, after refitting to a new set of parameters for the combinatorial background.

Table 1: Systematic Study Example: Bin 7 in Run15pp North Arm, with the same combinatorial background initial parameters used for all Cases.

Case A	Ave FGH	Case F	Case G	Case H	Prelim
$2,845 \pm 66$	$2,843 \pm 68$	$2,766 \pm 75$	$2,883 \pm 64$	$2,881 \pm 64$	$2,746 \pm 64$

The results from Case A and the average of CaseFGH are consistent, which verifies that the  $J/\psi$  extraction is not that sensitive to the correlated background shape. Therefore, we decided to use the results from case A (less free parameters) as the central value and the results from case FGH (more free parameters) for the systematic check.

### 6.4 Check on CaseFGH

Tony wondered how closely Case FGH matches Yue Hang's original correlated background shape, since there are two free parameters (aside from normalization), while Case A has one free parameter aside from normalization. Sanghoon suggested to take the mass ratios of the correlated

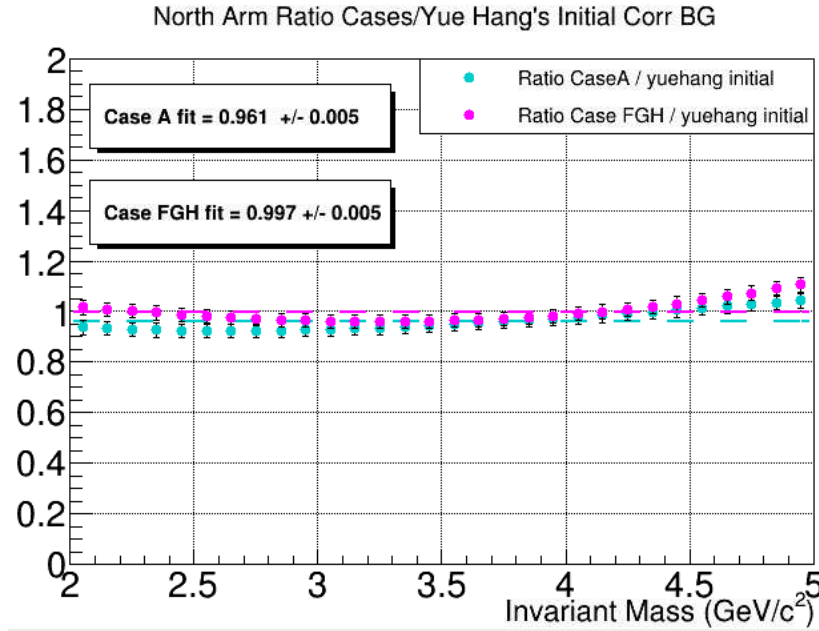


Figure 28: Run15pp North correlated background comparison between the ratios of Case FGH to Yue Hang's initial fit and Case A to Yue Hang's initial fit. bin 7 is shown (1.5 - 1.75 GeV/c).

background, with Case A compared with Yue Hang's initial fit and then to do the same with Case FGH. The results indicate that both Cases describe the initial correlated background quite well (see Figure 28).

## 6.5 Systematic Study Results

The systematic uncertainty as a function of  $p_T$  was plotted and a line of best fit was used to determine the overall value to assign as the correlated background systematic uncertainty. We used this approach for all systems and all measurements. The results are listed in Table 2. The fitted distributions for all systems and centralities are shown in Figures 28-34.

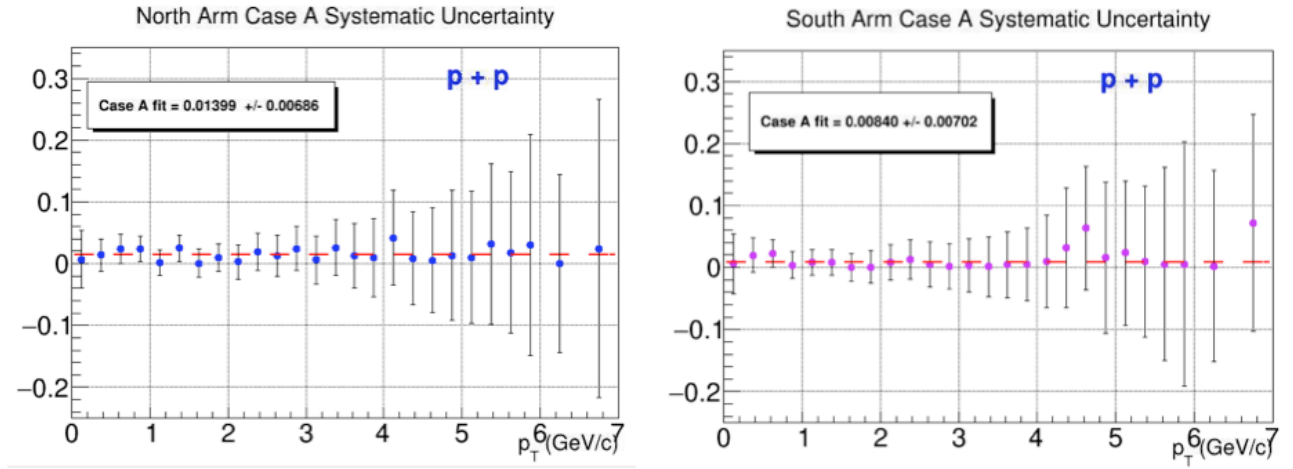


Figure 29: Run15pp correlated background fractional systematic uncertainty distributions for both North, left, and South Arms. The South arm uncertainty was rounded up to 1.00%

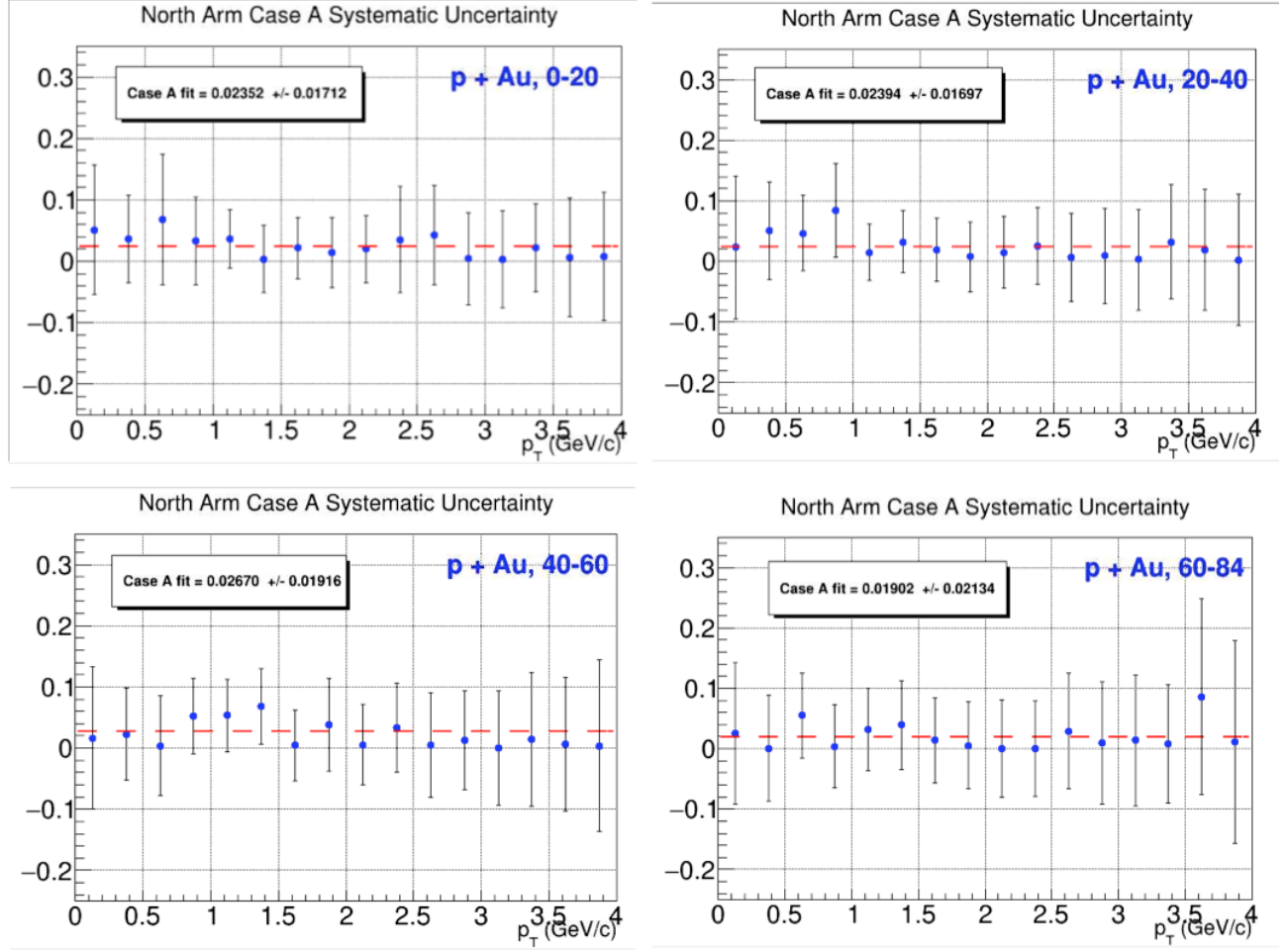


Figure 30: Run15pAu North correlated background fractional systematic uncertainty distributions for all centralities.

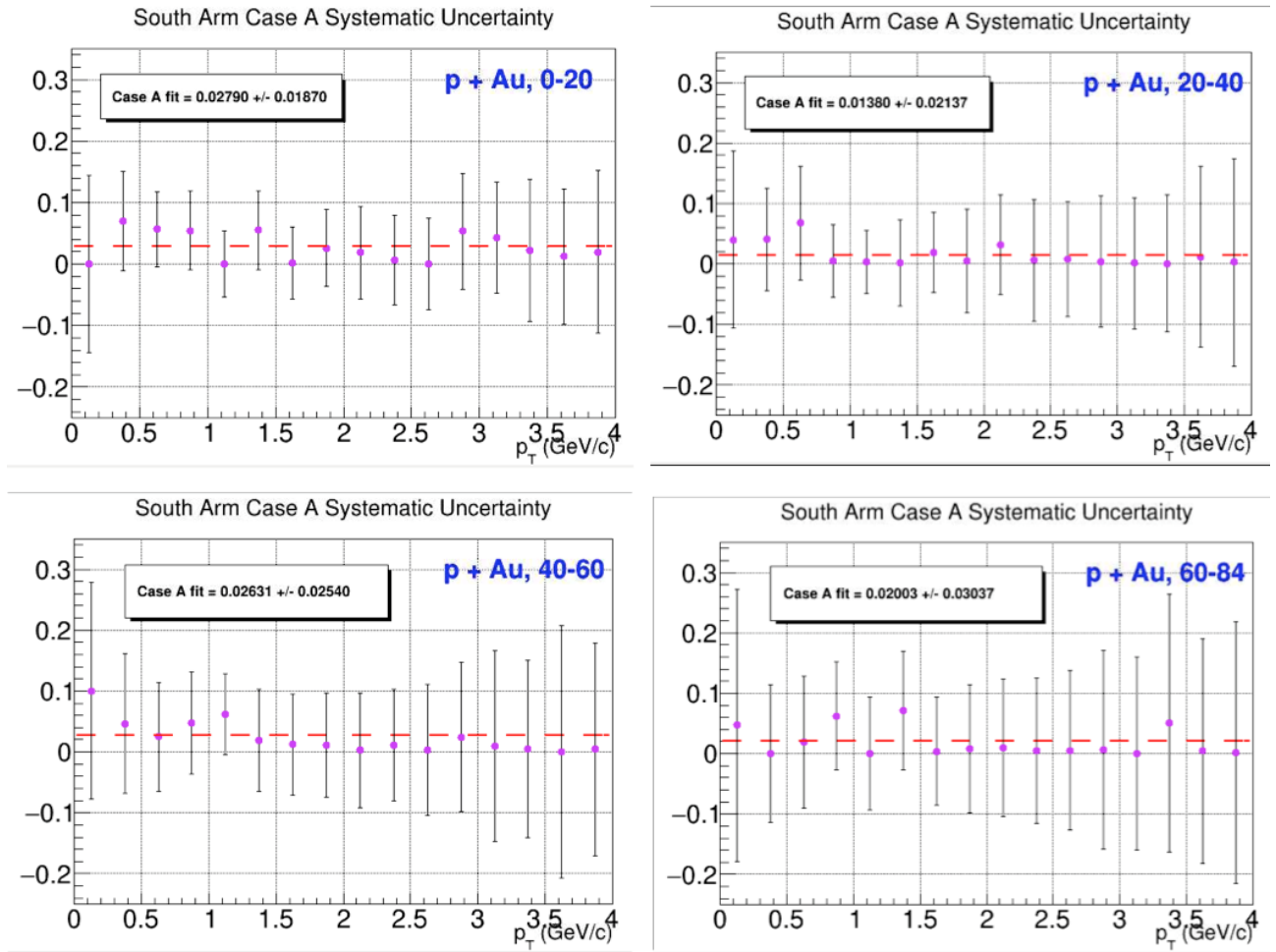


Figure 31: Run15pAu South correlated background fractional systematic uncertainty distributions for all centralities.

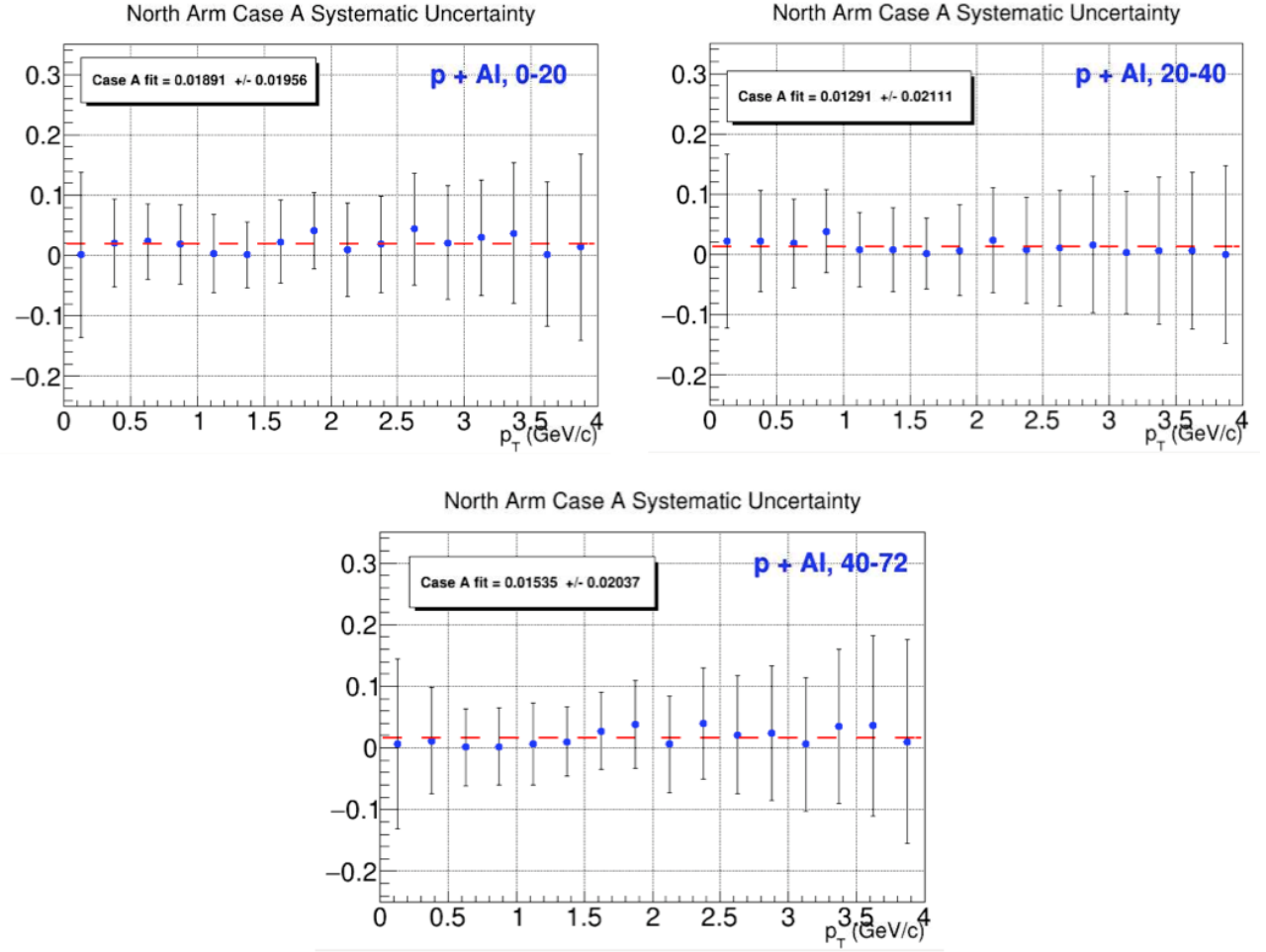


Figure 32: Run15pAl North correlated background fractional systematic uncertainty distributions for all centralities. Due to low statistics, Run15pp North systematic uncertainty ( $\sigma_{\text{corr}bg} = 1.4$ ) was used instead for all three centralities.



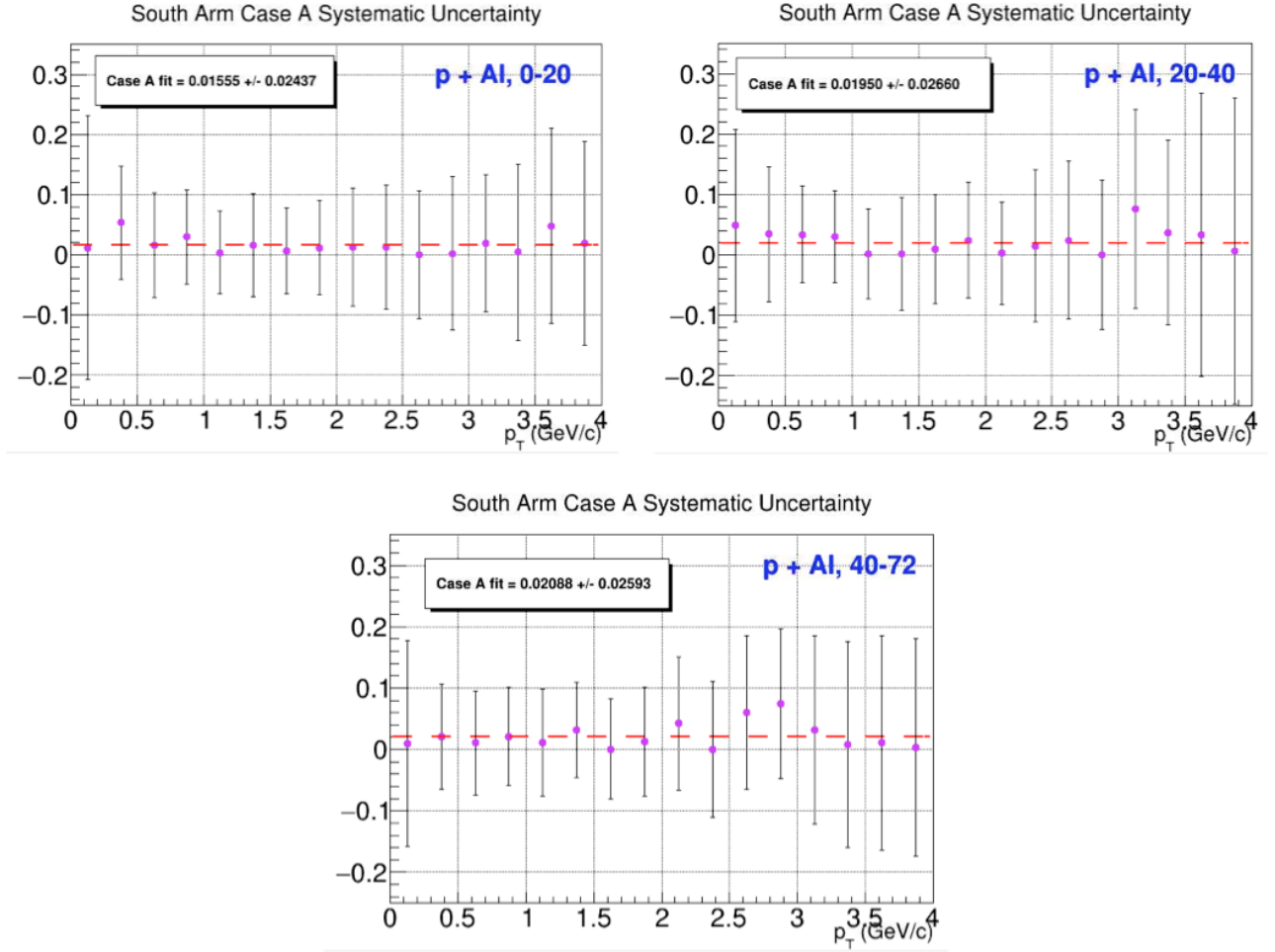


Figure 33: Run15pAl South correlated background fractional systematic uncertainty distributions for all centralities. Due to low statistics, Run15pp North systematic uncertainty ( $\sigma_{\text{corr}bg} = 1.0$ ) was used instead for all three centralities.

### 6.5.1 Run14HeAu Systematic Uncertainty

We determined the systematic uncertainty in the same manner for Run14HeAu as for the other systems, and the results are included here. But because of the low statistics, the systematic uncertainty results are more likely measuring statistical fluctuations as opposed to changes in the shape of the correlated background. For this reason, we have assigned the Run15pAu systematic uncertainty results to Run14HeAu for the 0-20 and 20-40 centrality bins. For the 40-88 Centrality range, we took the weighted average of 40-60 and 60-84 uncertainties in pAu, with the weight being the centrality binwidth.

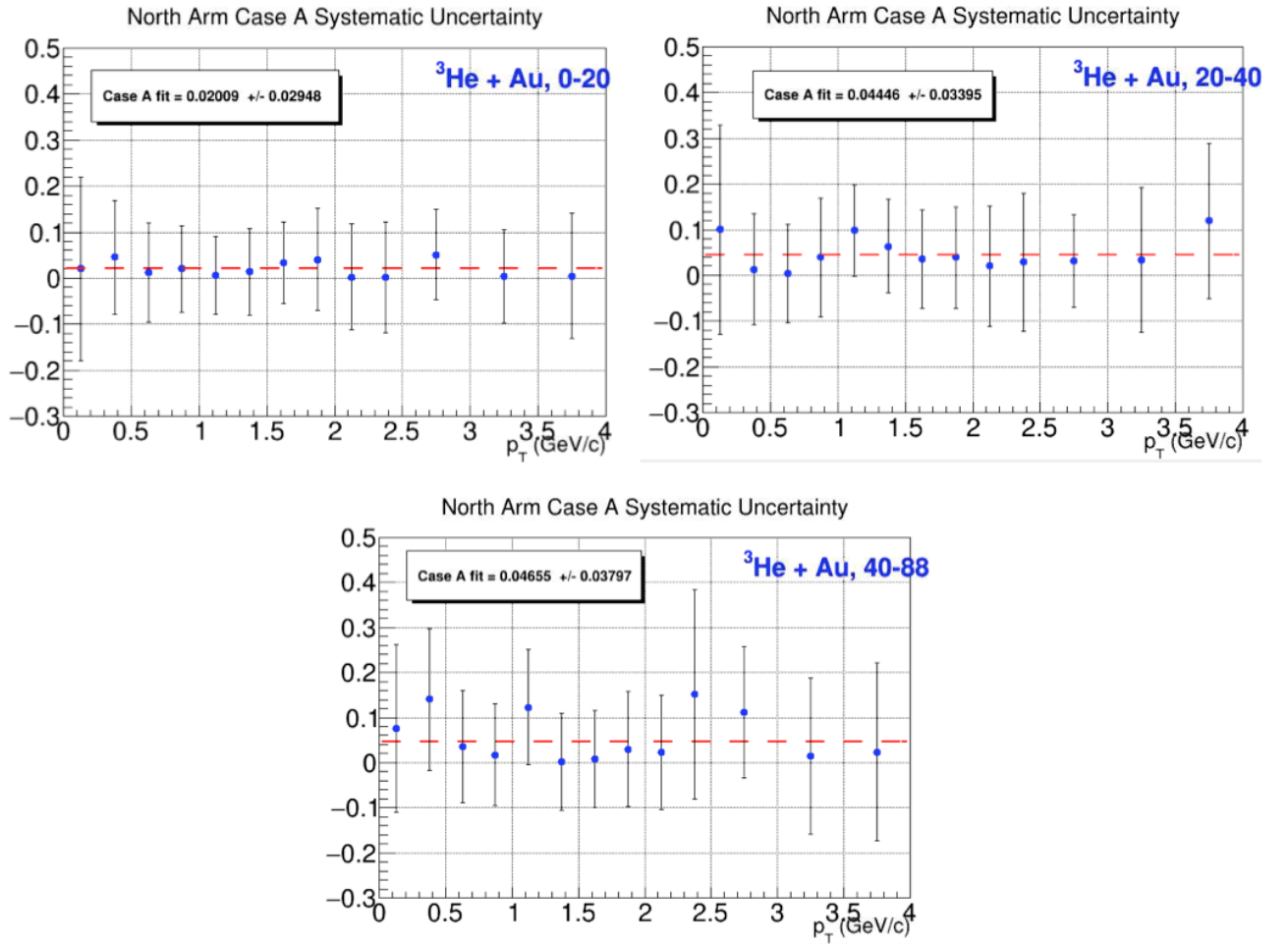


Figure 34: Run14HeAu North correlated background fractional systematic uncertainty distributions for all centralities. Please see above section "Run14HeAu Systematic Uncertainty" for details regarding the assignment of systematic uncertainty for this system.

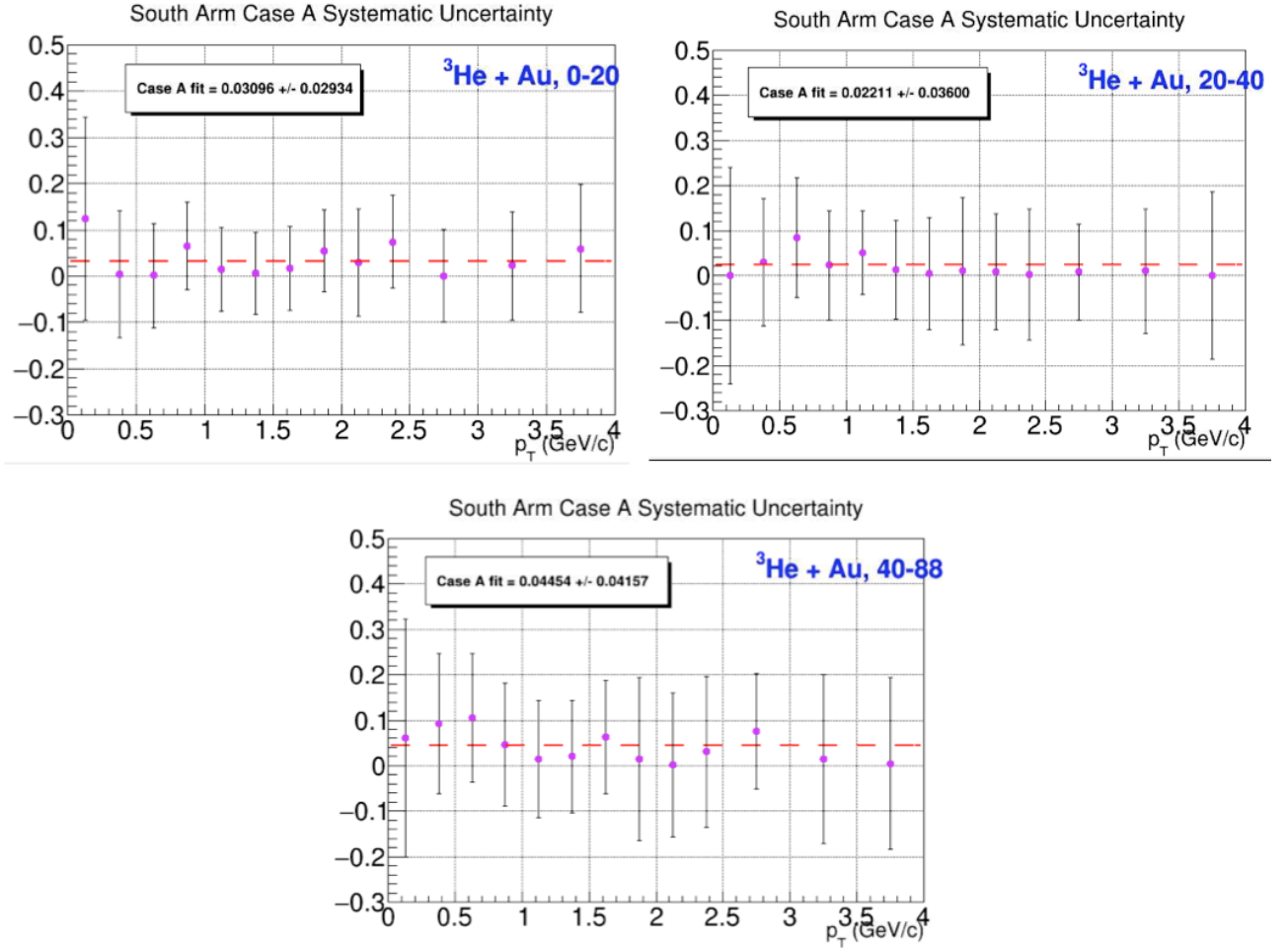


Figure 35: Run14HeAu South correlated background fractional systematic uncertainty distributions for all centralities. Please see the section “Run14HeAu Systematic Uncertainty” for details regarding the assignment of systematic uncertainty for this system.

Table 2: Correlated background fractional systematic uncertainty results. The value associated with the line of best fit through each  $p_T$  distribution was taken as the systematic uncertainty. The minimum bias uncertainties are the average of centrality uncertainties.

Arm	System	Centrality	$\sigma_{corrbg}$
North	Run15pp	-	1.40%
South	Run15pp	-	1.72%
North	Run15pAu	0-5	2.39%
		5-10	2.39%
		10-20	2.39%
		20-40	2.39%
		40-60	2.67%
		60-84	1.90%
		MinBias	2.33%
South	Run15pAu	0-5	2.79%
		5-10	2.79%
		10-20	2.79%
		0-20	2.79%
		20-40	1.38%
		20-40	1.38%
		40-60	2.54%
		60-84	2.00%
		MinBias	2.18%
North	Run15pAl	0-20	1.40%
		20-40	1.40%
		40-72	1.40%
		MinBias	1.40%
South	Run15pAl	0-20	1.72%
		20-40	1.72%
		40-72	1.72%
		MinBias	1.72%
North	Run14HeAu	0-20	2.35%
		20-40	2.39%
		40-88	2.25%
		MinBias	2.33%
South	Run14HeAu	0-20	2.79%
		20-40	1.38%
		40-88	2.25%
		MinBias	2.14 %

## 7 Run15pp Checks on $J/\psi$ Counts

### 7.1 Sum Over $p_T$

We refit the previous results for  $J/\psi$  vs.  $p_T$  (AN1391) to ensure results were consistent despite different analysis methods used. The results are compared with Case FGH counts as well. See Figure 36.

NORTH ARM												SOUTH ARM					
pt [GeV/c]	Case A	Case FGH	AN 1391	Case F	Case G	Case H	pt [GeV/c]	Case A	Case FGH	AN 1391	Case F	Case G	Case H				
0.125	832 +/- 51	857 +/- 37	795 +/- 35	856 +/- 38	858 +/- 35	857 +/- 39	0.125	720 +/- 33	736 +/- 39	678 +/- 32	772 +/- 39	669 +/- 34	767 +/- 43				
0.375	2246 +/- 59	2213 +/- 63	2147 +/- 58	2210 +/- 68	2153 +/- 62	2278 +/- 58	0.375	2048 +/- 54	2091 +/- 48	1975 +/- 57	2122 +/- 53	2079 +/- 43	2073 +/- 48				
0.625	2848 +/- 74	2753 +/- 82	2737 +/- 67	2708 +/- 80	2795 +/- 77	2756 +/- 88	0.625	2690 +/- 60	2715 +/- 88	2621 +/- 65	2700 +/- 107	2719 +/- 77	2727 +/- 80				
0.875	3680 +/- 78	3486 +/- 74	3413 +/- 74	3308 +/- 64	3450 +/- 78	3699 +/- 80	0.875	3299 +/- 77	3222 +/- 113	3266 +/- 73	3296 +/- 109	3194 +/- 117	3176 +/- 114				
1.125	3687 +/- 82	3721 +/- 79	3548 +/- 77	3644 +/- 88	3760 +/- 75	3759 +/- 75	1.125	3528 +/- 68	3526 +/- 91	3446 +/- 58	3527 +/- 90	3525 +/- 89	3525 +/- 93				
1.375	3237 +/- 71	3182 +/- 89	3045 +/- 68	3167 +/- 97	3094 +/- 102	3287 +/- 69	1.375	3066 +/- 70	3081 +/- 86	3024 +/- 67	3110 +/- 79	3065 +/- 92	3068 +/- 87				
1.625	2877 +/- 64	2843 +/- 68	2746 +/- 64	2766 +/- 75	2883 +/- 64	2881 +/- 64	1.625	2796 +/- 64	2745 +/- 74	2708 +/- 91	2746 +/- 82	2691 +/- 90	2797 +/- 51				
1.875	2512 +/- 59	2463 +/- 64	2367 +/- 61	2370 +/- 74	2510 +/- 60	2508 +/- 60	1.875	2185 +/- 55	2132 +/- 56	2107 +/- 56	2138 +/- 55	2090 +/- 56	2167 +/- 56				
2.125	1966 +/- 54	1941 +/- 57	1847 +/- 53	1914 +/- 65	1953 +/- 53	1955 +/- 53	2.125	1743 +/- 44	1701 +/- 61	1666 +/- 53	1713 +/- 50	1658 +/- 83	1732 +/- 49				
2.375	1638 +/- 48	1588 +/- 52	1530 +/- 66	1581 +/- 49	1549 +/- 58	1635 +/- 49	2.375	1424 +/- 44	1399 +/- 60	1347 +/- 45	1417 +/- 59	1367 +/- 76	1412 +/- 44				
2.625	1284 +/- 42	1253 +/- 57	1215 +/- 57	1260 +/- 61	1216 +/- 68	1284 +/- 43	2.625	1073 +/- 38	1042 +/- 49	1013 +/- 39	1043 +/- 49	1015 +/- 61	1069 +/- 36				
2.875	1086 +/- 38	1052 +/- 51	1043 +/- 39	1058 +/- 46	1003 +/- 69	1096 +/- 37	2.875	961 +/- 35	936 +/- 41	905 +/- 36	938 +/- 40	931 +/- 50	940 +/- 34				
3.125	868 +/- 34	854 +/- 36	838 +/- 34	830 +/- 40	867 +/- 33	866 +/- 34	3.125	737 +/- 31	707 +/- 35	711 +/- 31	709 +/- 38	681 +/- 36	731 +/- 30				
3.375	704 +/- 31	684 +/- 42	675 +/- 31	690 +/- 39	656 +/- 57	704 +/- 30	3.375	542 +/- 27	546 +/- 28	536 +/- 28	543 +/- 31	551 +/- 26	544 +/- 27				
3.625	520 +/- 27	509 +/- 29	493 +/- 27	488 +/- 32	518 +/- 27	520 +/- 27	3.625	457 +/- 24	445 +/- 28	437 +/- 26	445 +/- 25	439 +/- 35	452 +/- 25				
3.875	378 +/- 23	377 +/- 27	354 +/- 24	377 +/- 30	377 +/- 23	378 +/- 27	3.875	342 +/- 21	334 +/- 27	334 +/- 23	336 +/- 26	329 +/- 33	337 +/- 22				
4.125	275 +/- 21	261 +/- 24	247 +/- 20	251 +/- 17	256 +/- 35	275 +/- 19	4.125	231 +/- 17	234 +/- 17	216 +/- 18	233 +/- 17	234 +/- 17	234 +/- 17				
4.375	231 +/- 17	227 +/- 18	212 +/- 18	227 +/- 19	228 +/- 17	227 +/- 17	4.375	154 +/- 15	154 +/- 15	142 +/- 16	153 +/- 15	154 +/- 14	156 +/- 17				
4.625	180 +/- 15	176 +/- 15	170 +/- 16	174 +/- 15	177 +/- 15	176 +/- 15	4.625	145 +/- 13	132 +/- 19	130 +/- 15	149 +/- 13	107 +/- 17	140 +/- 27				
4.875	125 +/- 13	121 +/- 13	118 +/- 14	117 +/- 15	123 +/- 12	124 +/- 13	4.875	86 +/- 10	84 +/- 11	84 +/- 12	83 +/- 12	83 +/- 12	87 +/- 11				
5.125	105 +/- 12	102 +/- 11	103 +/- 12	99 +/- 12	102 +/- 11	105 +/- 12	5.125	92 +/- 11	84 +/- 13	84 +/- 12	81 +/- 14	81 +/- 14	90 +/- 11				
5.375	91 +/- 12	84 +/- 11	83 +/- 12	76 +/- 11	93 +/- 13	83 +/- 10	5.375	83 +/- 11	84 +/- 11	77 +/- 10	84 +/- 10	84 +/- 11	84 +/- 10				
5.625	75 +/- 10	74 +/- 10	68 +/- 10	71 +/- 11	75 +/- 10	75 +/- 10	5.625	53 +/- 9	53 +/- 9	46 +/- 9	53 +/- 9	53 +/- 8	53 +/- 9				
5.875	44 +/- 9	41 +/- 9	38 +/- 8	38 +/- 8	42 +/- 10	43 +/- 8	5.875	34 +/- 7	34 +/- 7	27 +/- 7	34 +/- 7	34 +/- 7	34 +/- 7				
6.25	72 +/- 9	69 +/- 10	64 +/- 9	69 +/- 10	69 +/- 9	69 +/- 10	6.25	49 +/- 8	49 +/- 12	47 +/- 15	49 +/- 9	-	48 +/- 15				
6.75	32 +/- 7	32 +/- 7	27 +/- 7	32 +/- 7	-	32 +/- 7	6.75	46 +/- 8	42 +/- 10	39 +/- 8	39 +/- 13	-	45 +/- 8				
sum:	31593	30965	29,921				sum:	28583	28,309	27,667							
pt int:	31452 +/- 215	30714	29,597				pt int:	28511 +/- 205	28,689	28,288							
sum/pt int % diff:	0.45%	0.81					sum/pt int % diff:	0.25%									
Case A/FGH pt int % diff:	2.37%						Case A/FGH pt int % diff:	0.62%									
Case A/prelim pt int % diff:	5.82%						Case A/prelim pt int % diff:	0.79%									

Figure 36: Run15pp North and South arm  $p_T$  check. Case A is consistent with Case FGH, and Case A as the central value is consistent with  $p_T$  integrated results.

## 7.2 Sum Over Rapidity

We refit the preliminary results for  $J/\psi$  vs. rapidity (AN1354) to ensure results were consistent despite different analysis methods used. The results are compared with Case FGH counts as well. See Figure 37.

Run15pp	NORTH					
rap center	Case A	Ave FGH	Case F	Case G	Case H	AN 1354
1.325	2,082 +/- 54	2,034 +/- 58	1,949 +/- 73	2,086 +/- 51	2,065 +/- 51	1,974 +/- 58
1.575	10,583 +/- 120	10,201 +/- 154	10,062 +/- 161	9,926 +/- 180	10,614 +/- 121	9,997 +/- 186
1.825	12,170 +/- 138	11,949 +/- 177	11,850 +/- 172	11,659 +/- 224	12,337 +/- 136	11,431 +/- 192
2.075	7,040 +/- 109	7,088 +/- 161	7,283 +/- 112	6,725 +/- 262	7,255 +/- 108	6,554 +/- 233
sum:	31,875	31,272	31,144	30,396	32,271	29,956
MB	31,487 +/- 215	30,714 +/- 274	30,351 +/- 279	29,975 +/- 327	31,817 +/- 217	29,399 +/- 279
sum/MB % diff:	1.22%	1.80%	2.56%	1.39%	1.42%	
sum CaseA/Case FGH % diff		1.89%				
Case A/Case FGH MB % diff:		2.45%				
sum Case A/ prelim % diff:		6.21%				
Run15pp	SOUTH					
rap center	Case A	Ave Case FGH	Case F	Case G	Case H	AN 1354
-1.325	3,151 +/- 66	3,085	2,934 +/- 103	3,147 +/- 65	3,174 +/- 65	2,907 +/- 125
-1.575	12,079 +/- 132	12,033	11,696 +/- 143	12,196 +/- 193	12,206 +/- 129	11,341 +/- 203
-1.825	10,645 +/- 124	10,757	10,604 +/- 120	10,824 +/- 94	10,842 +/- 118	10,918 +/- 192
-2.075	2,978 +/- 63	3,113	3,138 +/- 64	3,095 +/- 64	3,105 +/- 66	3,017 +/- 87
sum:	28,853	28,988	28,372	29,262	29,327	28,183
MB	28,511 +/- 205	28,689 +/- 195	28,145 +/- 229	28,942 +/- 153	28,981 +/- 202	28,207 +/- 282
sum/MB % diff	1.19%	1.04%	0.80%	1.10%	1.34%	
sum Case A/Case FGH % diff		-0.47%				
Case A/Case FGH MB % diff:		-0.62%				
sum Case A/ prelim % diff:		2.35%				

Figure 37: Run15pp forward and backward rapidity check. Case A is consistent with Case FGH, and Case A as the central value is consistent with rapidity integrated results.

## 8 Run15pAu Checks on $J/\psi$ Counts

The same checks were performed on Run15pAu as Run15pp, in addition to several more needed to confirm centrality results.

### 8.1 Sum Over $p_T$

pt [GeV/c]	pAu North	pAu South
0.125	421 +/-24	218 +/- 19
0.375	1074 +/-43	723 +/- 33
0.625	1393 +/-47	841 +/- 40
0.875	1818 +/-56	1196 +/- 46
1.125	1873 +/-51	1439 +/- 46
1.375	1775 +/-51	1118 +/- 45
1.625	1732 +/-78	1195 +/- 68
1.875	1433 +/-49	928 +/- 40
2.125	1270 +/-37	819 +/- 37
2.375	1053 +/-36	663 +/- 31
2.625	875 +/-36	551 +/- 28
2.875	769 +/-45	464 +/- 26
3.125	646 +/-30	357 +/- 22
3.375	566 +/-28	304 +/- 21
3.625	389 +/-22	245 +/- 18
3.875	310 +/-20	179 +/- 16
4.125	252 +/-18	142 +/- 10
4.375	168 +/-14	125 +/- 13
4.625	161 +/-15	82 +/- 11
4.875	144 +/-13	61 +/- 9
5.125	107 +/-11	41 +/- 7
5.375	86 +/-10	36 +/- 7
5.625	68 +/-9	28 +/- 6
5.875	57 +/-8	17 +/- 5
6.25	55 +/-8	19 +/- 5
6.75	41 +/-8	18 +/- 5
SUM	18535	11810
Min Bias	18328 +/- 175	11661 +/- 152
% diff	1.12%	1.65%
AN1354	18194 +/- 224	11602 +/- 193

Figure 38: Centrality Integrated Results for Run15pAu.

### 8.2 Sum Over Rapidity

We refit the preliminary results for  $J/\psi$  vs. rapidity (AN1354) to ensure results were consistent despite different analysis methods used. The results are compared with Case FGH counts as well.

### 8.3 Sum Over Centrality

We checked if the sum of Case A  $p_T$  counts over each centrality bin is consistent with the sum of the average of Cases F, G and H. We also checked if the resulting sum is consistent with the  $p_T$  integrated fit value for each centrality range.

Run15pAu	NORTH					
rap center	Case A	Ave FGH	Case F	Case G	Case H	AN 1354
1.325	1393 +/- 43	1346 +/- 51	1347 +/- 49	1350 +/- 53	1342 +/- 51	1334 +/- 60
1.575	6635 +/- 100	6436 +/- 123	6622 +/- 101	6335 +/- 136	6350 +/- 131	6464 +/- 128
1.825	6736 +/- 107	6651 +/- 126	6736 +/- 107	6603 +/- 140	6614 +/- 131	6822 +/- 136
2.075	3674 +/- 83	3860 +/- 108	3870 +/- 93	3853 +/- 113	3858 +/- 117	3793 +/- 99
sum:	18438	18,293	18,379	18,141	18,164	18,413
MB	18328 +/- 175	18112 +/- 248	18197 +/- 236	18118 +/- 244	18021 +/- 263	18194 +/- 224
sum/MB % diff:	0.60%	0.99%	1.00%	0.13%	2.15%	
sum CaseA/Case FGH % diff		0.79%				
Case A/Case FGH MB % diff:		1.19%				
sum Case A/ prelim % diff:		0.73%				
Run15pAu	SOUTH					
rap center	Case A	Ave Case FGH	Case F	Case G	Case H	AN 1354
-1.325	1579 +/- 52	1570 +/- 56	1571 +/- 53	1568 +/- 60	1572 +/- 55	1521 +/- 57
-1.575	5297 +/- 100	5076 +/- 126	5124 +/- 107	4969 +/- 144	5136 +/- 127	4910 +/- 155
-1.825	3887 +/- 78	3895 +/- 91	3916 +/- 90	3886 +/- 115	3884 +/- 68	4138 +/- 80
-2.075	913 +/- 40	968 +/- 44	950 +/- 52	979 +/- 40	976 +/- 39	973 +/- 39
sum:	11676	11,509	11561	11,402	11,568	12,595
MB	11661 +/- 152	11622 +/- 155	11667 +/- 136	11637 +/- 143	11561 +/- 185	11602 +/- 193
sum/MB % diff	0.13%	-0.98%	-0.91%	-2.04%	0.06%	
sum Case A/Case FGH % diff		1.44%				
Case A/Case FGH MB % diff:		0.34%				
sum Case A/ prelim % diff:		0.51%				

Figure 39: Run15pAu rapidity checks. Top: Forward rapidity. Case A is consistent with Case FGH, and Case A as the central value is consistent with rapidity integrated results in both directions.

centrality 0-20			Run15pAu North Arm				
pt [GeV/c]	Case A	Case FGH	Case F	Case G	Case H		
0.125	139 +/- 15	147 +/- 14	150 +/- 13	139 +/- 14	150 +/- 14		
0.375	345 +/- 26	346 +/- 24	357 +/- 23	344 +/- 23	337 +/- 25		
0.625	461 +/- 31	483 +/- 25	481 +/- 26	484 +/- 25	484 +/- 25		
0.875	577 +/- 35	560 +/- 36	560 +/- 32	561 +/- 39	558 +/- 37		
1.125	655 +/- 31	679 +/- 31	694 +/- 30	-	664 +/- 31		
1.375	595 +/- 32	593 +/- 40	590 +/- 32	591 +/- 44	599 +/- 43		
1.625	555 +/- 30	569 +/- 36	568 +/- 34	573 +/- 39	567 +/- 35		
1.875	506 +/- 29	499 +/- 33	491 +/- 30	500 +/- 29	506 +/- 40		
2.125	432 +/- 25	429 +/- 27	429 +/- 27	425 +/- 30	434 +/- 24		
2.375	337 +/- 23	325 +/- 26	336 +/- 29	310 +/- 24	329 +/- 24		
2.625	300 +/- 21	288 +/- 21	297 +/- 21	275 +/- 22	291 +/- 21		
2.875	276 +/- 21	277 +/- 20	276 +/- 20	280 +/- 20	275 +/- 20		
3.125	220 +/- 18	220 +/- 18	226 +/- 18	221 +/- 17	213 +/- 19		
3.375	209 +/- 16	211 +/- 17	210 +/- 17	206 +/- 17	216 +/- 16		
3.625	133 +/- 13	132 +/- 12	132 +/- 13	131 +/- 10	132 +/- 13		
3.875	117 +/- 12	118 +/- 13	118 +/- 13	120 +/- 12	117 +/- 13		
4.25	143 +/- 14	127 +/- 13	131 +/- 12	124 +/- 14	125 +/- 14		
4.75	120 +/- 12	122 +/- 12	122 +/- 12	-	121 +/- 13		
6	145 +/- 13	148 +/- 15	148 +/- 16	-	149 +/- 13		
sum	6263	6273					
pt int:	6185 +/- 104						
Case A sum/Case A pt int % diff:			1.25%				
Case A sum/Case FGH sum % diff:			-0.16%				

centrality 0-20			Run15pAu South Arm				
pt [GeV/c]	Case A	Case FGH	Case F	Case G	Case H		
0.125	87 +/- 12	88 +/- 12	83 +/- 11	83 +/- 12	98 +/- 12		
0.375	300 +/- 24	321 +/- 21	307 +/- 22	315 +/- 21	340 +/- 18		
0.625	360 +/- 24	394 +/- 35	389 +/- 31	397 +/- 51	397 +/- 25		
0.875	482 +/- 33	456 +/- 36	460 +/- 36	394 +/- 42	515 +/- 30		
1.125	617 +/- 27	617 +/- 36	632 +/- 30	617 +/- 33	603 +/- 46		
1.375	466 +/- 29	501 +/- 32	502 +/- 31	499 +/- 35	500 +/- 32		
1.625	516 +/- 32	518 +/- 42	518 +/- 42	519 +/- 42	518 +/- 42		
1.875	406 +/- 25	426 +/- 25	426 +/- 25	427 +/- 25	427 +/- 25		
2.125	374 +/- 31	363 +/- 26	365 +/- 25	358 +/- 26	365 +/- 27		
2.375	292 +/- 21	303 +/- 20	308 +/- 20	301 +/- 18	301 +/- 23		
2.625	254 +/- 20	259 +/- 20	256 +/- 19	260 +/- 19	260 +/- 23		
2.875	181 +/- 17	172 +/- 18	180 +/- 17	157 +/- 18	179 +/- 17		
3.125	157 +/- 16	148 +/- 16	149 +/- 16	141 +/- 17	153 +/- 15		
3.375	123 +/- 14	121 +/- 14	122 +/- 14	118 +/- 13	122 +/- 14		
3.625	117 +/- 13	119 +/- 13	118 +/- 13	119 +/- 13	119 +/- 13		
3.875	75 +/- 11	74 +/- 11	-	73 +/- 11	74 +/- 10		
4.25	106 +/- 11	104 +/- 12	103 +/- 12	106 +/- 12	-		
4.75	69 +/- 9	65 +/- 9	61 +/- 8	68 +/- 9	61 +/- 9		
6	72 +/- 9	66 +/- 10	71 +/- 9	62 +/- 11	74 +/- 10		
sum	5054	5115					
pt int:	4968 +/- 91						
Case A sum/Case A pt int % diff:			1.72%				
Case A sum/Case FGH sum % diff:			-1.20%				



centrality 20-40			Run15pAu North Arm			
pt [GeV/c]	Case A	Case FGH	Case F	Case G	Case H	
0.125	100 +/- 12	105 +/- 11	105 +/- 11	105 +/- 10	105 +/- 12	
0.375	294 +/- 23	309 +/- 22	313 +/- 21	307 +/- 22	307 +/- 24	
0.625	377 +/- 24	401 +/- 26	399 +/- 28	401 +/- 25	402 +/- 24	
0.875	491 +/- 36	439 +/- 35	435 +/- 29	437 +/- 36	444 +/- 39	
1.125	556 +/- 28	563 +/- 27	588 +/- 27	521 +/- 26	579 +/- 27	
1.375	517 +/- 27	516 +/- 28	523 +/- 27	511 +/- 28	513 +/- 31	
1.625	505 +/- 27	513 +/- 32	521 +/- 32	513 +/- 27	505 +/- 37	
1.875	429 +/- 25	425 +/- 30	423 +/- 30	425 +/- 34	428 +/- 25	
2.125	363 +/- 22	364 +/- 21	366 +/- 21	363 +/- 21	363 +/- 21	
2.375	318 +/- 20	309 +/- 21	320 +/- 19	294 +/- 22	314 +/- 21	
2.625	254 +/- 17	251 +/- 18	254 +/- 19	256 +/- 18	242 +/- 18	
2.875	212 +/- 17	210 +/- 18	211 +/- 18	216 +/- 17	204 +/- 18	
3.125	178 +/- 14	177 +/- 15	179 +/- 15	172 +/- 15	178 +/- 15	
3.375	135 +/- 13	130 +/- 14	135 +/- 12	123 +/- 14	133 +/- 14	
3.625	114 +/- 12	115 +/- 12	125 +/- 11	114 +/- 12	107 +/- 12	
3.875	90 +/- 10	91 +/- 10	91 +/- 10	91 +/- 10	91 +/- 11	
4.25	134 +/- 14	134 +/- 13	134 +/- 13	134 +/- 13	134 +/- 13	
4.75	68 +/- 10	67 +/- 10	68 +/- 10	66 +/- 10	69 +/- 9	
6	121 +/- 12	114 +/- 13	115 +/- 14	114 +/- 13	122 +/- 11	
sum	5256	5233				
pt int:	5174 +/- 90					
Case A sum/Case A pt Int % diff:			1.57%			
Case A sum/Case FGH sum % diff:			-0.44%			

centrality 20-40			Run15pAu South Arm			
pt [GeV/c]	Case A	Case FGH	Case F	Case G	Case H	
0.125	62 +/- 9	63 +/- 9	64 +/- 8	61 +/- 9	64 +/- 9	
0.375	198 +/- 16	209 +/- 17	210 +/- 17	209 +/- 17	209 +/- 17	
0.625	227 +/- 19	212 +/- 25	207 +/- 21	213 +/- 25	214 +/- 30	
0.875	330 +/- 18	344 +/- 26	345 +/- 25	343 +/- 27	343 +/- 28	
1.125	413 +/- 23	391 +/- 25	321 +/- 24	436 +/- 23	416 +/- 27	
1.375	309 +/- 24	298 +/- 30	280 +/- 23	303 +/- 41	311 +/- 25	
1.625	321 +/- 24	319 +/- 23	323 +/- 22	306 +/- 26	327 +/- 22	
1.875	225 +/- 20	226 +/- 17	233 +/- 18	220 +/- 15	226 +/- 18	
2.125	213 +/- 18	220 +/- 19	220 +/- 18	220 +/- 17	220 +/- 21	
2.375	155 +/- 16	156 +/- 16	155 +/- 16	157 +/- 16	155 +/- 16	
2.625	146 +/- 17	142 +/- 15	145 +/- 15	140 +/- 16	141 +/- 15	
2.875	126 +/- 15	127 +/- 13	126 +/- 13	127 +/- 14	127 +/- 13	
3.125	108 +/- 12	108 +/- 12	107 +/- 12	109 +/- 12	107 +/- 11	
3.375	100 +/- 11	99 +/- 11	99 +/- 11	100 +/- 11	100 +/- 11	
3.625	64 +/- 10	65 +/- 10	65 +/- 10	66 +/- 11	64 +/- 9	
3.875	44 +/- 8	45 +/- 8	46 +/- 8	45 +/- 8	44 +/- 8	
4.25	90 +/- 10	87 +/- 11	84 +/- 11	-	90 +/- 10	
4.75	48 +/- 8	47 +/- 8	46 +/- 8	48 +/- 8	40 +/- 10	
6	50 +/- 7	49 +/- 8	49 +/- 7	49 +/- 8	50 +/- 7	
sum	3228	3207				
pt int:	3208 +/- 111					
Case A sum/Case A pt Int % diff:			0.62%			
Case A sum/Case FGH sum % diff:			0.65%			

centrality 40-60			Run15pAu North Arm			
pt [GeV/c]	Case A	Case FGH	Case F	Case G	Case H	
0.125	96 +/- 10	99 +/- 11	99 +/- 11	99 +/- 11	98 +/- 11	
0.375	254 +/- 19	260 +/- 18	260 +/- 18	260 +/- 18	260 +/- 18	
0.625	286 +/- 23	287 +/- 28	294 +/- 24	289 +/- 27	278 +/- 34	
0.875	406 +/- 27	424 +/- 25	417 +/- 27	426 +/- 24	428 +/- 24	
1.125	407 +/- 23	408 +/- 27	452 +/- 23	-	364 +/- 30	
1.375	407 +/- 25	435 +/- 24	435 +/- 23	435 +/- 23	436 +/- 24	
1.625	414 +/- 24	407 +/- 24	406 +/- 26	406 +/- 22	410 +/- 23	
1.875	267 +/- 21	252 +/- 20	289 +/- 20	209 +/- 22	258 +/- 19	
2.125	264 +/- 17	274 +/- 19	273 +/- 19	274 +/- 18	274 +/- 19	
2.375	210 +/- 17	203 +/- 16	199 +/- 16	202 +/- 16	209 +/- 17	
2.625	178 +/- 14	181 +/- 16	188 +/- 14	180 +/- 17	176 +/- 15	
2.875	166 +/- 14	170 +/- 14	170 +/- 14	170 +/- 15	170 +/- 15	
3.125	140 +/- 13	142 +/- 13	145 +/- 13	144 +/- 14	138 +/- 12	
3.375	101 +/- 11	103 +/- 11	103 +/- 11	103 +/- 11	103 +/- 11	
3.625	104 +/- 11	103 +/- 11	103 +/- 11	104 +/- 11	102 +/- 12	
3.875	62 +/- 8	62 +/- 9	62 +/- 9	62 +/- 9	62 +/- 9	
4.25	86 +/- 10	87 +/- 10	86 +/- 11	87 +/- 10	87 +/- 10	
4.75	71 +/- 10	78 +/- 10	84 +/- 10	-	72 +/- 10	
6	77 +/- 10	79 +/- 10	79 +/- 10	-	79 +/- 10	
sum	3998	4054				
pt int:	3968 +/- 80					
Case A sum/Case A pt Int % diff:			0.75%			
Case A sum/Case FGH sum % diff:			-1.37%			

centrality 40-60			Run15pAu South Arm			
pt [GeV/c]	Case A	Case FGH	Case F	Case G	Case H	
0.125	47 +/- 11	52 +/- 9	50 +/- 9	49 +/- 8	57 +/- 10	
0.375	136 +/- 15	129 +/- 15	128 +/- 14	131 +/- 14	129 +/- 15	
0.625	144 +/- 17	176 +/- 15	169 +/- 15	180 +/- 15	180 +/- 15	
0.875	208 +/- 19	199 +/- 18	206 +/- 15	195 +/- 20	195 +/- 19	
1.125	280 +/- 18	263 +/- 22	293 +/- 18	231 +/- 25	265 +/- 22	
1.375	214 +/- 21	229 +/- 18	-	227 +/- 18	231 +/- 18	
1.625	224 +/- 22	225 +/- 17	223 +/- 17	225 +/- 17	225 +/- 18	
1.875	179 +/- 16	176 +/- 16	180 +/- 16	170 +/- 16	179 +/- 15	
2.125	155 +/- 15	155 +/- 15	160 +/- 13	148 +/- 16	156 +/- 15	
2.375	124 +/- 13	127 +/- 12	129 +/- 13	126 +/- 12	125 +/- 12	
2.625	99 +/- 10	99 +/- 11	100 +/- 11	99 +/- 11	99 +/- 10	
2.875	81 +/- 11	83 +/- 11	88 +/- 11	77 +/- 11	84 +/- 11	
3.125	52 +/- 8	53 +/- 8	53 +/- 8	53 +/- 9	53 +/- 8	
3.375	53 +/- 8	53 +/- 8	52 +/- 8	53 +/- 8	53 +/- 8	
3.625	32 +/- 6	35 +/- 7	34 +/- 7	36 +/- 7	35 +/- 7	
3.875	37 +/- 7	37 +/- 6	38 +/- 6	38 +/- 6	37 +/- 7	
4.25	42 +/- 7	43 +/- 7	42 +/- 8	-	43 +/- 7	
4.75	22 +/- 5	23 +/- 5	23 +/- 5	22 +/- 5	23 +/- 5	
6	26 +/- 7	26 +/- 8	26 +/- 8	26 +/- 8	26 +/- 8	
sum	2155	2183				
pt int:	2128 +/- 75					
Case A sum/Case A pt Int % diff:			2.19%			
Case A sum/Case FGH sum % diff:			-1.29%			

centrality 60-84			Run15pAu North Arm			
pt [GeV/c]	Case A	Case FGH	Case F	Case G	Case H	
0.125	81 +/- 10	85 +/- 10	84 +/- 10	85 +/- 10	87 +/- 9	
0.375	197 +/- 17	198 +/- 17	198 +/- 18	198 +/- 17	198 +/- 17	
0.625	287 +/- 20	298 +/- 21	292 +/- 20	301 +/- 20	301 +/- 22	
0.875	352 +/- 24	350 +/- 25	352 +/- 26	351 +/- 23	348 +/- 28	
1.125	295 +/- 21	304 +/- 18	302 +/- 16	313 +/- 19	298 +/- 20	
1.375	303 +/- 22	290 +/- 23	285 +/- 22	311 +/- 20	275 +/- 27	
1.625	268 +/- 21	271 +/- 19	261 +/- 17	286 +/- 17	265 +/- 21	
1.875	233 +/- 17	234 +/- 17	233 +/- 17	234 +/- 17	234 +/- 17	
2.125	198 +/- 16	198 +/- 16	198 +/- 16	198 +/- 16	198 +/- 16	
2.375	183 +/- 16	183 +/- 15	183 +/- 15	183 +/- 15	183 +/- 15	
2.625	145 +/- 14	149 +/- 14	149 +/- 14	149 +/- 14	149 +/- 14	
2.875	115 +/- 12	115 +/- 13	115 +/- 13	115 +/- 13	115 +/- 12	
3.125	107 +/- 12	103 +/- 13	101 +/- 14	105 +/- 12	103 +/- 14	
3.375	108 +/- 12	109 +/- 12	108 +/- 14	110 +/- 11	110 +/- 11	
3.625	47 +/- 7	40 +/- 7	41 +/- 7	40 +/- 7	40 +/- 7	
3.875	37 +/- 7	38 +/- 7	38 +/- 7	38 +/- 7	38 +/- 7	
4.25	63 +/- 9	64 +/- 9	64 +/- 9	64 +/- 9	64 +/- 9	
4.75	44 +/- 8	45 +/- 8	46 +/- 8	-	45 +/- 8	
6	57 +/- 9	53 +/- 8	53 +/- 9	54 +/- 8	56 +/- 8	
sum	3118	3130				
pt int:	3039 +/- 69					
Case A sum/Case A pt Int % diff:			2.57%			
Case A sum/Case FGH sum % diff:			-0.38%			

centrality 60-84			Run15pAu South Arm			
pt [GeV/c]	Case A	Case FGH	Case F	Case G	Case H	
0.125	30 +/- 7	31 +/- 7	32 +/- 7	31 +/- 8	31 +/- 7	
0.375	102 +/- 14	99 +/- 13	100 +/- 13	99 +/- 12	97 +/- 14	
0.625	120 +/- 15	121 +/- 12	121 +/- 12	121 +/- 12	121 +/- 12	
0.875	159 +/- 14	169 +/- 15	163 +/- 15	171 +/- 14	171 +/- 14	
1.125	134 +/- 13	135 +/- 14	136 +/- 17	136 +/- 13	135 +/- 13	
1.375	130 +/- 14	140 +/- 14	139 +/- 14	141 +/- 14	141 +/- 14	
1.625	142 +/- 14	143 +/- 14	143 +/- 14	143 +/- 15	143 +/- 14	
1.875	109 +/- 11	111 +/- 11	111 +/- 9	112 +/- 12	111 +/- 12	
2.125	96 +/- 12	92 +/- 11	95 +/- 11	88 +/- 11	94 +/- 11	
2.375	82 +/- 10	84 +/- 10	84 +/- 10	84 +/- 10	84 +/- 10	
2.625	63 +/- 9	64 +/- 9	64 +/- 9	64 +/- 9	64 +/- 8	
2.875	60 +/- 8	59 +/- 9	60 +/- 10	59 +/- 9	59 +/- 9	
3.125	44 +/- 7	44 +/- 7	43 +/- 6	44 +/- 7	44 +/- 7	
3.375	28 +/- 6	26 +/- 6	26 +/- 6	25 +/- 6	27 +/- 6	
3.625	29 +/- 6	29 +/- 6	29 +/- 6	-	30 +/- 6	
3.875	22 +/- 5	23 +/- 5	-	22 +/- 5	23 +/- 5	
4.25	28 +/- 6	28 +/- 6	28 +/- 6	28 +/- 6	29 +/- 6	
4.75	20 +/- 4	20 +/- 4	20 +/- 4	20 +/- 4	-	
6	18 +/- 4	13 +/- 4	14 +/- 4	-	12 +/- 4	
sum	1416	1432				
pt int:	1386 +/- 43					
Case A sum/Case A pt Int % diff:			2.14%			
Case A sum/Case FGH sum % diff:			1.12%			

## 8.4 $\sigma$ vs $p_T$

During an fvtx meeting, it was requested by Xuan Li to plot the width of the  $J/\psi$  peak versus  $p_T$  as an additional check on the Run15pAu centrality, because the peak looked narrow at low  $p_T$ . The plots for each centrality range in both the north and south arms as well as the  $p_T$  integrated widths as a function of centrality are shown in 40 and 41.

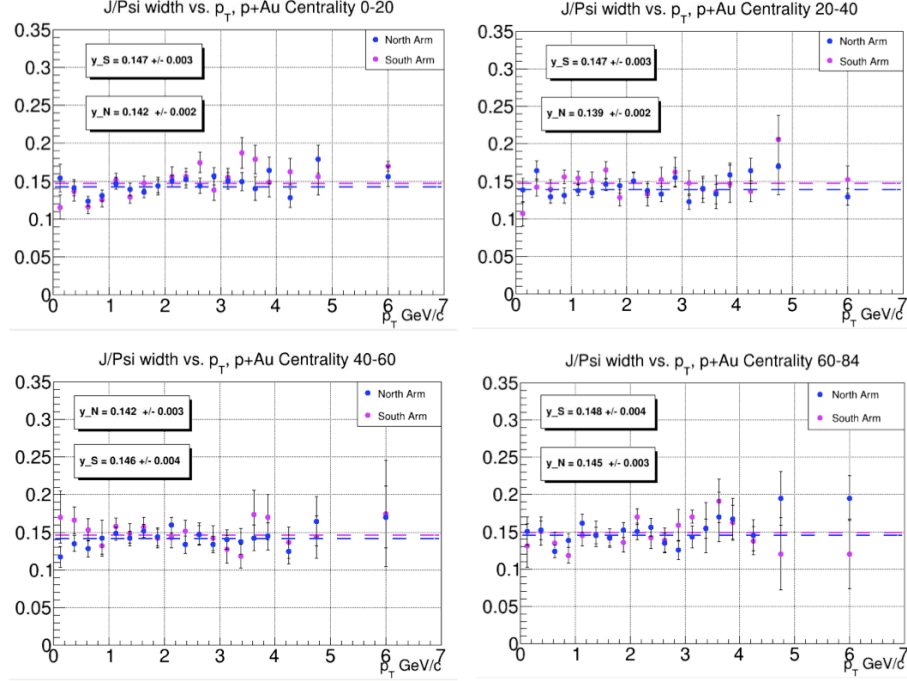


Figure 40: Run15pAu  $J/\psi$  width check as a function of  $p_T$  and centrality. The muon arms consistently measures approximately 140 MeV for  $\sigma$ .

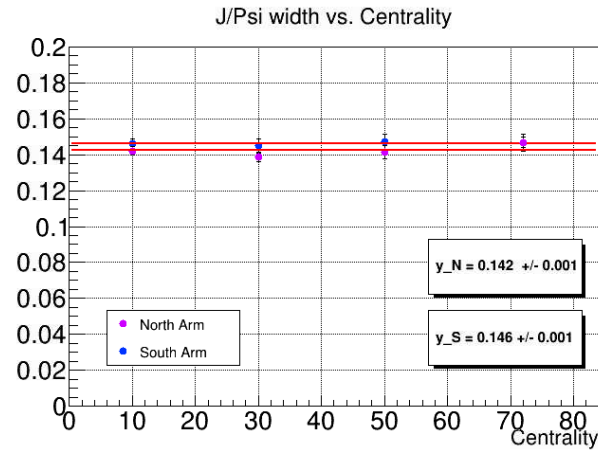


Figure 41: Run15pAu North and South arms  $p_T$  integrated width as function of centrality.

## 9 Run15pAl Checks on $J/\psi$ Counts

All of the same checks used for Run15pAu were used for Run15pAl.

### 9.1 Sum over $p_T$

pt [GeV/c]	pAl North	pAl South
0.125	258 +/- 22	164 +/- 19
0.375	831 +/- 38	523 +/- 31
0.625	1056 +/- 43	750 +/- 40
0.875	1251 +/- 45	818 +/- 38
1.125	1231 +/- 45	801 +/- 37
1.375	1208 +/- 42	882 +/- 36
1.625	1050 +/- 40	736 +/- 35
1.875	934 +/- 38	560 +/- 30
2.125	783 +/- 32	491 +/- 28
2.375	597 +/- 29	367 +/- 26
2.625	501 +/- 28	317 +/- 24
2.875	466 +/- 28	266 +/- 22
3.125	392 +/- 23	227 +/- 18
3.375	284 +/- 20	161 +/- 15
3.625	240 +/- 18	117 +/- 12
3.875	146 +/- 14	88 +/- 11
4.25	226 +/- 17	102 +/- 13
4.75	137 +/- 14	51 +/- 8
5.5	139 +/- 13	67 +/- 9
6.5	50 +/- 8	11 +/- 4
SUM	11780	7500
Min Bias	11738 +/- 138	7455 +/- 115
% diff	0.36%	0.60%
AN1354	11085 +/- 190	6567 +/- 206

Figure 42: Centrality Integrated Results for Run15pAl.

### 9.2 Sum over Rapidity

We refit the preliminary results for  $J/\psi$  vs. rapidity (AN1354) to ensure results were consistent despite different analysis methods used. The results are compared with Case FGH counts as well.

### 9.3 Sum over Centrality

We checked if the sum of Case A  $p_T$  counts over each centrality bin is consistent with the sum of the average of Cases F, G and H. We also checked if the resulting sum is consistent with the  $p_T$  integrated fit value for each centrality range.

### 9.4 $\sigma$ vs. $p_T$

During an fvtx meeting, it was requested by Xuan Li to plot the width of the  $J/\psi$  peak versus  $p_T$  as an additional check on the Run15pAu centrality, because the peak looked narrow at low  $p_T$ . We continue the same check here with Run15pAl.

Run15pAl	NORTH					
rap center	Case A	Ave FGH	Case F	Case G	Case H	AN 1354
1.325	853 +/- 33	825	813 +/- 43	822 +/- 41	841 +/- 32	843 +/- 47
1.575	4004 +/- 77	3893	3844 +/- 78	3811 +/- 113	4023 +/- 76	3785 +/- 95
1.825	4406 +/- 84	4309	4297 +/- 103	4149 +/- 153	4482 +/- 84	4125 +/- 121
2.075	2615 +/- 66	2646	2691 +/- 70	2506 +/- 73	2742 +/- 65	2539 +/- 87
sum:	11878	11,673	11,645	11,288	12,088	11,292
MB	11738 +/- 138	11502 +/- 168	11354 +/- 165	11281 +/- 205	11872 +/- 135	11085 +/- 190
sum/MB % diff:	1.19%	1.48%	2.51%	0.06%	1.80%	
sum CaseA/Case FGH % diff		1.73%				
Case A/Case FGH MB % diff:		2.03%				
sum Case A/ prelim % diff:		5.72%				
Run15pAl	SOUTH					
rap center	Case A	Ave Case FGH	Case F	Case G	Case H	AN 1354
-1.325	907 +/- 36	885	842 +/- 48	906 +/- 34	906 +/- 35	682 +/- 54
-1.575	3288 +/- 72	3,277	3233 +/- 74	3299 +/- 80	3300 +/- 70	2920 +/- 234
-1.825	2497 +/- 65	2,584	2543 +/- 68	2576 +/- 53	2632 +/- 49	2364 +/- 107
-2.075	766 +/- 42	792	768 +/- 41	795 +/- 32	814 +/- 38	601 +/- 47
sum:	7458	7,538	7386	7,576	7,652	6,567
MB	7455 +/- 115	7458 +/- 111	7212 +/- 114	7544 +/- 111	7617 +/- 108	6567 +/- 206
sum/MB % diff	0.04%	1.07%	2.38%	0.42%	0.46%	
sum Case A/Case FGH % diff		1.07%				
Case A/Case FGH MB % diff:		0.04%				
sum Case A/ prelim % diff:		12.70%				

Figure 43: Run15pAl forward and backward rapidity check. Case A is consistent with Case FGH, and Case A as the central value is consistent with rapidity integrated results.

## 10 Run14HeAu Checks on $J/\psi$ Counts

All of the same checks used for Run15pAu were used for Run14HeAu.

### 10.1 Sum over $p_T$

pt [GeV/c]	HeAu North	HeAu South
0.125	78 +/- 11	68 +/- 11
0.375	196 +/- 17	241 +/- 20
0.625	323 +/- 21	273 +/- 22
0.875	347 +/- 25	433 +/- 48
1.125	406 +/- 25	501 +/- 27
1.375	381 +/- 22	447 +/- 23
1.625	364 +/- 24	391 +/- 24
1.875	322 +/- 21	366 +/- 24
2.125	250 +/- 20	265 +/- 19
2.375	193 +/- 17	239 +/- 18
2.625	214 +/- 17	238 +/- 18
2.875	135 +/- 15	151 +/- 16
3.125	128 +/- 12	113 +/- 12
3.375	89 +/- 13	93 +/- 11
3.625	85 +/- 11	89 +/- 13
3.875	55 +/- 8	59 +/- 9
4.25	86 +/- 12	73 +/- 10
4.75	60 +/- 8	45 +/- 8
6	56 +/- 9	52 +/- 9
SUM	3769	4138
Min Bias	3804 +/- 88	4069 +/- 103
% diff	0.92%	1.68%
AN1354	3825 +/- 91	3987 +/- 118

Figure 44: Centrality Integrated Results for Run14HeAu.

### 10.2 Sum over Rapidity

We refit the preliminary results for  $J/\psi$  vs. rapidity (AN1354) to ensure results were consistent despite different analysis methods used. The results are compared with Case FGH counts as well.

### 10.3 Sum over Centrality

As with the other systems, we checked if the sum of Case A  $p_T$  counts over each centrality bin is consistent with the sum of the average of Cases F, G and H. We also checked if the resulting sum is consistent with the  $p_T$  integrated fit value for each centrality range.

### 10.4 $\sigma$ vs. $p_T$

During an fvtx meeting, it was requested by Xuan Li to plot the width of the  $J/\psi$  peak versus  $p_T$  as an additional check on the Run15pAu centrality, because the peak looked narrow at low  $p_T$ . We continued the same check here with Run14HeAu.

Run14HeAu	NORTH					
rap center	Case A	Ave FGH	Case F	Case G	Case H	AN 1354
1.325	325 +/- 21	316 +/- 34	317 +/- 40	315 +/- 39	317 +/- 22	334 +/- 21
1.575	1346 +/- 49	1311 +/- 56	1303 +/- 49	1322 +/- 45	1309 +/- 75	1318 +/- 62
1.825	1503 +/- 54	1459 +/- 75	1437 +/- 51	1466 +/- 83	1475 +/- 90	1552 +/- 56
2.075	639 +/- 34	667 +/- 36	677 +/- 35	663 +/- 34	661 +/- 39	686 +/- 29
sum:	3812	3,753	3,734	3,766	3,762	3,890
MB	3804 +/- 88	3764 +/- 106	3741 +/- 80	3768 +/- 128	3783 +/- 111	3825 +/- 91
sum/MB % diff:	0.21%	0.29%	-0.19%	-0.05%	2.79%	
sum Case A/Case FGH % diff		1.56%				
Case A/Case FGH MB % diff:		1.06%				
sum Case A/ prelim % diff:		2.03%				

Run14HeAu	SOUTH					
rap center	Case A	Ave Case FGH	Case F	Case G	Case H	AN 1354
-1.325	505 +/- 31	514 +/- 29	512 +/- 29	515 +/- 29	515 +/- 29	508 +/- 28
-1.575	1684 +/- 64	1529 +/- 75	1560 +/- 67	1405 +/- 87	1622 +/- 72	1455 +/- 83
-1.825	1427 +/- 62	1447 +/- 86	1471 +/- 69	1427 +/- 68	1441 +/- 120	1454 +/- 71
-2.075	477 +/- 41	492 +/- 32	490 +/- 33	493 +/- 32	493 +/- 32	484 +/- 27
sum:	4093	3,982	4033	3,840	4,071	3,901
MB	4069 +/- 103	3912 +/- 163	3986 +/- 103	3852 +/- 271	3898 +/- 114	3987 +/- 118
sum/MB % diff	0.59%	1.77%	1.17%	-0.31%	2.08%	
sum Case A/Case FGH % diff		2.75%				
Case A/Case FGH MB % diff:		3.93%				
sum Case A/ prelim % diff:		5.23%				

Figure 45: Run14HeAu forward and backward rapidity check. Case A is consistent with Case FGH, and Case A as the central value is consistent with rapidity integrated results.

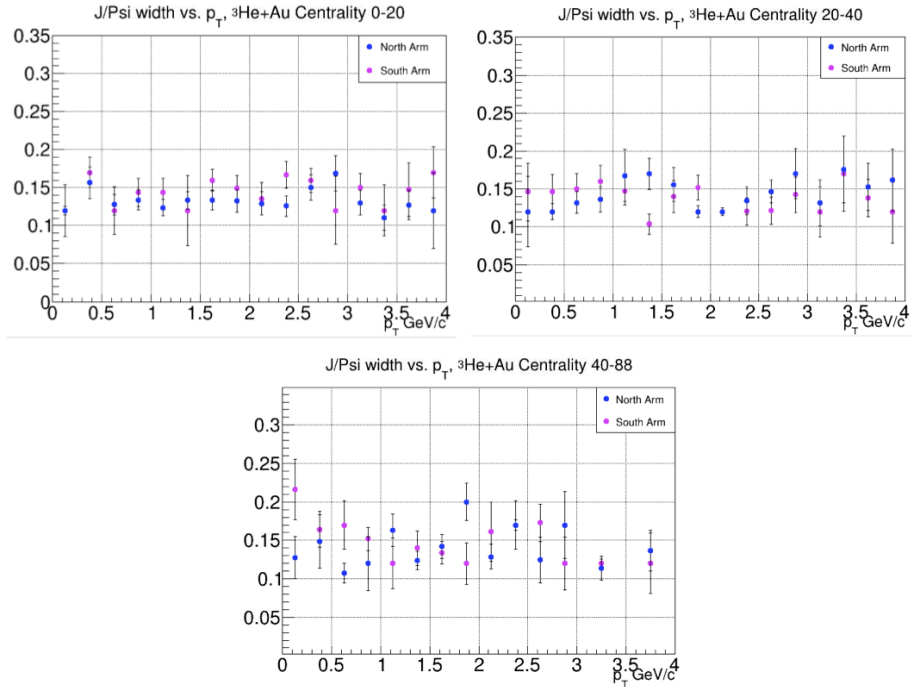
centrality 0-20			Run14HeAu North Arm				
pt [GeV/c]	Case A	Case FGH	Case F	Case G	Case H		
0.125	29 +/- 6	29 +/- 5	29 +/- 5	29 +/- 6	28 +/- 6		
0.375	78 +/- 10	82 +/- 11	82 +/- 11	81 +/- 11	81 +/- 12		
0.625	115 +/- 12	116 +/- 12	116 +/- 12	116 +/- 12	116 +/- 12		
0.875	136 +/- 13	133 +/- 16	133 +/- 20	133 +/- 14	133 +/- 14		
1.125	162 +/- 14	162 +/- 16	158 +/- 21	164 +/- 14	163 +/- 14		
1.375	148 +/- 14	150 +/- 13	150 +/- 13	150 +/- 13	150 +/- 13		
1.625	159 +/- 14	164 +/- 14	168 +/- 14	161 +/- 14	-		
1.875	119 +/- 13	114 +/- 18	115 +/- 13	114 +/- 17	114 +/- 22		
2.125	100 +/- 12	99 +/- 12	99 +/- 12	99 +/- 12	100 +/- 12		
2.375	82 +/- 10	82 +/- 10	82 +/- 10	82 +/- 10	82 +/- 10		
2.75	131 +/- 13	138 +/- 13	139 +/- 13	137 +/- 13	137 +/- 14		
3.25	105 +/- 11	105 +/- 11	104 +/- 11	105 +/- 11	105 +/- 11		
3.75	60 +/- 8	60 +/- 8	59 +/- 8	60 +/- 8	60 +/- 8		
sum	1424	1433					
pt int:							
Case A sum/Case A pt Int % diff:							
Case A sum/Case FGH sum % diff:							
Case A pt Int/Case FGH pt Int % diff:							

centrality 0-20			Run14HeAu South Arm			
pt [GeV/c]	Case A	Case FGH	Case F	Case G	Case H	
0.125	23 +/- 5	20 +/- 6	20 +/- 5	23 +/- 7	18 +/- 8	
0.375	105 +/- 14	105 +/- 15	109 +/- 13	100 +/- 18	106 +/- 14	
0.625	120 +/- 14	120 +/- 14	120 +/- 14	120 +/- 14	120 +/- 14	
0.875	198 +/- 19	185 +/- 19	188 +/- 20	173 +/- 20	194 +/- 18	
1.125	215 +/- 19	218 +/- 19	212 +/- 20	-	225 +/- 18	
1.375	184 +/- 16	185 +/- 17	190 +/- 16	184 +/- 17	181 +/- 18	
1.625	188 +/- 17	191 +/- 16	182 +/- 17	196 +/- 16	196 +/- 16	
1.875	184 +/- 16	173 +/- 24	184 +/- 23	166 +/- 28	169 +/- 20	
2.125	124 +/- 14	120 +/- 14	126 +/- 14	109 +/- 15	125 +/- 13	
2.375	126 +/- 13	117 +/- 14	105 +/- 16	120 +/- 14	126 +/- 13	
2.75	154 +/- 15	154 +/- 15	154 +/- 15	155 +/- 15	154 +/- 16	
3.25	90 +/- 10	88 +/- 11	-	87 +/- 11	89 +/- 11	
3.75	73 +/- 10	68 +/- 12	70 +/- 11	66 +/- 16	68 +/- 9	
sum	1783	1746				
pt int:						
Case A sum/Case A pt Int % diff:						
Case A sum/Case FGH sum % diff:						
Case A pt Int/Case FGH pt Int % diff:						

centrality 20-40						centrality 20-40					
Run14HeAu North Arm						Run14HeAu South Arm					
pt [GeV/c]	Case A	Case FGH	Case F	Case G	Case H	pt [GeV/c]	Case A	Case FGH	Case F	Case G	Case H
0.125	24 +/- 6	27 +/- 5	26 +/- 5	27 +/- 5	27 +/- 5	0.125	23 +/- 6	23 +/- 6	23 +/- 6	23 +/- 5	-
0.375	83 +/- 10	84 +/- 10	83 +/- 10	83 +/- 10	84 +/- 10	0.375	81 +/- 11	79 +/- 11	76 +/- 11	85 +/- 10	77 +/- 11
0.625	102 +/- 11	102 +/- 11	103 +/- 11	101 +/- 11	102 +/- 11	0.625	92 +/- 12	100 +/- 12	97 +/- 12	101 +/- 12	101 +/- 12
0.875	88 +/- 11	91 +/- 12	91 +/- 12	91 +/- 11	91 +/- 12	0.875	121 +/- 15	118 +/- 16	127 +/- 15	115 +/- 16	113 +/- 17
1.125	133 +/- 13	120 +/- 16	134 +/- 13	93 +/- 22	134 +/- 13	1.125	149 +/- 14	141 +/- 17	139 +/- 21	141 +/- 15	143 +/- 15
1.375	114 +/- 12	107 +/- 13	103 +/- 12	108 +/- 13	108 +/- 13	1.375	118 +/- 13	117 +/- 14	117 +/- 14	117 +/- 14	116 +/- 13
1.625	99 +/- 11	96 +/- 13	99 +/- 11	91 +/- 17	98 +/- 11	1.625	122 +/- 15	123 +/- 15	122 +/- 14	122 +/- 15	124 +/- 15
1.875	105 +/- 12	109 +/- 11	109 +/- 11	109 +/- 11	109 +/- 11	1.875	97 +/- 16	98 +/- 16	97 +/- 18	98 +/- 14	98 +/- 16
2.125	74 +/- 10	76 +/- 10	77 +/- 10	75 +/- 10	75 +/- 10	2.125	78 +/- 10	78 +/- 10	77 +/- 10	79 +/- 9	77 +/- 10
2.375	64 +/- 10	66 +/- 9	65 +/- 9	66 +/- 9	66 +/- 9	2.375	68 +/- 10	68 +/- 10	71 +/- 9	64 +/- 12	69 +/- 10
2.75	120 +/- 12	123 +/- 12	122 +/- 12	124 +/- 12	-	2.75	115 +/- 12	116 +/- 12	116 +/- 12	116 +/- 12	116 +/- 12
3.25	53 +/- 8	54 +/- 8	54 +/- 8	55 +/- 8	55 +/- 8	3.25	60 +/- 8	60 +/- 9	59 +/- 8	61 +/- 8	61 +/- 9
3.75	41 +/- 7	36 +/- 8	38 +/- 8	35 +/- 8	35 +/- 9	3.75	40 +/- 7	40 +/- 7	39 +/- 7	40 +/- 7	39 +/- 7
sum	1099	1091				sum	1165	1161			
pt int:						pt int:					
Case A sum/Case A pt Int % diff:						Case A sum/Case A pt Int % diff:					
Case A sum/Case FGH sum % diff:						Case A sum/Case FGH sum % diff:					
Case A pt Int/Case FGH pt Int % diff:						Case A pt Int/Case FGH pt Int % diff:					

centrality 40-88						centrality 40-88					
Run14HeAu North Arm						Run14HeAu South Arm					
pt [GeV/c]	Case A	Case FGH	Case F	Case G	Case H	pt [GeV/c]	Case A	Case FGH	Case F	Case G	Case H
0.125	30 +/- 5	32 +/- 3	-	29 +/- 5	-	0.125	19 +/- 5	20 +/- 5	20 +/- 5	19 +/- 5	22 +/- 5
0.375	53 +/- 8	46 +/- 9	49 +/- 9	44 +/- 9	44 +/- 9	0.375	58 +/- 9	53 +/- 10	52 +/- 9	50 +/- 11	56 +/- 9
0.625	83 +/- 10	86 +/- 11	85 +/- 10	86 +/- 12	86 +/- 11	0.625	72 +/- 10	65 +/- 11	64 +/- 11	61 +/- 12	68 +/- 11
0.875	85 +/- 10	86 +/- 10	85 +/- 9	87 +/- 10	87 +/- 10	0.875	70 +/- 9	73 +/- 9	73 +/- 9	73 +/- 10	73 +/- 9
1.125	87 +/- 11	76 +/- 12	71 +/- 11	77 +/- 12	79 +/- 13	1.125	70 +/- 9	69 +/- 9	67 +/- 9	71 +/- 9	-
1.375	101 +/- 11	102 +/- 11	102 +/- 11	101 +/- 11	102 +/- 11	1.375	87 +/- 11	88 +/- 11	92 +/- 10	87 +/- 11	87 +/- 12
1.625	96 +/- 10	96 +/- 11	96 +/- 11	95 +/- 11	96 +/- 11	1.625	94 +/- 12	100 +/- 11	100 +/- 11	100 +/- 11	100 +/- 11
1.875	79 +/- 10	82 +/- 10	80 +/- 11	82 +/- 10	82 +/- 10	1.875	44 +/- 8	44 +/- 8	43 +/- 7	44 +/- 8	44 +/- 8
2.125	73 +/- 9	72 +/- 11	72 +/- 9	71 +/- 11	71 +/- 12	2.125	48 +/- 8	48 +/- 7	48 +/- 7	48 +/- 7	48 +/- 7
2.375	37 +/- 9	37 +/- 10	-	46 +/- 7	-	2.375	39 +/- 6	40 +/- 7	40 +/- 7	40 +/- 7	-
2.75	63 +/- 9	70 +/- 10	71 +/- 9	70 +/- 9	70 +/- 10	2.75	80 +/- 10	74 +/- 11	73 +/- 11	-	75 +/- 11
3.25	34 +/- 6	34 +/- 6	-	34 +/- 6	34 +/- 6	3.25	31 +/- 6	32 +/- 6	31 +/- 6	32 +/- 6	32 +/- 6
3.75	31 +/- 6	31 +/- 6	31 +/- 7	32 +/- 6	32 +/- 6	3.75	29 +/- 5	29 +/- 6	29 +/- 5	-	29 +/- 6
sum	852	843				sum	741	734			
pt int:						pt int:					
Case A sum/Case A pt Int % diff:						Case A sum/Case A pt Int % diff:					
Case A sum/Case FGH sum % diff:						Case A sum/Case FGH sum % diff:					
Case A pt Int/Case FGH pt Int % diff:						Case A pt Int/Case FGH pt Int % diff:					





### 10.4.1 Fixing the $J/\psi$ Width

However, the widths were not as well defined for Run4HeAu as in Run15pAu, due to low statistics. Tony suggested to fix the  $J/\psi$  width to the average value of pAu for the corresponding centrality range. Sanghoon further suggested that the width of the  $J/\psi$  peak be fixed to the width of the HeAu minimum bias fit, if statistics were good enough. The statistics were quite good (see Figure 46), and so this method was implemented for all HeAu fits. This method carries a systematic uncertainty with it, which we will discuss in the Type B systematic uncertainty section.

### 10.4.2 Fixing the Center of the $J/\psi$ Peak

Sanghoon additionally suggested to fix the center of the  $J/\psi$  peak after seeing the results from fixing the width. This also carries with it a systematic uncertainty that we will discuss in the Type B systematic uncertainty section.

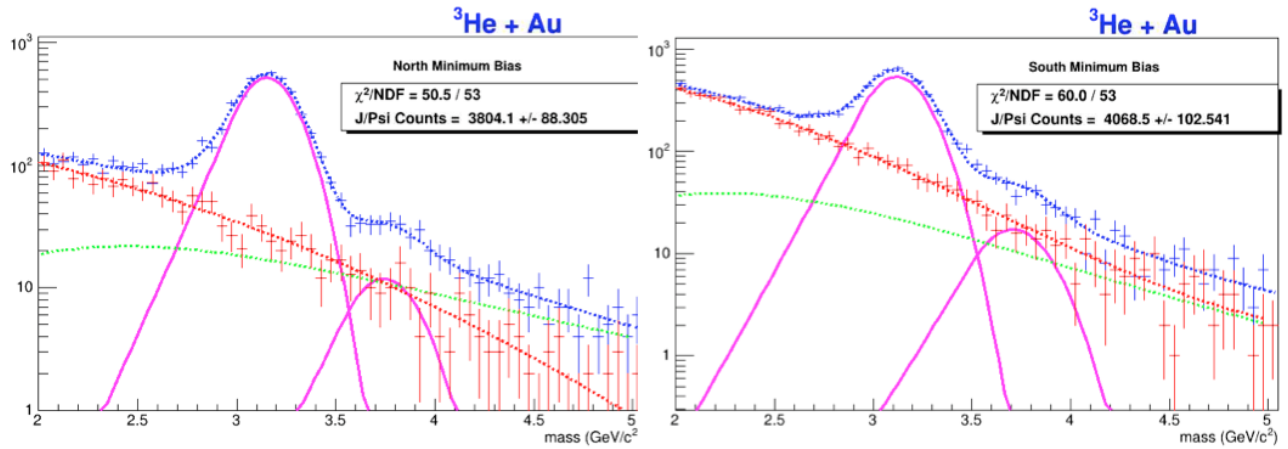


Figure 46: Run14HeAu Minimum Bias fits for the North, left, and South arm.

## 11 Bias Correction Factor

The bias correction factor is used in the nuclear modification factor for both centrality integrated and centrality dependent measurements. These factors were determined by James Nagle in the following three Analysis Notes: [AN 1207](#) (Run14HeAu), [AN 1265](#) (Run15pAu ) and [AN 1290](#) (Run15pAl). For additional information on how it is applied to the raw counts, see slides 23-28 in the following link: [bias correction factor c\(x\)](#)



## 12 Centralities

Initially we planned to analyze the Run15pAu data organized into 0-20, 20-40, 40-60 and 60-84% centrality bins, and all analysis prior to July 2019 showed these centrality ranges. However, in June 2019, Sanghoon completed a separate analysis on charged hadrons in p+Au and p+Al data, and the paper was released to the collaboration. Tony was interested in particular in Figure 10, which includes finer centrality binning for 0-20%.

Charged hadron paper: [PPG201](#)

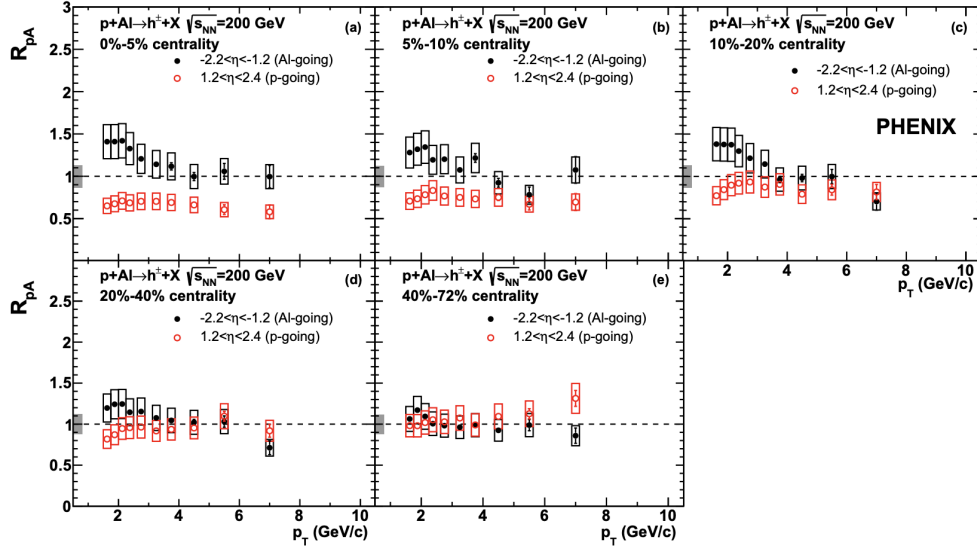
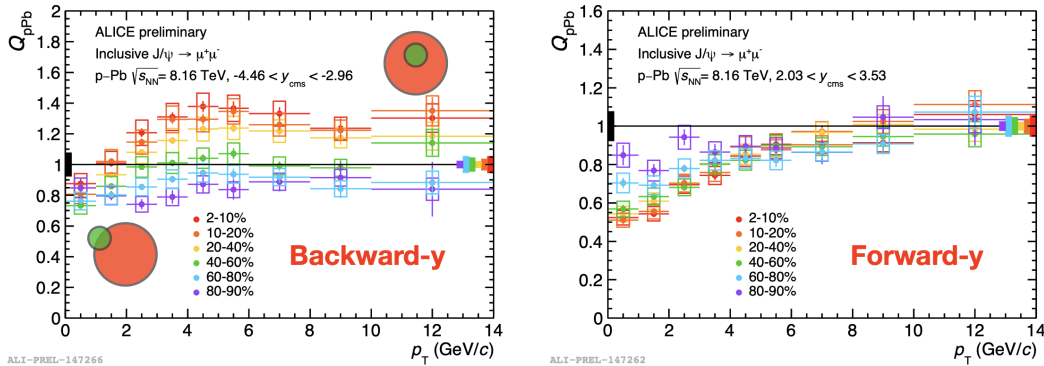


FIG. 10.  $R_{pA}$  of charged hadrons as a function of  $p_T$  at backward rapidity,  $-2.2 < \eta < -1.2$ , Al-going (filled [black] circles) and forward rapidity,  $1.4 < \eta < 2.4$ , p-going (open [red] circles) in various centrality classes of p+Al collisions at  $\sqrt{s_{NN}} = 200$  GeV.

Additionally, ALICE released new results at the Initial Stages 2019 conference on  $J/\psi \rightarrow \mu^+\mu^-$ , which also included finer centrality binning for 0-20%. **Therefore, it was decided in the FVTX meeting July 17, 2019 to include 0-5, 5-10 and 10-20 for Run15pAu, but keep 0-20 p+Au to compare with p+Al and He+Au.** Initial Stages 2019 presentation: [ALICE Results](#)



## 13 NEW: 0-5-10-20% pAu Analysis

As discussed in the last section, the decision to add finer centrality binning came at the end of the analysis. For this reason, we have added the finer centrality binning results in a separate section.

### 13.1 Checks

We performed the same checks that were done for Run15pAu 0-20-40-60-84 centrality. The sum over  $p_T$  and the sum over rapidity are independent of centrality. Therefore, the only relevant check is the sum over centrality.

	Run15pAu 0-5	Run15pAu 5-10	Run15pAu 10-20			Run15pAu 0-5	Run15pAu 5-10	Run15pAu 10-20
	NORTH	NORTH	NORTH			SOUTH	SOUTH	SOUTH
bin	Counts	Counts	Counts		bin	Counts	Counts	Counts
1	30 +/- 6	31 +/- 6	70 +/- 9		1	31 +/- 7	23 +/- 5	36 +/- 7
2	86 +/- 13	93 +/- 10	150 +/- 14		2	82 +/- 14	78 +/- 11	139 +/- 18
3	134 +/- 14	112 +/- 13	224 +/- 18		3	118 +/- 16	108 +/- 13	177 +/- 17
4	136 +/- 14	147 +/- 15	301 +/- 21		4	136 +/- 20	129 +/- 20	241 +/- 19
5	156 +/- 15	163 +/- 17	325 +/- 21		5	179 +/- 19	171 +/- 15	251 +/- 18
6	185 +/- 16	149 +/- 15	263 +/- 21		6	153 +/- 16	157 +/- 14	201 +/- 18
7	157 +/- 14	138 +/- 13	261 +/- 20		7	162 +/- 16	131 +/- 13	215 +/- 17
8	149 +/- 14	117 +/- 13	230 +/- 19		8	147 +/- 14	127 +/- 13	172 +/- 15
9	104 +/- 11	127 +/- 12	204 +/- 16		9	119 +/- 14	87 +/- 13	155 +/- 14
10	82 +/- 12	83 +/- 10	169 +/- 16		10	102 +/- 11	74 +/- 11	117 +/- 15
11	80 +/- 10	68 +/- 9	157 +/- 15		11	85 +/- 11	66 +/- 9	90 +/- 10
12	67 +/- 9	59 +/- 10	143 +/- 13		12	52 +/- 9	41 +/- 7	88 +/- 11
13	60 +/- 9	53 +/- 9	102 +/- 11		13	56 +/- 8	42 +/- 8	55 +/- 8
14	52 +/- 8	67 +/- 9	87 +/- 10		14	46 +/- 8	16 +/- 4	55 +/- 8
15	41 +/- 7	31 +/- 6	60 +/- 8		15	32 +/- 8	25 +/- 6	53 +/- 8
16	28 +/- 6	25 +/- 6	60 +/- 8		16	22 +/- 5	22 +/- 6	31 +/- 7
17	40 +/- 7	41 +/- 7	61 +/- 8		17	43 +/- 7	20 +/- 6	42 +/- 7
18	24 +/- 5	28 +/- 6	55 +/- 8		18	19 +/- 5	19 +/- 5	24 +/- 6
19	36 +/- 6	32 +/- 6	72 +/- 9		19	15 +/- 5	15 +/- 5	30 +/- 6
SUM	1647	1563	2994		SUM	1600	1351	2175
pT int	1629 +/- 53	1552 +/- 52	2970 +/- 71		pT int	1538 +/- 49	1328 +/- 44	2124 +/- 65
% diff	1.10%	0.71%	0.80%		% diff	3.95%	1.72%	2.37%

### 13.2 Summary of Analysis Method

Because 0-5-10-20 is much finer binning than 0-20, we decided to fix the  $J/\psi$  lineshape to prevent against statistical fluctuations from low statistics. For the systematic uncertainty related to doing this, we used the results from the HeAu study, since this study used Run15pAu 0-20 centrality anyway (for better statistics). See section 6.5.1 for more information.

We also did not calculate a new correlated background uncertainty for 0-5-10-20, and instead used the uncertainty results already determined using the Run15pAu 0-20 centrality (see section 6.5).

Also, for this finer centrality, we were able to fit all the way up to 7 GeV/c. Therefore all Run15pAu results for centrality integrated and centrality dependence are over the range 0-7 GeV/c, and all Run15pAu centrality dependence has the same binning.

## 14 Binshift Corrections

Binshift corrections were applied as outlined in AN 1391. For  $R_{AB}$  measurements, binshift corrections were applied to both the pp invariant yield as well as the AA invariant yield. The corrections are listed by system in the following order: Run15pp, Run15pAu, Run15pAl and Run14HeAu.

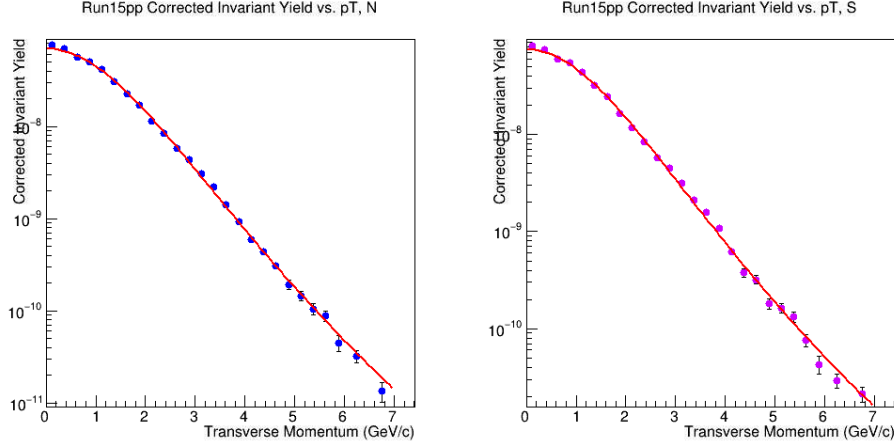


Figure 47: Run15pp North and South invariant yield binshift correction fits.

	NORTH Run15pp	SOUTH Run15pp
pt[GeV/c]	binshift corrections	binshift corrections
0.125	0.997643	0.997524
0.375	0.997994	0.997915
0.625	0.99865	0.998643
0.875	0.999534	0.999613
1.125	1.00055	1.00071
1.375	1.0016	1.00183
1.625	1.00261	1.00287
1.875	1.00352	1.00379
2.125	1.00429	1.00455
2.375	1.00491	1.00514
2.625	1.00537	1.00556
2.875	1.0057	1.00584
3.125	1.00591	1.00599
3.375	1.00601	1.00604
3.625	1.00603	1.00601
3.875	1.00599	1.00592
4.125	1.00589	1.00579
4.375	1.00576	1.00563
4.625	1.00559	1.00544
4.875	1.00542	1.00524
5.125	1.00522	1.00503
5.375	1.00503	1.00482
5.625	1.00483	1.00462
5.875	1.00463	1.00441
6.25	1.01746	1.01656
6.75	1.01598	1.01508

Figure 48: Run15pp North and South invariant yield binshift corrections.

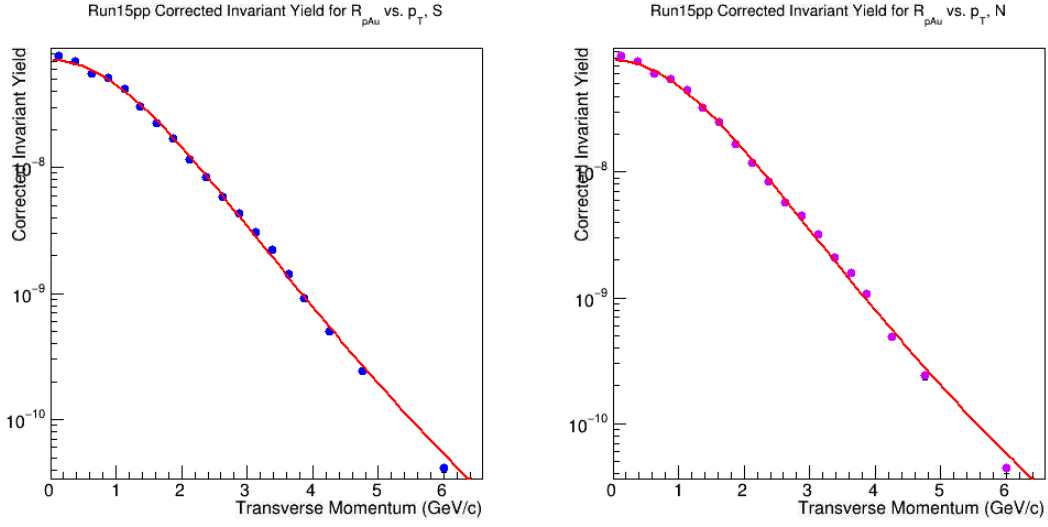


Figure 49: Run15pp North and South invariant yield binshift correction fits for pAu Centrality. All pAu centrality fits share the same  $p_T$  binning, therefore only one set of pp yields (and corrections) are necessary.

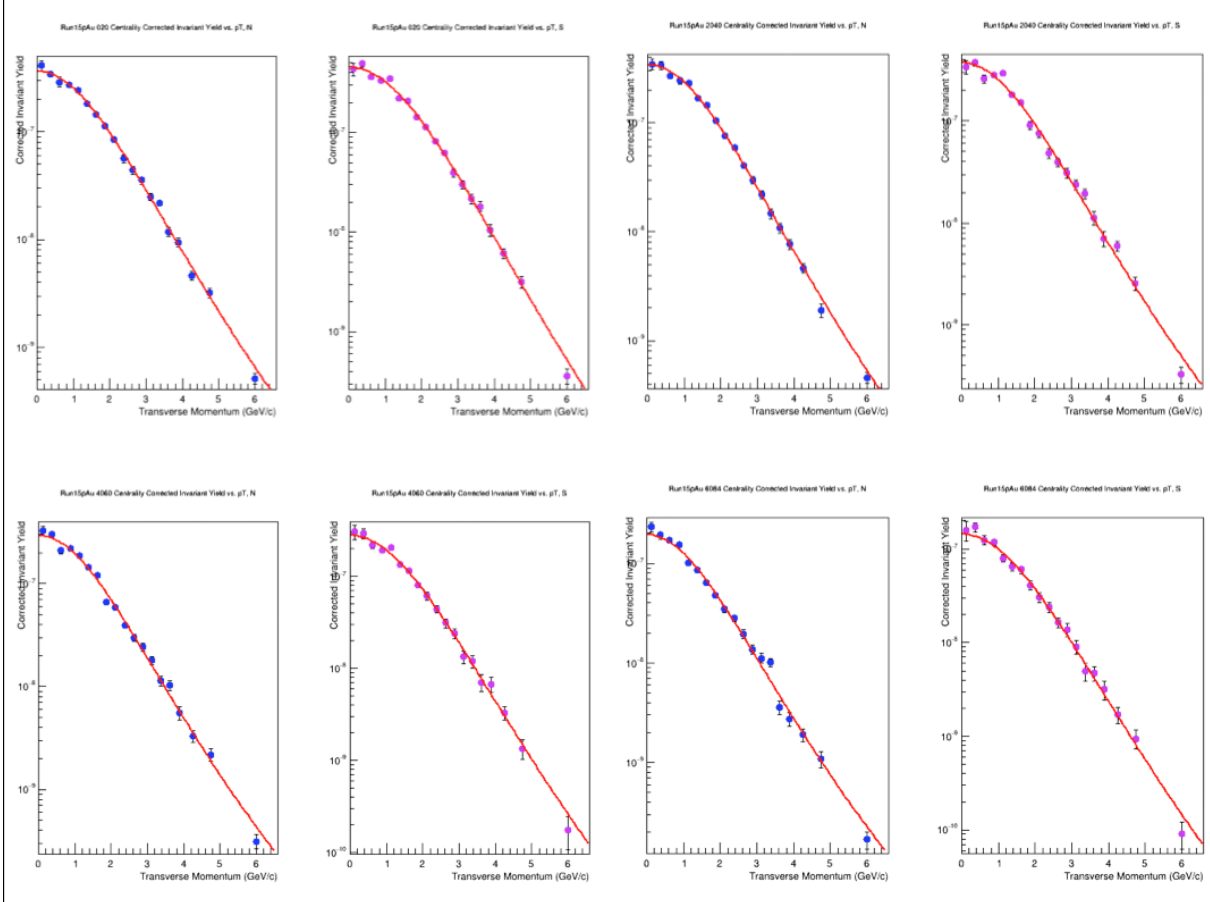


Figure 50: Run15pAu North and South invariant yield binshift correction fits. Larger centralities shown.

	Run15pAu NORTH	0-20 Centrality	20-40 Centrality	40-60 Centrality	60-84 Centrality
pt [GeV/c]	pp binshift corrections	pAu binshift corrections	pAu binshift corrections	pAu binshift corrections	pAu binshift corrections
0.125	0.99759	0.99806	0.998382	0.997817	0.99770
0.375	0.99796	0.99830	0.998536	0.998128	0.99805
0.625	0.99865	0.99876	0.998833	0.998707	0.99868
0.875	0.99958	0.99938	0.999257	0.999482	0.99953
1.125	1.00063	1.00010	0.999782	1.00036	1.00050
1.375	1.00170	1.00086	1.00038	1.00127	1.00147
1.625	1.00271	1.00161	1.00102	1.00212	1.00239
1.875	1.00360	1.00231	1.00168	1.00288	1.00319
2.125	1.00434	1.00292	1.00233	1.00351	1.00386
2.375	1.00492	1.00343	1.00295	1.004	1.00437
2.625	1.00534	1.00384	1.00352	1.00437	1.00474
2.875	1.00562	1.00414	1.00403	1.00461	1.00498
3.125	1.00578	1.00436	1.00448	1.00476	1.00512
3.375	1.00585	1.00449	1.00486	1.00482	1.00517
3.625	1.00583	1.00456	1.00518	1.00482	1.00515
3.875	1.00575	1.00457	1.00543	1.00476	1.00507
4.25	1.02236	1.01812	1.02288	1.01853	1.01966
4.75	1.02096	1.01739	1.02362	1.0174	1.01838
6	1.30000	1.25564	1.41067	1.24618	1.25917

Figure 51: North binshift correction values for Run15pAu and Run15pp invariant yields. All centralities shown.

	Run15pAu SOUTH	0-20 Centrality	20-40 Centrality	40-60 Centrality	60-84 Centrality
pt [GeV/c]	pp binshift corrections	pAu binshift corrections	pAu binshift corrections	pAu binshift corrections	pAu binshift corrections
0.125	0.99746	0.99823	0.997936	0.998043	0.99805
0.375	0.99788	0.99842	0.998208	0.998278	0.99829
0.625	0.99865	0.99878	0.998719	0.998726	0.99873
0.875	0.99966	0.99929	0.999413	0.999346	0.99935
1.125	1.00080	0.99992	1.00022	1.00009	1.00008
1.375	1.00193	1.00060	1.00107	1.00089	1.00088
1.625	1.00298	1.00132	1.0019	1.00171	1.00169
1.875	1.00387	1.00203	1.00265	1.0025	1.00246
2.125	1.00459	1.00271	1.00331	1.00322	1.00317
2.375	1.00513	1.00332	1.00386	1.00385	1.00379
2.625	1.00550	1.00386	1.00428	1.00438	1.00431
2.875	1.00573	1.00432	1.0046	1.00482	1.00473
3.125	1.00584	1.00469	1.00481	1.00515	1.00505
3.375	1.00585	1.00499	1.00494	1.00539	1.00528
3.625	1.00578	1.00521	1.005	1.00555	1.00543
3.875	1.00567	1.00537	1.00499	1.00564	1.00551
4.25	1.02182	1.02205	1.0197	1.02276	1.02224
4.75	1.02023	1.02207	1.01881	1.02231	1.02177
6	1.28320	1.35857	1.27562	1.34856	1.33856

Figure 52: South binshift correction values for Run15pAu and Run15pp invariant yields. All centralities shown.

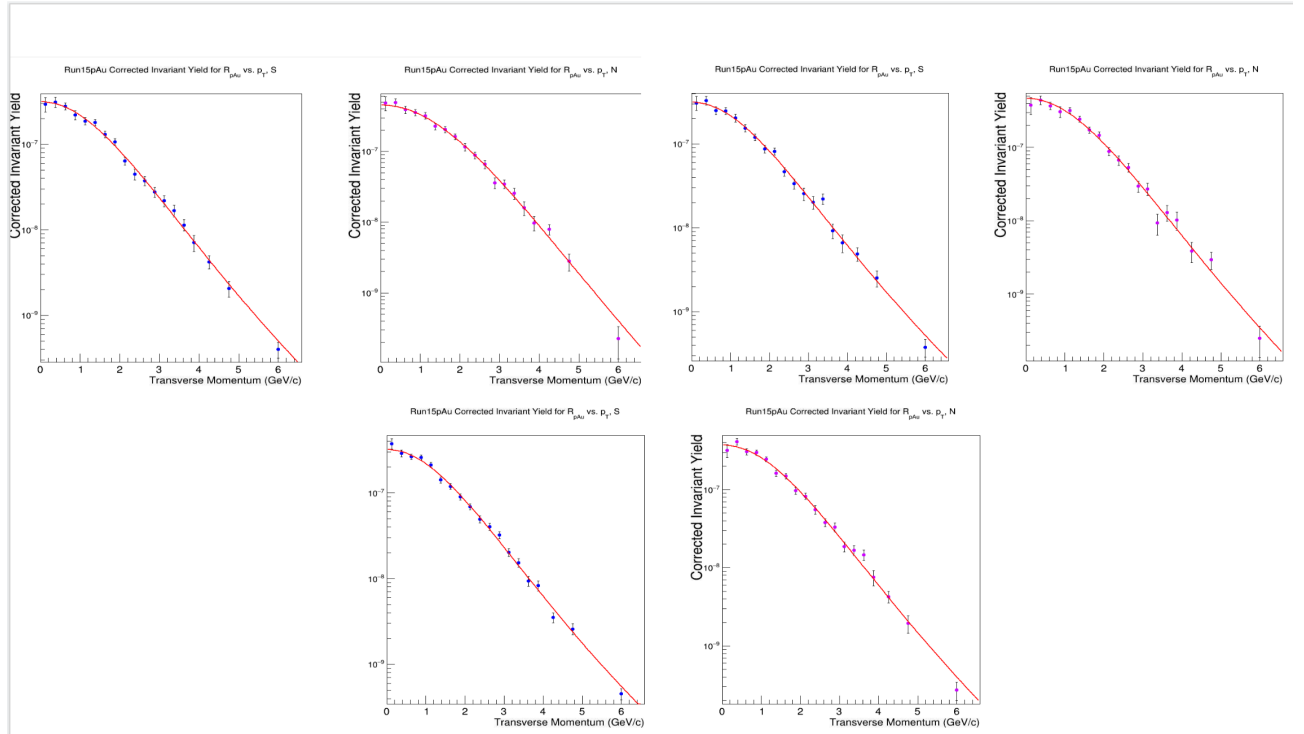


Figure 53: Run15pAu North and South invariant yield binshift correction fits. Finer centralities shown.

	Run15pAu NORTH	0-5 Centrality	5-10 Centrality	10-20 Centrality
pt [GeV/c]	pp binshift corrections	pAu binshift corrections	pAu binshift corrections	pAu binshift corrections
0.125	0.99761	0.998039	0.997994	0.997949
0.375	0.99798	0.998284	0.998253	0.998222
0.625	0.99865	0.998747	0.99874	0.998734
0.875	0.99956	0.999379	0.999401	0.999425
1.125	1.0006	1.00012	1.00017	1.00022
1.375	1.00165	1.0009	1.00097	1.00104
1.625	1.00266	1.00167	1.00176	1.00184
1.875	1.00355	1.00239	1.00247	1.00255
2.125	1.00429	1.00302	1.00309	1.00317
2.375	1.00487	1.00355	1.00361	1.00366
2.625	1.0053	1.00397	1.00401	1.00404
2.875	1.00559	1.00429	1.0043	1.0043
3.125	1.00576	1.00451	1.0045	1.00448
3.375	1.00584	1.00466	1.00462	1.00457
3.625	1.00583	1.00473	1.00467	1.0046
3.875	1.00576	1.00475	1.00467	1.00457
4.25	1.02242	1.01883	1.0184	1.01791
4.75	1.02105	1.01809	1.01755	1.01697
6	1.30251	1.26733	1.25556	1.24348

	Run15pAu SOUTH	0-5 Centrality	5-10 Centrality	10-20 Centrality
pt [GeV/c]	pp binshift corrections	pAu binshift corrections	pAu binshift corrections	pAu binshift corrections
0.125	0.9975	0.998338	0.997934	0.997969
0.375	0.99791	0.998499	0.998196	0.998227
0.625	0.99865	0.998811	0.998694	0.998715
0.875	0.99964	0.999255	0.99938	0.999384
1.125	1.00074	0.999807	1.0002	1.00017
1.375	1.00186	1.00044	1.00108	1.00101
1.625	1.00289	1.00111	1.00196	1.00185
1.875	1.00379	1.00181	1.00281	1.00264
2.125	1.00451	1.0025	1.00357	1.00334
2.375	1.00507	1.00315	1.00424	1.00393
2.625	1.00546	1.00376	1.00479	1.00442
2.875	1.0057	1.00431	1.00522	1.00479
3.125	1.00583	1.00479	1.00555	1.00506
3.375	1.00585	1.0052	1.00578	1.00524
3.625	1.0058	1.00555	1.00593	1.00534
3.875	1.0057	1.00582	1.006	1.00538
4.25	1.02201	1.02458	1.0241	1.02145
4.75	1.02048	1.02542	1.02348	1.02072
6	1.28869	1.44721	1.36436	1.31291

Figure 54: South binshift correction values for Run15pAu and Run15pp invariant yields. Finer centralities shown.

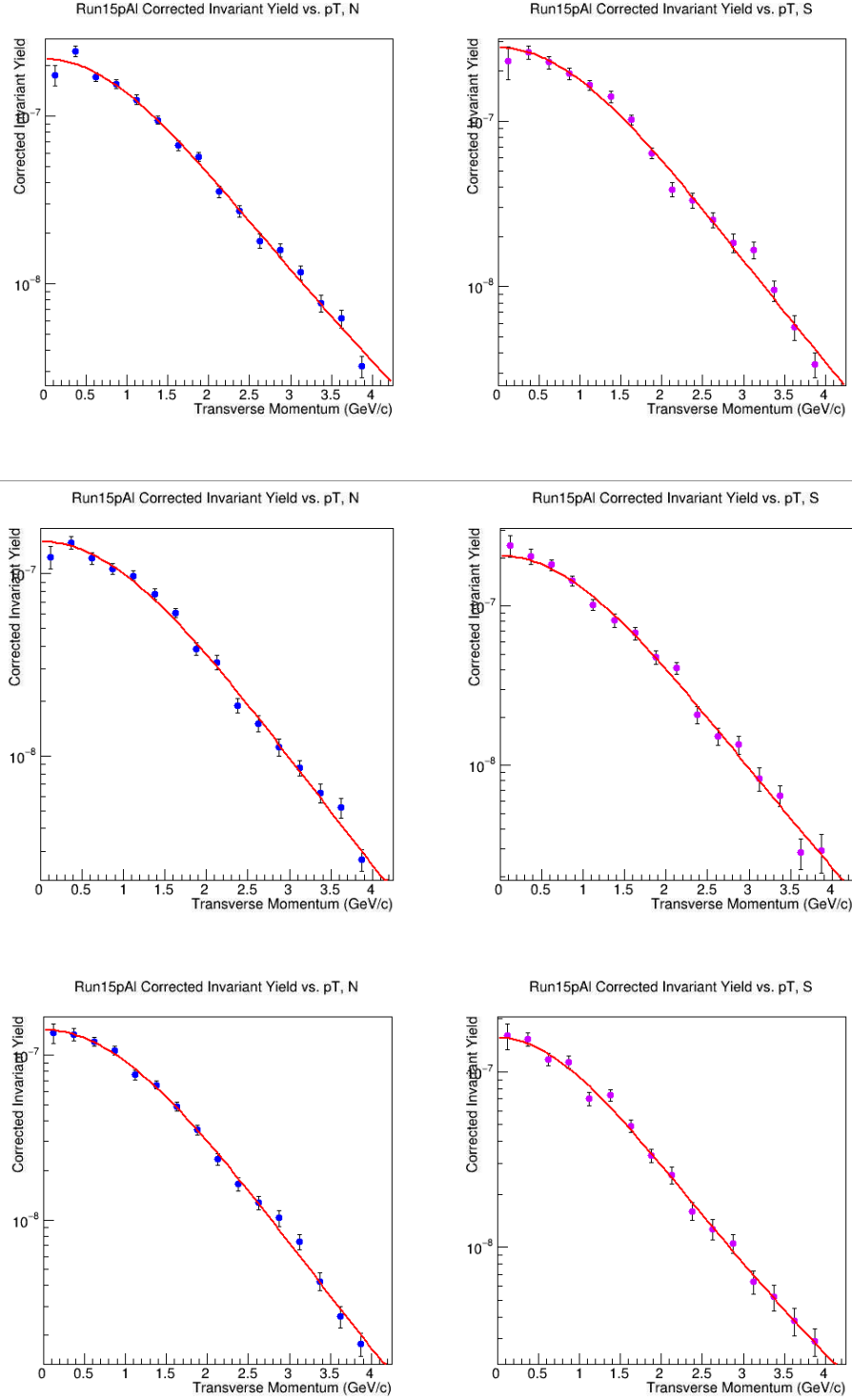


Figure 55: Run15pAl North and South invariant yield binshift correction fits. All centralities shown. The  $pp$  invariant yields used in the nuclear modification factor  $R_{pAl}$  share the same  $p_T$  binning as Run15pAu, and are shown in Figure 51.



	Run15pAl NORTH	0-20 Centrality	20-40 Centrality	40-72 Centrality
pt [GeV/c]	pp binshift corrections	pAl binshift corrections	pAl binshift corrections	pAl binshift corrections
0.125	0.99761	0.99745	0.997842	0.997648
0.375	0.99798	0.99790	0.998144	0.998001
0.625	0.99865	0.99871	0.998709	0.99866
0.875	0.99956	0.99974	0.999467	0.999542
1.125	1.00060	1.00084	1.00033	1.00055
1.375	1.00165	1.00188	1.00123	1.00158
1.625	1.00266	1.00277	1.00207	1.00257
1.875	1.00355	1.00348	1.00283	1.00344
2.125	1.00429	1.00399	1.00347	1.00417
2.375	1.00487	1.00433	1.00397	1.00475
2.625	1.00530	1.00452	1.00435	1.00518
2.875	1.00559	1.00460	1.00461	1.00547
3.125	1.00576	1.00458	1.00477	1.00564
3.375	1.00584	1.00450	1.00485	1.00572
3.625	1.00583	1.00437	1.00485	1.00572
3.875	1.00576	1.00421	1.00481	1.00566
	Run15pAl SOUTH	0-20 Centrality	20-40 Centrality	40-72 Centrality
pt [GeV/c]	pp binshift corrections	pAl binshift corrections	pAl binshift corrections	pAl binshift corrections
0.125	0.99750	0.99760	0.997454	0.997155
0.375	0.99791	0.99797	0.997878	0.997737
0.625	0.99865	0.99867	0.998658	0.998761
0.875	0.99964	0.99959	0.999682	1.00001
1.125	1.00074	1.00063	1.00082	1.00126
1.375	1.00186	1.00167	1.00194	1.00236
1.625	1.00289	1.00264	1.00296	1.00322
1.875	1.00379	1.00347	1.00383	1.00383
2.125	1.00451	1.00414	1.00451	1.00422
2.375	1.00507	1.00465	1.00501	1.00442
2.625	1.00546	1.00501	1.00534	1.00447
2.875	1.00570	1.00523	1.00554	1.00442
3.125	1.00583	1.00535	1.00562	1.0043
3.375	1.00585	1.00537	1.00561	1.00414
3.625	1.00580	1.00532	1.00553	1.00395
3.875	1.00570	1.00523	1.0054	1.00375

Figure 56: North and South Arm binshift correction values for Run15pAl and Run15pp invariant yields. All centralities shown.

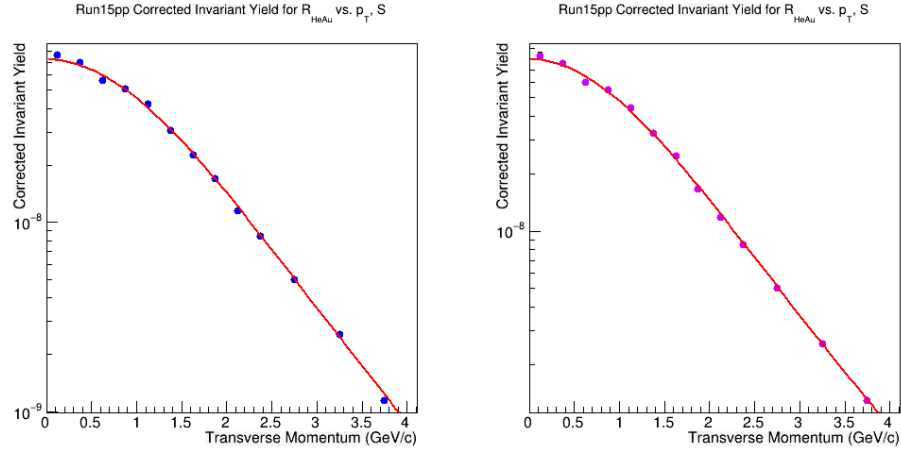


Figure 57: Run15pp North and South invariant yield binshift correction fits for HeAu Centrality. All HeAu centrality fits share the same  $p_T$  binning, therefore only one set of pp yields (and corrections) are necessary.

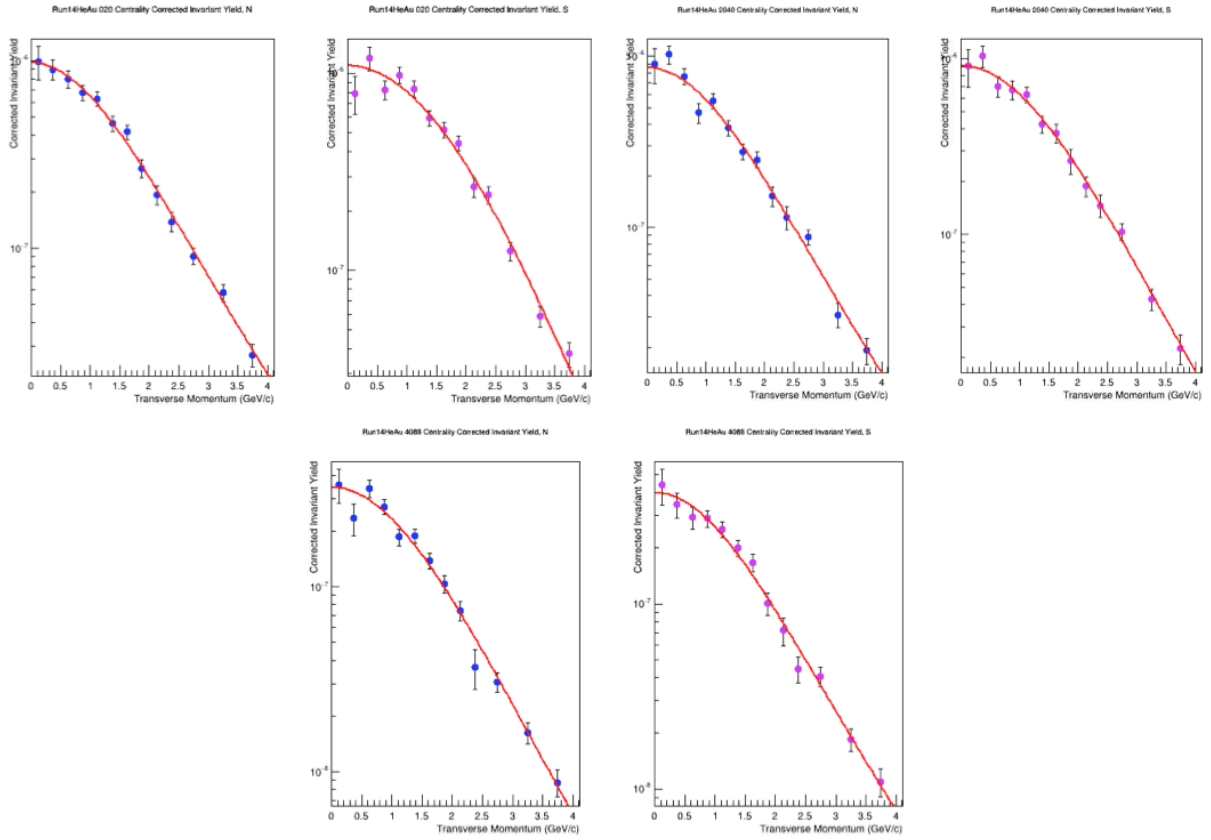


Figure 58: Run14HeAu North and South invariant yield binshift correction fits. All centralities shown.

	Run14HeAu NORTH	0-20 Centrality	20-40 Centrality	40-88 Centrality
pt [GeV/c]	pp binshift corrections	HeAu binshift corrections	HeAu binshift corrections	HeAu binshift corrections
0.125	0.99747	0.99779	0.997659	0.997596
0.375	0.99789	0.99813	0.998026	0.997961
0.625	0.99867	0.99874	0.998702	0.998645
0.875	0.99969	0.99954	0.999587	0.999562
1.125	1.00080	1.00043	1.00056	1.00061
1.375	1.00190	1.00129	1.00153	1.00169
1.625	1.00289	1.00207	1.00241	1.00272
1.875	1.00371	1.00272	1.00314	1.00364
2.125	1.00436	1.00323	1.00372	1.00441
2.375	1.00482	1.00360	1.00415	1.00503
2.75	1.02095	1.01571	1.01813	1.02271
3.25	1.02146	1.01615	1.0187	1.02431
3.75	1.02077	1.01566	1.01818	1.02439
	Run14HeAu SOUTH	0-20 Centrality	20-40 Centrality	4088 Centrality
pt [GeV/c]	pp binshift corrections	HeAu binshift corrections	HeAu binshift corrections	HeAu binshift corrections
0.125	0.99726	0.99841	0.998017	0.997313
0.375	0.99777	0.99855	0.998266	0.997838
0.625	0.99869	0.99883	0.998736	0.998764
0.875	0.99986	0.99924	0.999379	0.999896
1.125	1.00110	0.99974	1.00013	1.00104
1.375	1.00227	1.00033	1.00094	1.00205
1.625	1.00326	1.00098	1.00173	1.00286
1.875	1.00404	1.00166	1.00247	1.00344
2.125	1.00459	1.00235	1.00312	1.00381
2.375	1.00495	1.00303	1.00367	1.00401
2.75	1.02083	1.01594	1.01721	1.01631
3.25	1.02058	1.02042	1.01919	1.01556
3.75	1.01936	1.02393	1.0199	1.01423

Figure 59: North, top, and South binshift correction values for Run14HeAu and Run15pp invariant yields. All centralities shown.

## 15 Uncertainties: Type A, B and C

### 15.1 Type A: Statistical Uncertainty

The Type A statistical uncertainty present in this analysis arises from only one source: the uncertainty in the  $J/\psi$  yield.

### 15.2 Type B: Systematic Uncertainty

All Type B systematic uncertainties taken into consideration in this analysis, aside from the correlated background shape and fixing the  $J/\psi$  lineshape (see section 12.2.1), were determined by Matt Durham and Sanghoon Lim in AN 1354. These include background normalization, trigger efficiency,  $J/\psi$  polarization, run to run variation, phi matching and initial shape. The same procedure and uncertainties were used for the centrality dependent nuclear modification factor as for the centrality integrated nuclear modification factor. In particular, the systematic uncertainty on  $J/\psi$  polarization cancels out when calculating  $R_{AB}$  by assuming the same polarization between pp and pAl, pp and pAu, and pp and  $^3\text{HeAu}$ .

#### 15.2.1 Run14HeAu: Fixing the $J/\psi$ Width and Center of the Peak

As previously mentioned, the statistics were low for Run14HeAu  $J/\psi$  analysis as a function of  $p_T$  and centrality. To remedy this, we fixed the center of the  $J/\psi$  peak as well as the width of the  $J/\psi$  peak to the HeAu minimum bias results. The HeAu minimum bias was fit using the  $p_T$  integrated pAu correlated background result as initial parameters, using the Case ‘A’ fit.

The systematic uncertainty for fixing the  $J/\psi$  peak and width was determined using the Run15pAu data set, since the statistics were too low in Run14HeAu to accurately determine this effect. Since both the width and the center of the peak were fixed to the same value for all centrality bins, the systematic uncertainty is independent of centrality. We selected the centrality bin with the highest statistics, Run15pAu 0-20. Following the suggestions by Tony and Sanghoon described in 10.4.1 and 10.4.2, the pAu MB data was fit and the bestfit results for the width and the center of the  $J/\psi$  peak were extracted.

We then refit the pAu 0-20 spectra with the width and the center of the peak fixed to the minimum bias values shown in the above figures. Taking the minimum bias results as the central value, we calculated the systematic uncertainty following the same formula used in Sanghoon’s method for the correlated background systematic study. The results are shown on the next page.

### 15.3 Type C: Global Uncertainty

The global uncertainties in the centrality dependent  $R_{AB}$  are due to the BBC uncertainty, the  $N_{coll}$  estimation and also from the bias correction factors. These are the same sources of global uncertainty that were present in the centrality integrated  $R_{AB}$ . Please refer to the table on the next page for a complete list of centrality dependent global errors. A weighted average was taken to determine the uncertainties for the 40-88 range in Run14HeAu as well as the 0-20 range in Run15pAl (see section 17.1: Rebinning Centralities for more details).

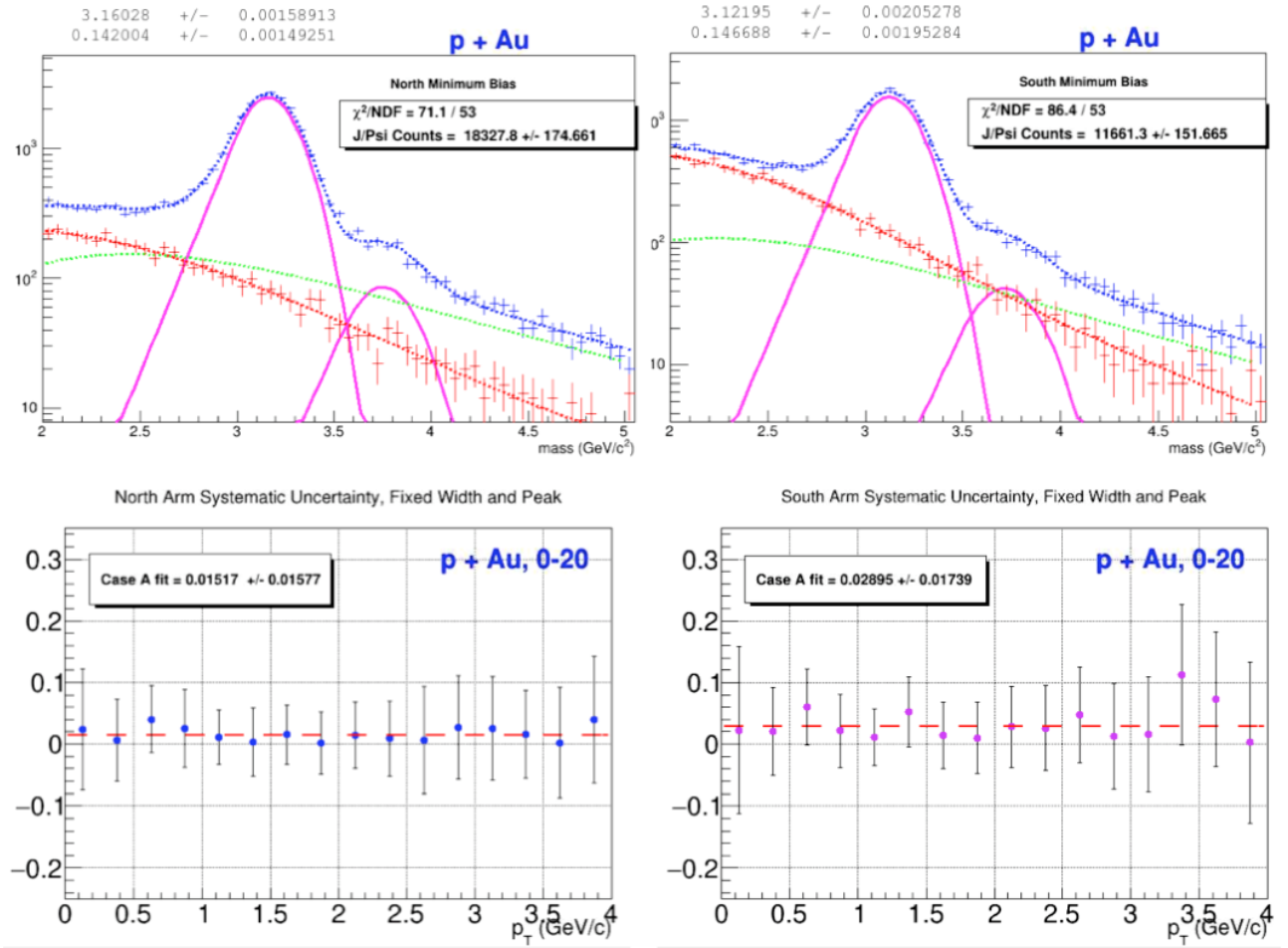


Figure 60: Top: Run15pAu MB fit for the North and South Arms. The bestfit values for the  $J/\psi$  width and the center of the peak are shown. Bottom: Run14HeAu systematic uncertainty results for fixing the width and the center of the  $J/\psi$  peak. Run15pAu data was used for more reliable statistics.

Table 3: Run15pp, Run15pAu, Run15pAl and Run14HeAu Type B systematic uncertainties included in the nuclear modification factor  $R_{AB}$ . Results for all centralities and transverse momenta shown as a range.

System	Corr. BG	Run Var.	Initial Shape	Trigger eff.	BG Norm	Lineshape
Run15pp N	1.4%	4.0%	2.0%	1.0 - 1.7%	neg	-
Run15pp S	1.7%	4.7%	2.0%	1.0 - 2.6%	neg	-
Run15pAu N	1.9 - 2.7%	1.6%	2.0%	1.0 - 1.7%	1.0%	-
Run15pAu S	1.4 - 2.8%	3.5%	2.0%	1.0 - 4.8%	4.4%	-
Run15pAl N	1.40%	2.8%	2.0%	1.0 - 1.8%	1.0%	-
Run15pAl S	1.79%	3.3%	2.0%	2.0 - 4.6%	1.0%	-
Run14HeAu N	2.3 - 2.4%	1.5%	2.0%	1.0 - 2.4%	1.0%	1.5%
Run14HeAu S	1.4 - 2.8%	5.0%	2.0%	1.0 - 2.4%	2.7%	2.9%
p+Au N (0-5-10-20%)	1.9 - 2.7%	1.6%	2.0%	1.0 - 1.7%	1.0%	1.5%
p+Au S (0-5-10-20%)	1.4 - 2.8%	3.5%	2.0%	1.0 - 4.8%	4.4%	2.9%

Table 4: Type C fractional systematic uncertainties for all centralities.

Centrality	System	$N_{coll}$	bias correction	Reference	BBC (Ref: AN1354)	Total
0-100	Run15pp	-	-	-	10%	10%
0-5	Run15pAu	6.19%	1.16%	AN1265	10%	11.82%
5-10		5.95%	1.11%	AN1265	10%	11.69%
10-20		6.76%	1.06%	AN1265	10%	12.12%
0-20		6.10%	1.11%	AN1265	10%	11.77%
20-40		6.56%	1.02%	AN1265	10%	12.00%
40-60		6.82%	0.98%	AN1265	10%	12.14%
60-84		7.69%	6.00%	AN1265	10%	13.97%
0-84		6.38%	1.63%	AN1265	10%	11.97%
0-20	Run15pAl	7.42%	1.24%	AN1290	10%	12.51%
20-40		4.35%	2.22%	AN1290	10%	11.13%
40-72		5.88%	3.96%	AN1290	10%	12.26%
0-72		4.76%	2.50%	AN1290	10%	11.35%
0-20	Run14HeAu	7.62%	1.05%	AN1207	10%	12.62%
20-40		7.43%	0.99%	AN1207	10%	12.50%
40-88		8.12%	3.24 %	AN1207	10%	13.28%
0-88		6.73%	1.12%	AN1207	10%	12.11%

## 16 Trigger and Acceptance Reconstruction Efficiencies

Trigger efficiencies and acceptance reconstruction efficiencies in all systems were generated by Sanghoon Lim. This includes centrality/rapidity integrated Run15pAu, Run15pAl and Run14HeAu, and rapidity integrated Run15pp for the preliminary results presented in AN 1391. It also includes all centralities for Run15pAu, Run15pAl and Run14HeAu presented in this note.

In total, 36 efficiency files were needed for the analysis of  $J/\psi$  as a function of  $p_T$ . Sanghoon fit all efficiency histograms aside from Run15pp, as the  $p_T$  binning used was exactly the same. The figures below show Run15pAu acceptance and trigger efficiencies and their corresponding fits for the 0-20 centrality range in the North and South Arms. For a complete description of the methods Sanghoon used, see [AN 1354](#) section 3.

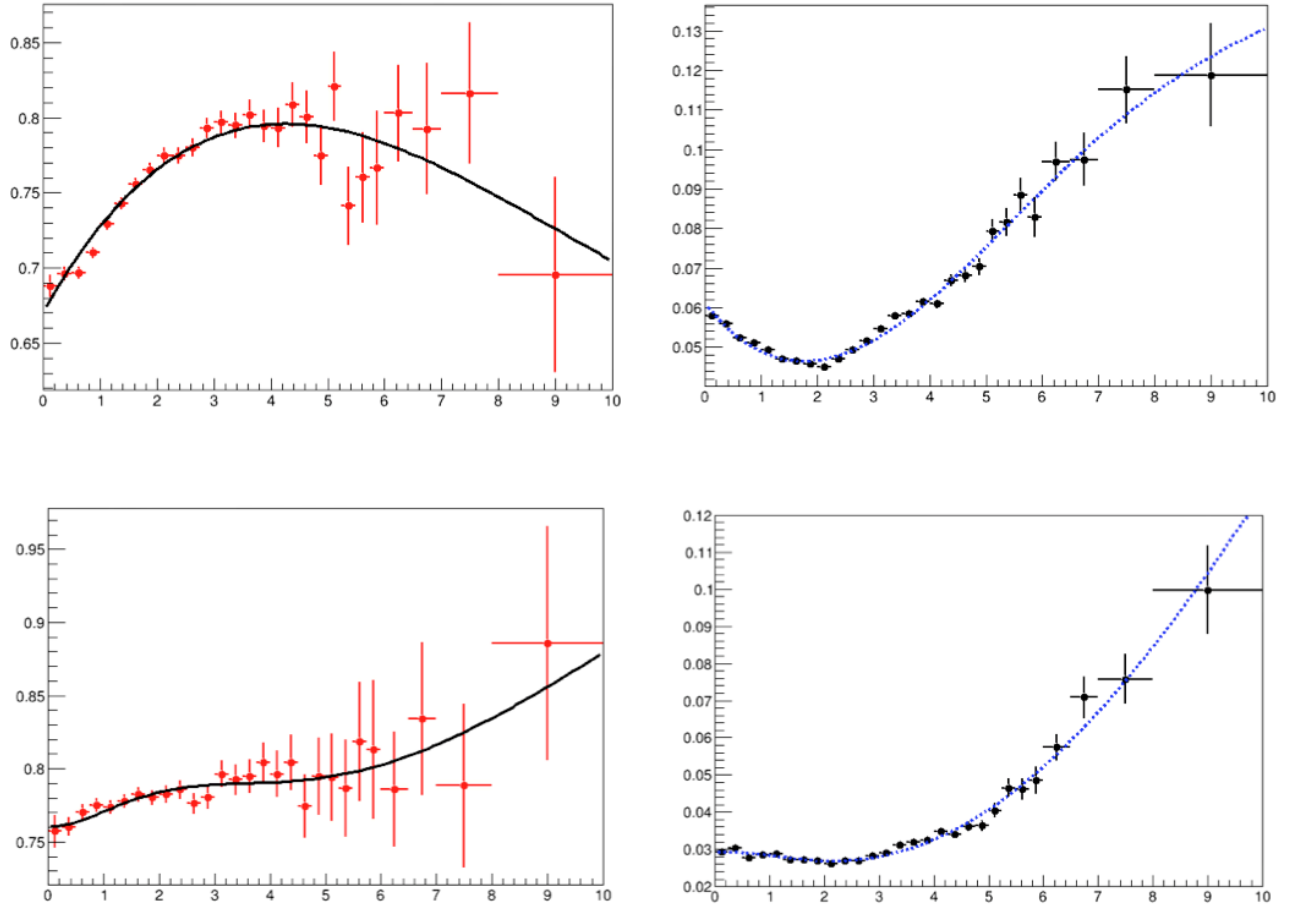


Figure 61: North Run15pAu efficiencies, top, and South for the 0-20 centrality range, with trigger efficiencies shown on the left and acceptance reconstruction efficiencies on the right. Generated by Sanghoon Lim.

## 17 Run15pp Results

The Run15pp results for  $J/\psi$  vs.  $p_T$  include the invariant cross section vs.  $p_T$ , the North to South invariant cross section ratio and comparison with PPG 104 results.

### 17.1 GEANT3/GEANT4 Discrepancy

Sanghoon Lim discovered a discrepancy between simulation results for GEANT3 as compared to GEANT4, which is the basis for the discrepancies between Run15pp and PPG104. These results were presented in the HI PWG meeting (April 4, 2019), and it was determined GEANT4 should be used. A summary of his study can be found in section 3.8 of AN 1354, and the link to his presentation is included below.

#### 17.1.1 Sanghoon's HI PWG Presentation

##### Comparison between G3 and G4

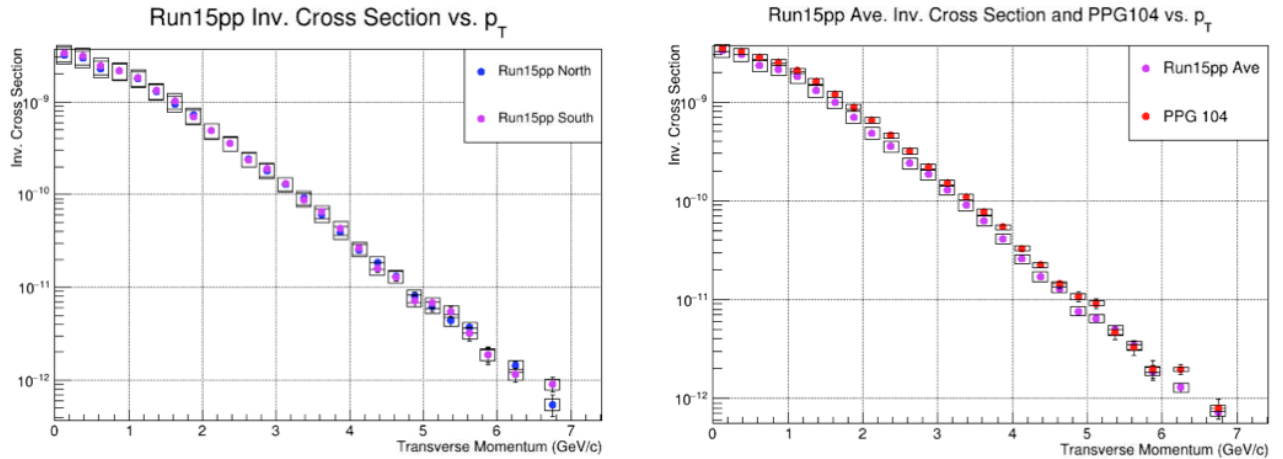


Figure 62: Invariant cross section results for Run15pp in both arms, left. Right: Average Run15pp cross sections compared with PPG104.



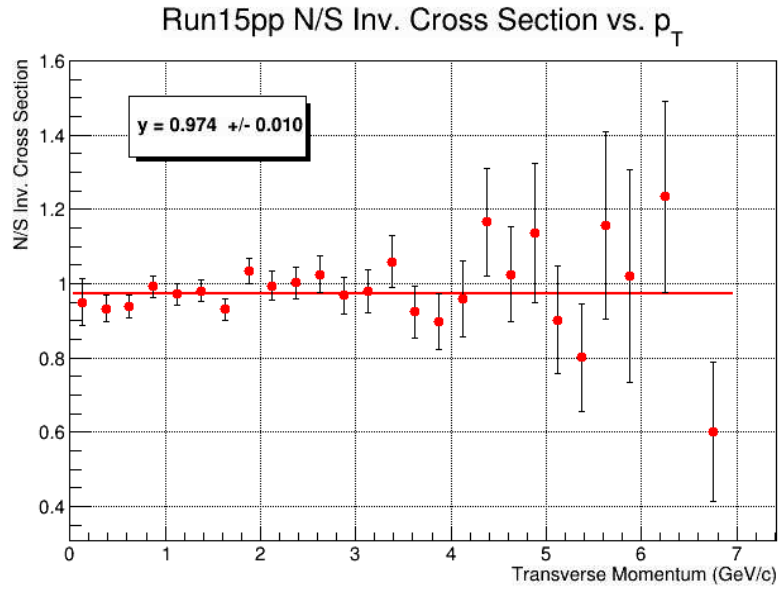


Figure 63: Ratio of the Run15pp North arm invariant cross section to the South arm invariant cross section.

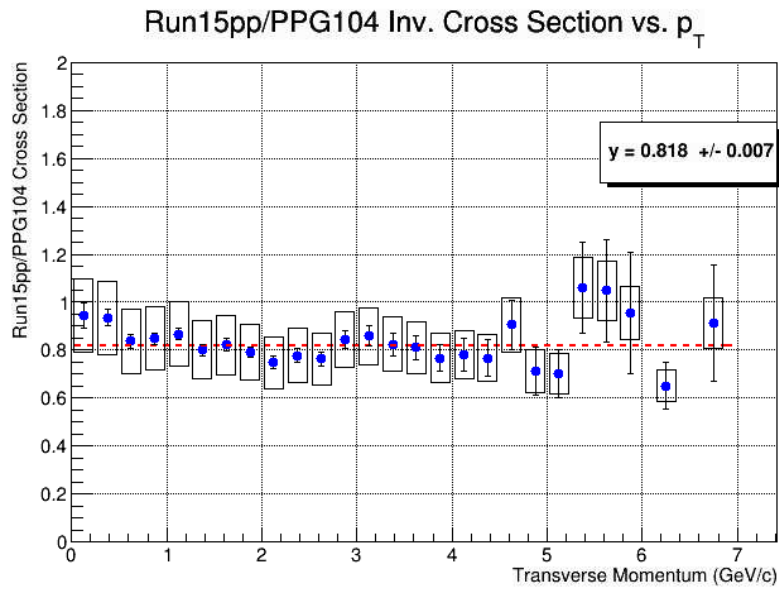


Figure 64: Ratio of the average of the Run15pp North and South arm invariant yields to PPG 104 results. Please see section 13.1 for more details.

## 18 Run15pAu Results

The Run15pAu results show  $R_{AB}$  as a function of  $p_T$  and centrality, and are compared with Run08dAu. Additional plots include  $R_{AB}$  vs.  $N_{coll}$  and the ratios of  $R_{pAu}/R_{dAu}$  per centrality range. Each pp yield in the nuclear modification factor was fit individually, and a binshift correction was applied.

### 18.1 Fraction of Events per Centrality Range

Sanghoon Lim found and corrected an error in the preliminary results concerning the fraction of events per centrality range.

According to AN 1265, “Note that the distribution is not perfectly flat due to the BBCLL1 z-vertex resolution dependence on multiplicity. This emphasizes that one must count events in each centrality category explicitly since centrality flattening is done for the unbiased wider range.”

In Run15pAu, the MuID 2D trigger was combined with different MB triggers (narrow-z, +/-30 cm, wide-z), so the flat centrality distribution for BBCLL1 trigger of +/-30 (by definition) is not flat for narrow-z. Therefore, to determine the correct fraction of events per centrality range for Run15pAu, we need to count the number of events from three BBCLL1 triggers combined with the 2D trigger in each centrality range. A slide showing the run numbers associated with each trigger combination is shown in Figure 65.

MuID/Muon LL1 trigger					
<ul style="list-style-type: none"> <li>Caution to use Run15 p+Au @ 200 GeV <ul style="list-style-type: none"> <li>Need to be careful for normalization (yield calculation)</li> </ul> </li> </ul>					
Run: start – 434028 combined with BBCLL1_narrowvtx		Run: 434033 – 434052 combined with BBCLL1_nowvertex		Run: 434134 – end combined with BBCLL1_nowvertex	
Name	Bit Mask	Name	Bit Mask	Name	Bit Mask
BBCLL1(>0 tubes)	0x00000001	BBCLL1(>0 tubes)	0x00000001	BBCLL1(>0 tubes)	0x00000001
BBCLL1(>0 tubes) novertex	0x00000002	BBCLL1(>0 tubes) novertex	0x00000002	BBCLL1(>0 tubes) novertex	0x00000002
ZDCLL1wide	0x00000004	ZDCLL1wide	0x00000004	ZDCLL1wide	0x00000004
BBCLL1(>0 tubes)_central35_narrowvtx	0x00000008	BBCLL1(>0 tubes)_central35_narrowvtx	0x00000008	BBCLL1(>0 tubes)_central35_narrowvtx	0x00000008
BBCLL1(>0 tubes) narrowvtx	0x00000010	BBCLL1(>0 tubes) narrowvtx	0x00000010	BBCLL1(>0 tubes) narrowvtx	0x00000010
ZDCNS	0x00000020	ZDCNS	0x00000020	ZDCNS	0x00000020
ERT_4x4b	0x00000040	ERT_4x4b	0x00000040	ERT_4x4b	0x00000040
ERT_4x4a&BBCLL1	0x00000080	ERT_4x4a&BBCLL1	0x00000080	ERT_4x4a&BBCLL1	0x00000080
ERT_4x4c&BBCLL1(narrow)	0x00000100	ERT_4x4c&BBCLL1(narrow)	0x00000100	ERT_4x4c&BBCLL1(narrow)	0x00000100
ERTLL1_E&BBCLL1(narrow)	0x00000200	ERTLL1_E&BBCLL1(narrow)	0x00000200	ERTLL1_E&BBCLL1(narrow)	0x00000200
FVTX_HighMult_N&BBCLL1(narrow)	0x00000400	FVTX_HighMult_N&BBCLL1(narrow)	0x00000400	FVTX_HighMult_N&BBCLL1(narrow)	0x00000400
FVTX_HighMult_S&BBCLL1(narrow)	0x00000800	FVTX_HighMult_S&BBCLL1(narrow)	0x00000800	FVTX_HighMult_S&BBCLL1(narrow)	0x00000800
MPC_N_A	0x00001000	MPC_N_A	0x00001000	MPC_N_A	0x00001000
MPC_S_A	0x00002000	MPC_S_A	0x00002000	MPC_S_A	0x00002000
MPC_S_C&ERTLL1_2x2	0x00004000	MPC_S_C&ERTLL1_2x2	0x00004000	MPC_S_C&ERTLL1_2x2	0x00004000
ZDCN	0x00008000	ZDCN	0x00008000	ZDCN	0x00008000
CLOCK	0x00010000	CLOCK	0x00010000	CLOCK	0x00010000
MPC_N_B	0x00020000	MPC_N_B	0x00020000	MPC_N_B	0x00020000
MPC_N_C&ERTLL1_2x2	0x00040000	MPC_N_C&ERTLL1_2x2	0x00040000	MPC_N_C&ERTLL1_2x2	0x00040000
ZDCS	0x00080000	ZDCS	0x00080000	ZDCS	0x00080000
MUIDLL1_N2D&BBCLL1narrow	0x00100000	MUIDLL1_N2D&BBCLL1novertex	0x00100000	MUIDLL1_N2D&BBCLL1	0x00100000
MUIDLL1_S2D&BBCLL1narrow	0x00200000	MUIDLL1_S2D&BBCLL1novertex	0x00200000	MUIDLL1_S2D&BBCLL1	0x00200000
MUIDLL1_N1D&BBCLL1narrow	0x00400000	MUIDLL1_N1D&BBCLL1novertex	0x00400000	MUIDLL1_N1D&BBCLL1	0x00400000
MUIDLL1_S1D&BBCLL1narrow	0x00800000	MUIDLL1_S1D&BBCLL1novertex	0x00800000	MUIDLL1_S1D&BBCLL1	0x00800000
MUON_N_SG3&MUIDLL1_1(D1H)&BBCLL1narrow(nppg)	0x01000000	MUON_N_SG3&MUIDLL1_1(D1H)&BBCLL1novertex(nppg)	0x01000000	MUON_N_SG3&MUIDLL1_1(D1H)&BBCLL1(nppg)	0x01000000
MUON_N_SG3&MUIDLL1_1(D1H)&BBCLL1narrow(nppg)	0x02000000	MUON_N_SG3&MUIDLL1_1(D1H)&BBCLL1novertex(nppg)	0x02000000	MUON_N_SG3&MUIDLL1_1(D1H)&BBCLL1(nppg)	0x02000000
MUON_N_SG3&BBCLL1narrow(nppg)	0x04000000	MUON_N_SG3&BBCLL1novertex(nppg)	0x04000000	MUON_N_SG3&BBCLL1(nppg)	0x04000000
MUON_N_SG3&BBCLL1narrow(nppg)	0x08000000	MUON_N_SG3&BBCLL1novertex(nppg)	0x08000000	MUON_N_SG3&BBCLL1(nppg)	0x08000000

17

Figure 65: Image credit: Sanghoon Lim. [Sanghoon's 2017 PHENIX summer school slides](#)

The fraction of events per centrality range  $\Delta x$  is included in the denominator of the invariant yield, which is needed to determine the nuclear modification factor as a function of centrality 'x':

$$dY_{AB}^{J/\psi}(x) = \frac{c(x) N_{AB}^{J/\psi}(x)}{2\pi p_T \Delta p_T \Delta y \epsilon_{trig}(x) \epsilon_{acc}(x) \Delta x N_{MB}} \quad (13)$$

$$R_{AB}(x) = \frac{dY_{AB}^{J/\psi}(x)}{N_{coll}(x) dY_{pp}^{J/\psi}} \quad (14)$$

For Run15pAu, Sanghoon directly counted the events and provided the following fraction of events per centrality range, listed in Table 5.

*Table 5: Run15pAu fraction of events per centrality range. All values determined by Sanghoon Lim using direct counting, as described in AN 1265.*

<i>Arm</i>	<i>Centrality</i>	<i>incorrect <math>\Delta x</math></i>	<i>correct <math>\Delta x</math></i>
North	0-5	0.05	0.06352
	5-10	0.05	0.06292
	10-20	0.10	0.1253
	0-20	0.20	0.2426
	20-40	0.20	0.2382
	40-60	0.20	0.2363
	60-84	0.24	0.2829
South	0-5	0.05	0.06087
	5-10	0.05	0.06013
	10-20	0.10	0.1196
	0-20	0.20	0.2431
	20-40	0.20	0.2381
	40-60	0.20	0.2361
	60-84	0.24	0.2826

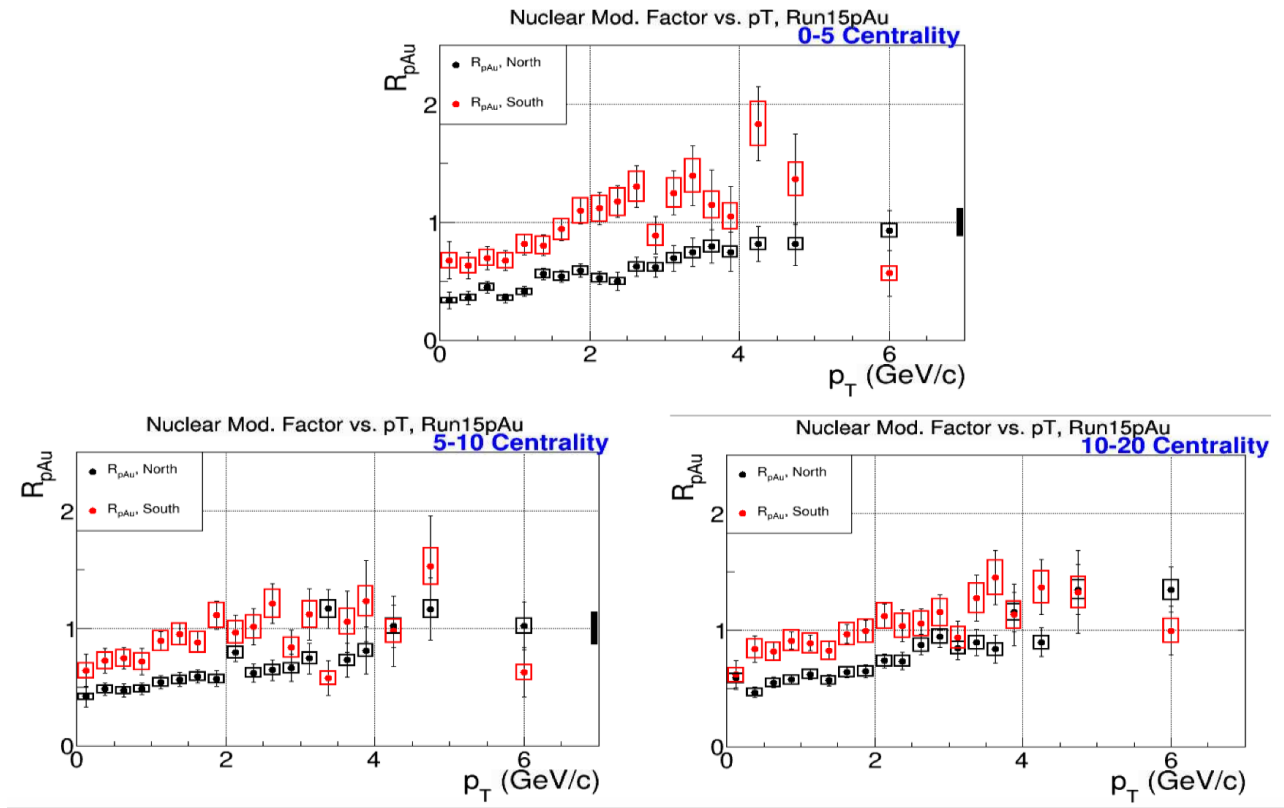


Figure 66: Run15pAu  $R_{pAu}$  vs.  $p_T$  for 0-5, 5-10, and 10-20 in both North and South Arms.

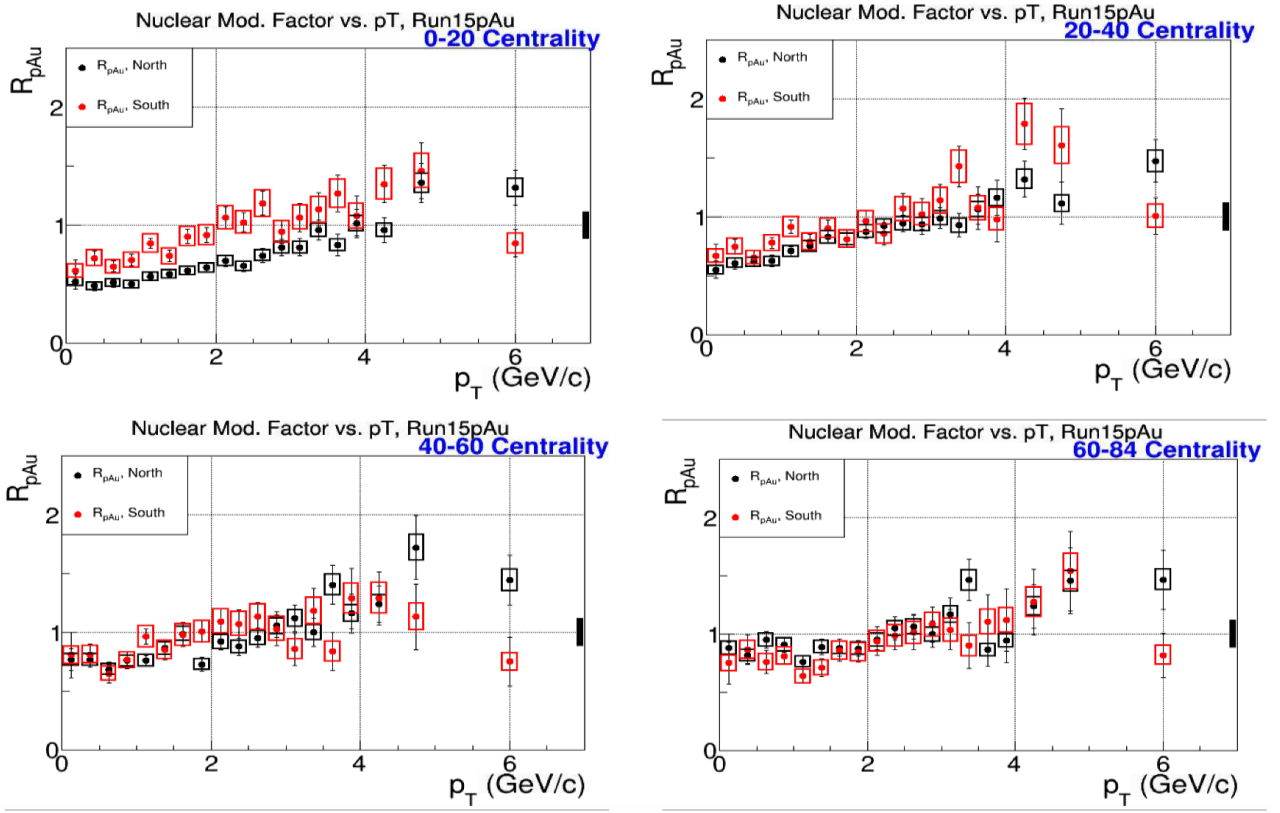


Figure 67: Run15pAu  $R_{pAu}$  vs.  $p_T$  for 0-20, 20-40, 40-60 and 60-84 in both North and South Arms.

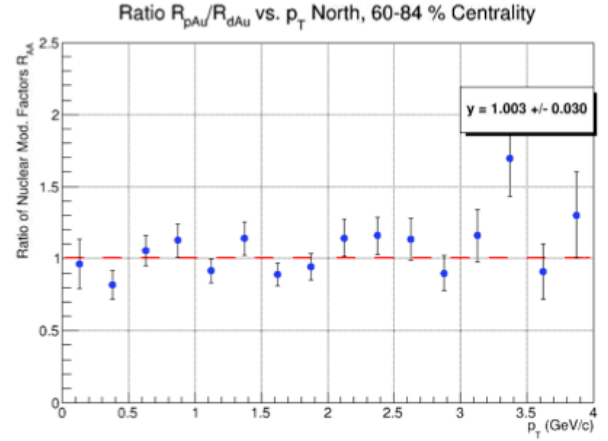
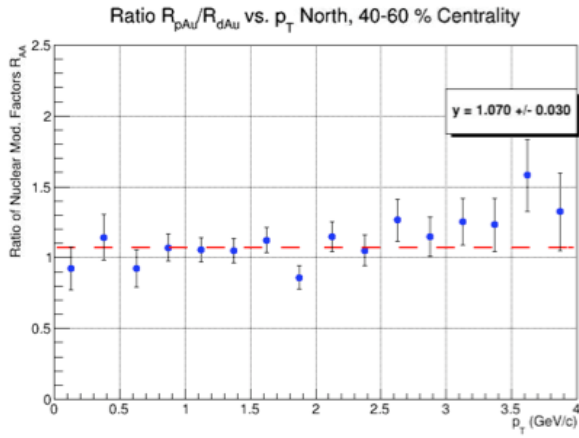
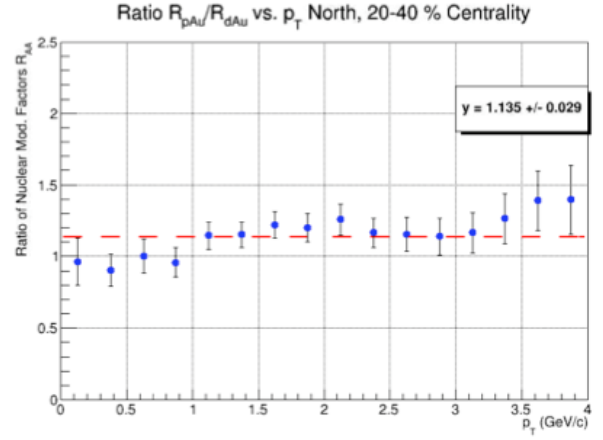
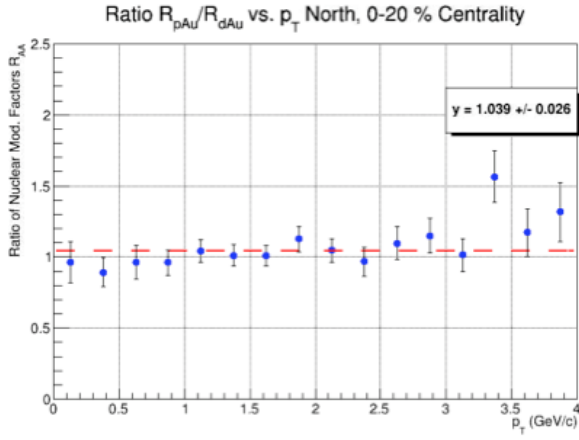


Figure 68: North Arm Results: The ratio of  $R_{pAu}/R_{dAu}$  for 0-20, 20-40, 40-60 and 60-84(60-88).

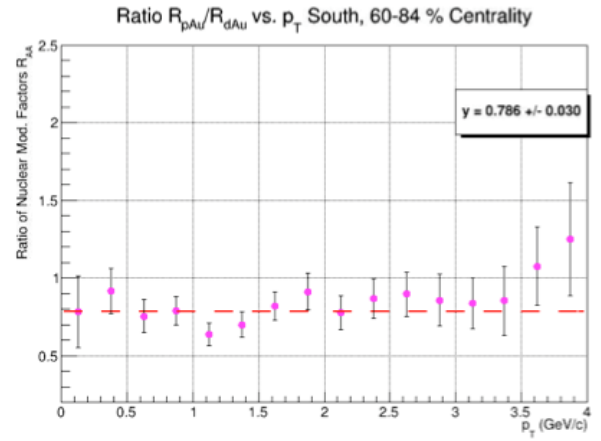
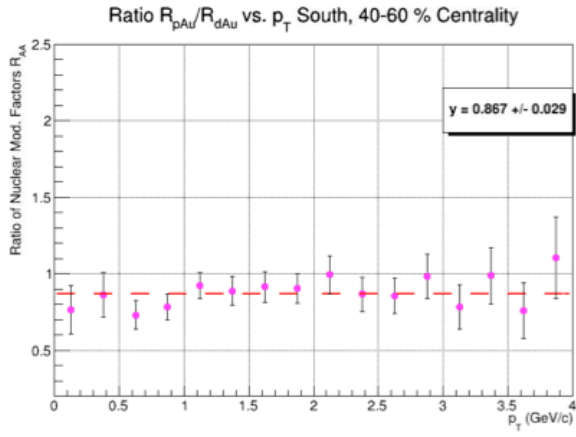
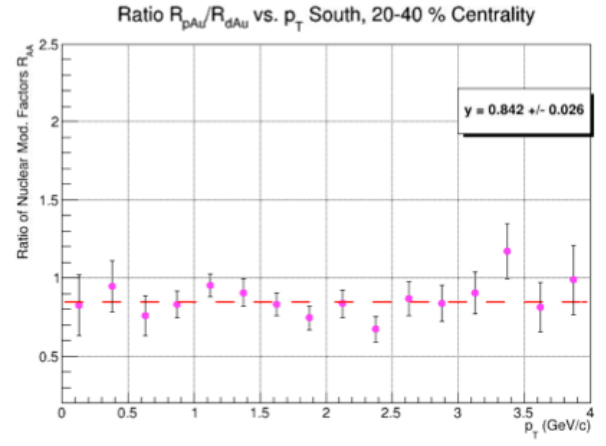
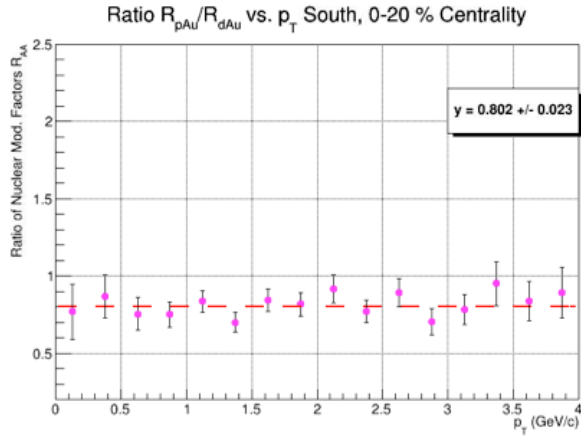


Figure 69: South Arm Results: The ratio of  $R_{pAu}/R_{dAu}$  for 0-20, 20-40, 40-60 and 60-84(60-88).

## 19 Run15pAl Results

The Run15pAu results show  $R_{AB}$  as a function of  $p_T$  and centrality, and are compared with Run08dAu. Additional plots include  $R_{AB}$  vs.  $N_{coll}$ , and the  $R_{AB}$  ratio of pAu to dAu. Each pp yield in the nuclear modification factor was fit individually, and a binshift correction was applied.

### 19.1 Fraction of Events per Centrality Range

Sanghoon Lim found and corrected an error in the preliminary results for Run15pAu and Run14HeAu, which extends to Run15pAl, concerning the fraction of events per centrality range. According to AN 1290, “high luminosity is an issue in the p+Al running.” “One normally expects a flat distribution as a function of run number (i.e. the same fraction of events in the 0-20% category for all runs). However, that is not what is observed due to double interactions.” “Users will need to check their specific analysis results and the impact of double interactions.” The fraction of events per centrality range  $\Delta x$  is included in the denominator of the invariant yield, which is needed to determine the nuclear modification factor as a function of centrality  $x$ :

$$Y_{AB}^{J/\psi}(x) = \frac{c(x)N_{AB}^{J/\psi}(x)}{2\pi p_T \Delta p_T \Delta y \epsilon_{trig}(x) \epsilon_{acc}(x) \Delta x N_{MB}} \quad (15)$$

$$R_{AB}(x) = \frac{dY_{AB}^{J/\psi}(x)}{N_{coll}(x) dY_{pp}^{J/\psi}} \quad (16)$$

#### 19.1.1 Sanghoon’s High Luminosity Study of Run15pAl

Sanghoon investigated the effects of double interactions in p+Al on pages 27-28 of [AN 1277](#). Sanghoon provided the following fraction of events per centrality range, listed in Table 6.

*Table 6: Run15pAl fraction of events per centrality range. All values determined by Sanghoon Lim.*

Arm	Centrality	incorrect $\Delta x$	correct $\Delta x$
North	0-20	0.20	0.2899
	20-40	0.20	0.277
	40-72	0.32	0.433
South	0-20	0.20	0.29
	20-40	0.20	0.277
	40-72	0.32	0.4327

### 19.2 Rebinning Centralities

We combined the 40-60 TH2D histogram with the 60-72 TH2D histogram using the same method as Run14HeAu, described in section 17.2.1. Taking a weighted average for the acceptance and MUID trigger efficiencies, the MUID trigger systematic error,  $N_{coll}$  and the bias correction factor were not necessary, as these were already binned in 40-72 centralities (AN 1207).



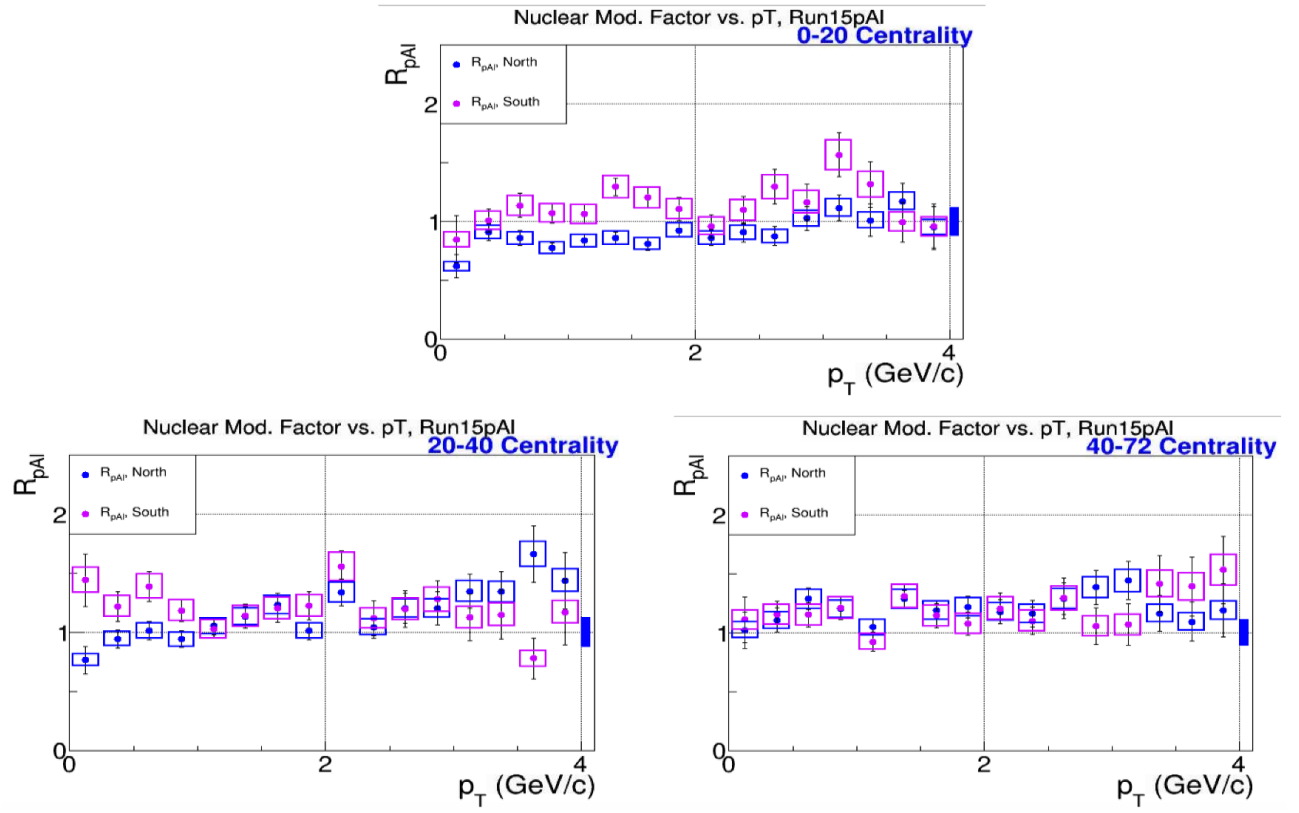


Figure 70: Run15pAl North and South  $R_{AB}$  vs.  $p_T$ . All centralities shown.

## 20 Run14HeAu Results

The Run14HeAu results show  $R_{AB}$  as a function of  $p_T$  and centrality, and are compared with Run15pAu. Additional plots include  $R_{AB}$  vs.  $N_{coll}$ , and the  $R_{AB}$  ratio of HeAu to pAu. Each pp yield in the nuclear modification factor was fit individually, and a binshift correction was applied. Please see section 14.1 for details on the  $p_T$  integrated  $N_{coll}$  calculation.

### 20.1 Fraction of Events per Centrality Range

Sanghoon Lim found and corrected an error in the preliminary results concerning the fraction of events per centrality range.

According to AN 1207, the 2D triggers are combined with BBCLL1 +/-30 cm, and the centrality distribution is flat. Therefore we can just take the ratio of centrality percentage between centrality bin and MB, and events do not need to be directly counted, as was necessary for Run15pAu. For example, the 0-20% range centrality for Run14HeAu would correspond to  $0.2/0.88 = 0.227$ .

The fraction of events per centrality range  $\Delta x$  is included in the denominator of the invariant yield, which is needed to determine the nuclear modification factor as a function of centrality  $x$ :

$$Y_{AB}^{J/\psi}(x) = \frac{c(x)N_{AB}^{J/\psi}(x)}{2\pi p_T \Delta p_T \Delta y \epsilon_{trig}(x) \epsilon_{acc}(x) \Delta x N_{MB}} \quad (17)$$

$$R_{AB}(x) = \frac{dY_{AB}^{J/\psi}(x)}{N_{coll}(x) dY_{pp}^{J/\psi}} \quad (18)$$

For Run14HeAu, Sanghoon determined the following fraction of events per centrality range, listed in Table 7.

Table 7: Run14HeAu fraction of events per centrality range. All values determined by Sanghoon Lim.

Arm	Centrality	incorrect $\Delta x$	correct $\Delta x$
North	0-20	0.20	0.227
	20-40	0.20	0.227
	40-88	0.48	0.545
South	0-20	0.20	0.227
	20-40	0.20	0.227
	40-88	0.48	0.545

### 20.2 Rebinning Centralities

The statistics were much lower in Run14HeAu than in Run15pAu, and it was necessary to combine the centrality range 40-60 with 60-88. To do this, we took the weighted average of  $N_{coll}$  from both centrality bins, and the weighted average of the bias correction factor from both centrality bins. The weight used in both cases was the centrality binwidth  $\Delta x = 0.2, 0.28$ .

To combine the acceptance and trigger efficiencies that Sanghoon generated, we again took the weighted average. The centrality bins 40-60 and 60-88 had been previously fit, and had their yields extracted. The weight used was then the yield for each  $p_T$  bin. This was also done for the trigger efficiency systematic error as well.

### 20.2.1 Combining TH2D Histograms

We combined the 40-60 TH2D histogram with the 60-88 TH2D histogram using the following method:

```
TH2D *t1;
TH2D *t2;

rootfile->GetObject("TH2D A", t1);
rootfile->GetObject("TH2D B", t2);

t2->Add(t1, 1);
t2->Write( );
```

The combining of two different TH2D histograms was checked by using the ROOT Method `TH2D->GetEntries( )`. We verified that the unlike-sign muon pairs in the North arm for the 40-60 and 60-88 centrality ranges summed to the `GetEntries( )` result of the newly combined TH2D. We verified the same in the South arm and found that all totals matched.

From the newly combined TH2D histogram, we used the `ProjectionX( )` method as described in AN 1391. We then verified that the sum of all projected histograms over the  $p_T$  range 0-12.0 GeV/c (which corresponds to 48 bins of width 0.25 GeV/c) totaled the same result returned using the ROOT Method:

```
TH2D->ProjectionX("ul", 1, 48)->GetEntries( );
```

### 20.3 $p_T$ Integrated $N_{coll}$

For the  $p_T$  integrated  $R_{AB}$  vs.  $N_{coll}$  plots, we took the weighted average over the same  $p_T$  range (0-7 GeV/c) for both Run15pAu  $R_{AB}$  data and Run08dAu  $R_{AB}$  data, the following formula:

$$R_{AB}(N_{coll}) = \frac{\sum_{p_T} R_{AB}(N_{coll}|p_T) dY_{p_T}^{pp}}{\sum_{p_T} dY_{p_T}^{pp}} \pm \frac{\sqrt{\sum_{p_T} \sigma_{p_T}^2 dY_{p_T}^{pp2}}}{\sum_{p_T} dY_{p_T}^{pp}} \quad (19)$$

where the weight used was the pp invariant yield. The information to reconstruct the pp invariant yield for Run08pp was found in the plain text tables for PPG125.

### 21 $\langle p_T^2 \rangle$ vs. $N_{coll}$

During an HI PWG meeting, Cesar de Silva requested to see the mean  $p_T^2$  vs.  $N_{coll}$  for pAu and  $^3\text{HeAu}$ . Tony had previously published results on  $J/\psi$  nuclear modification in Run08dAu (PPG125), and he calculated the mean pt squared in this paper (PRC). Tony also calculated it here for the requested systems. The two systems are compared up to a maximum  $p_T$  of 4.0 GeV/c.

## 22 Sum Over Centrality vs. Centrality Integrated

As a final cross check after all  $R_{AB}$  results were obtained, we compared the centrality-integrated results with the sum of centrality dependent results from the current analysis. To find the sum of centrality dependent results, we used the following formula:

$$R_{AB}^{sum}(p_T) = \left( \sum_x \frac{\Delta x R_{AB}(p_T|x) N_{coll}(x)}{c(x)} \right) \frac{c}{N_{coll}} \pm \sqrt{\left( R_{AB}(p_T|x) \frac{c}{N_{coll}} \right)^2 \left( \sum_x \frac{w_x \sigma_x}{R_{AB}(p_T|x)} \right)^2}, \quad (20)$$

where

$$w_x = \frac{\Delta x N_{coll}(x)}{c(x)} \quad (21)$$

where  $x$  is the centrality range,  $\Delta x$  is the fraction of events per centrality range and  $c(x)$  is the centrality-dependent bias correction factor. The factors ‘ $c$ ’ and ‘ $N_{coll}$ ’ are for the 0-100% centrality range.

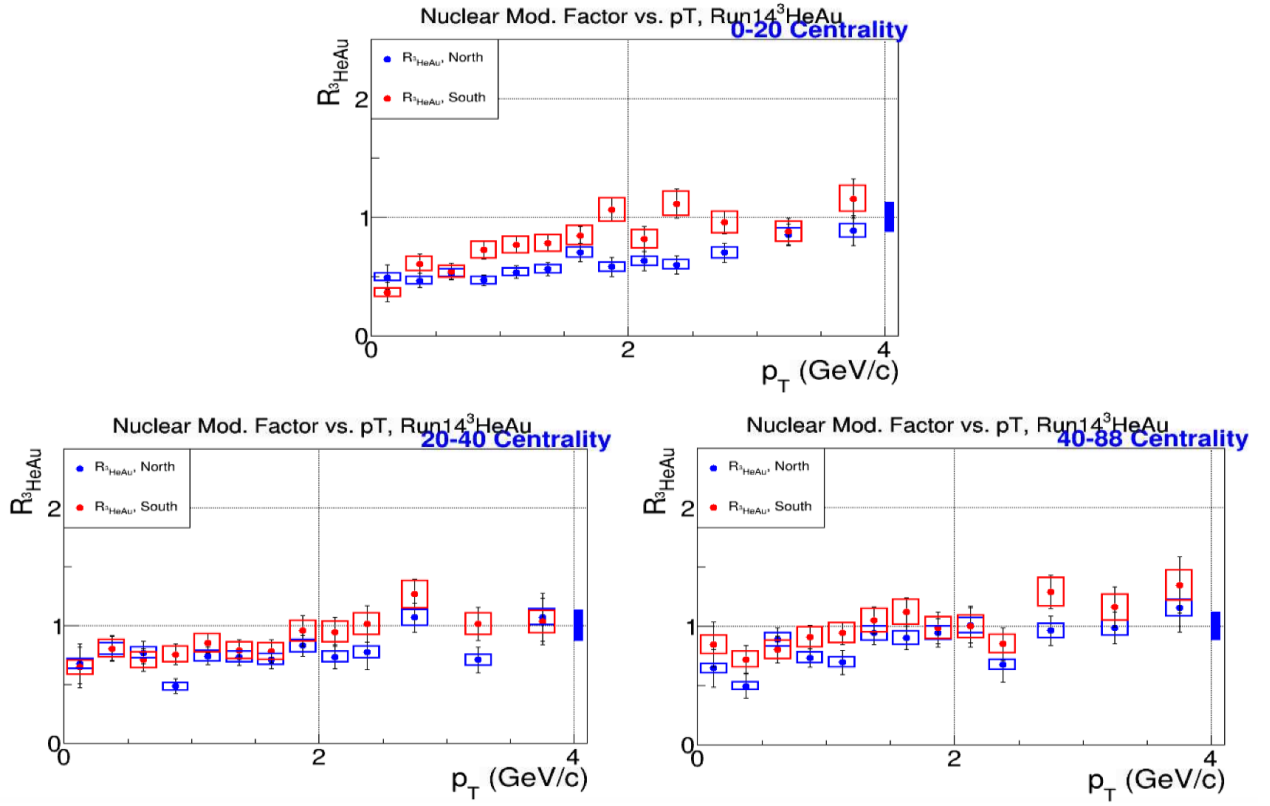


Figure 71: Run14HeAu North and South  $R_{AB}$  vs.  $p_T$ . All centralities shown.

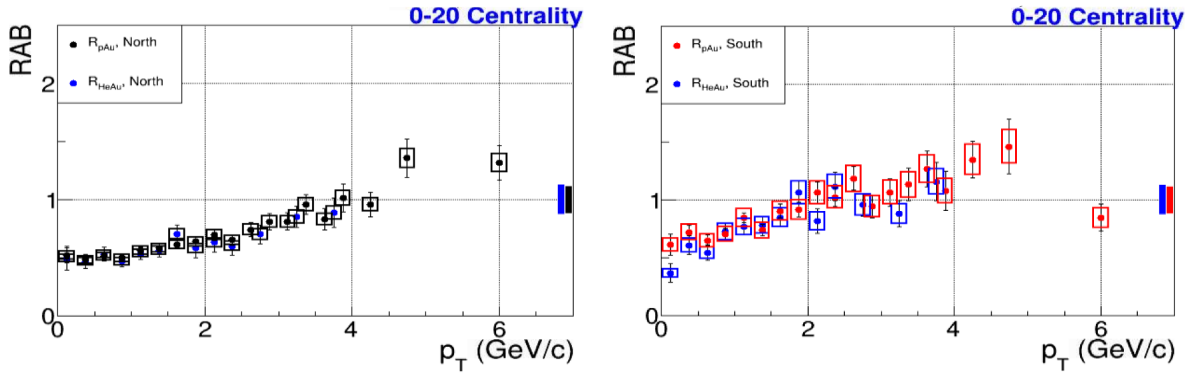


Figure 72: Run14HeAu  $R_{AB}$  vs.  $p_T$ , compared with Run15pAu. Centrality 0-20 shown for the North Arm, left, and South Arm.

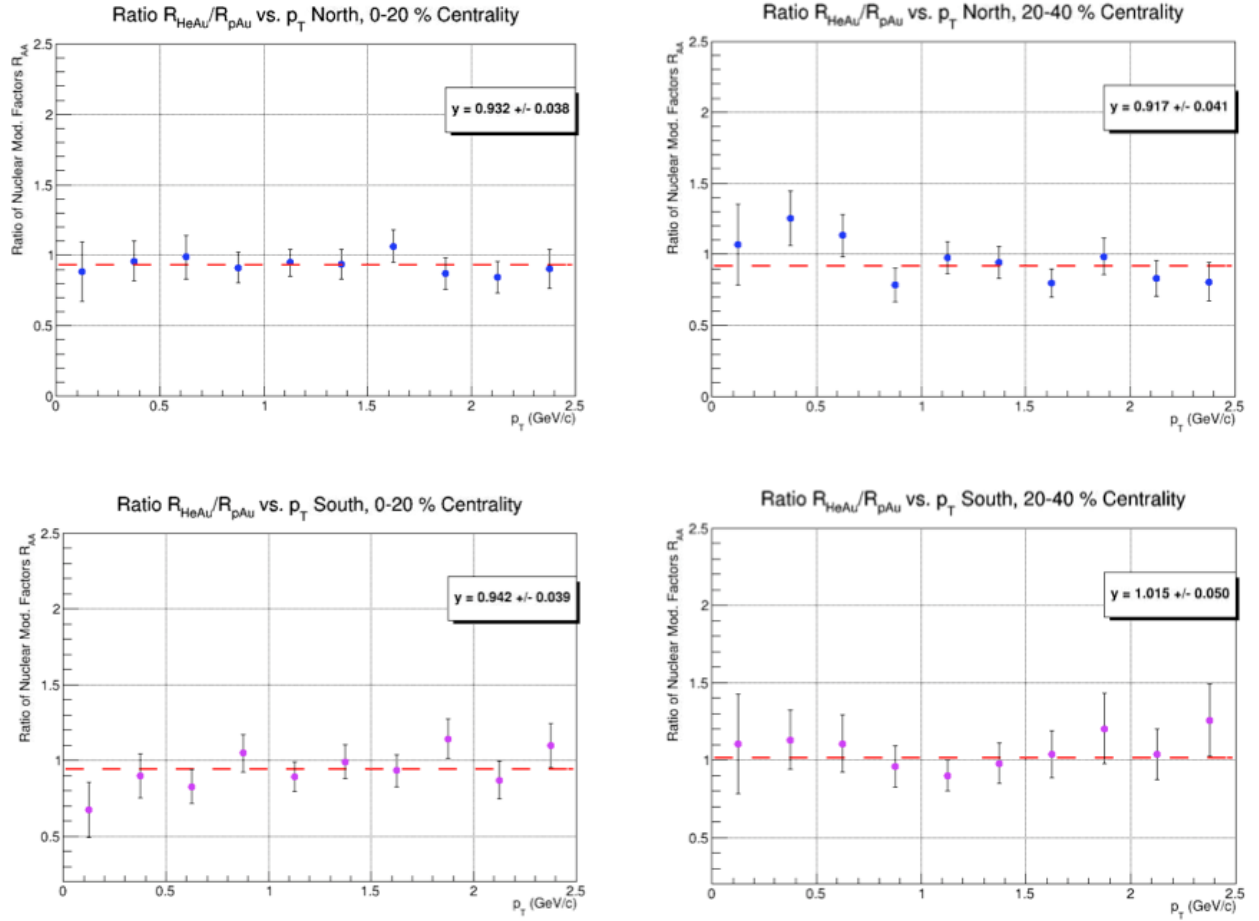


Figure 73: The ratio of  $R_{HeAu}/R_{pAu}$  for 0-20 and 20-40 centralities in the North, top, and South Arms.

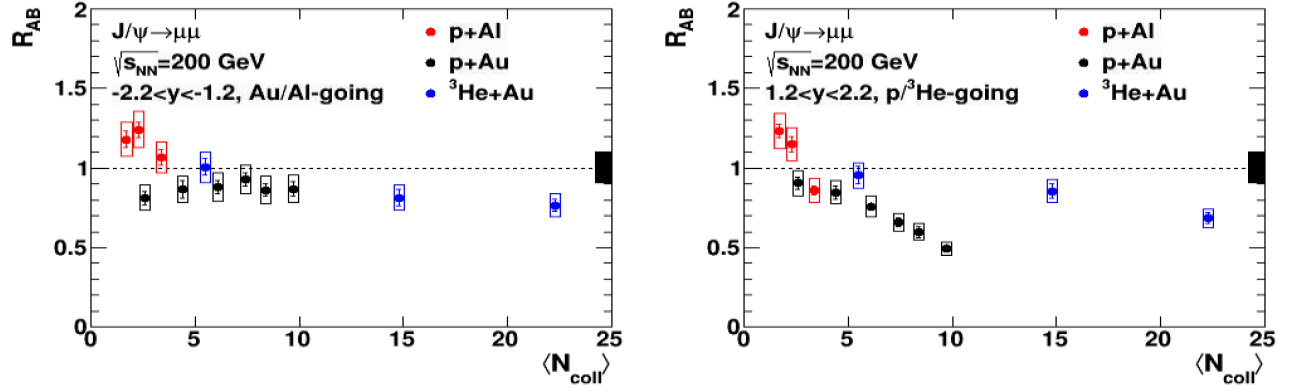


Figure 74:  $p_T$  Integrated  $R_{pAu}$  vs.  $N_{coll}$  for 0-5, 5-10, 10-20, 20-40, 40-60 and 60-84 in both North and South Arms. Also shown are  $p_T$  Integrated  $R_{pAl}$  for 0-20, 20-40, 40-72 and HeAu for 0-20, 20-40, 40-88.

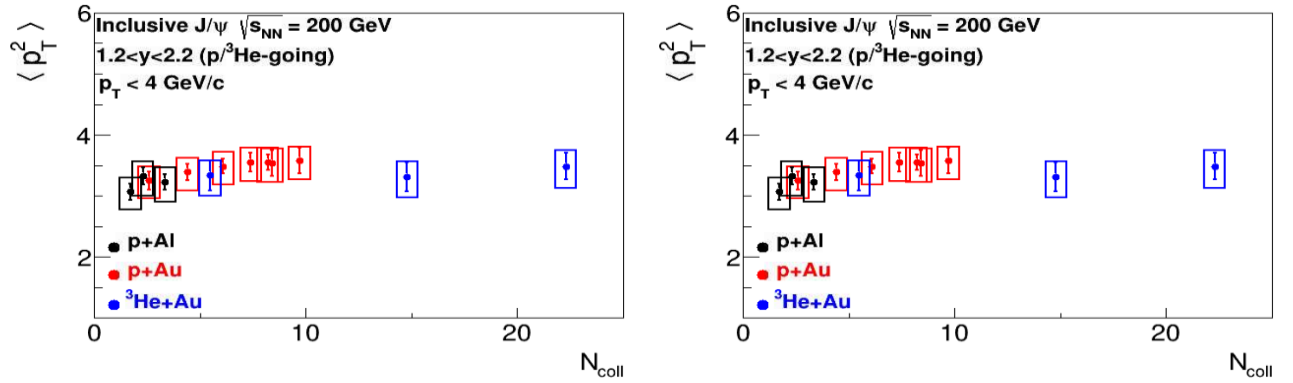


Figure 75:  $\langle p_T^2 \rangle$  vs.  $N_{coll}$  in the North, left, and South Arms for Run15pAl, Run15pAu and Run14HeAu.

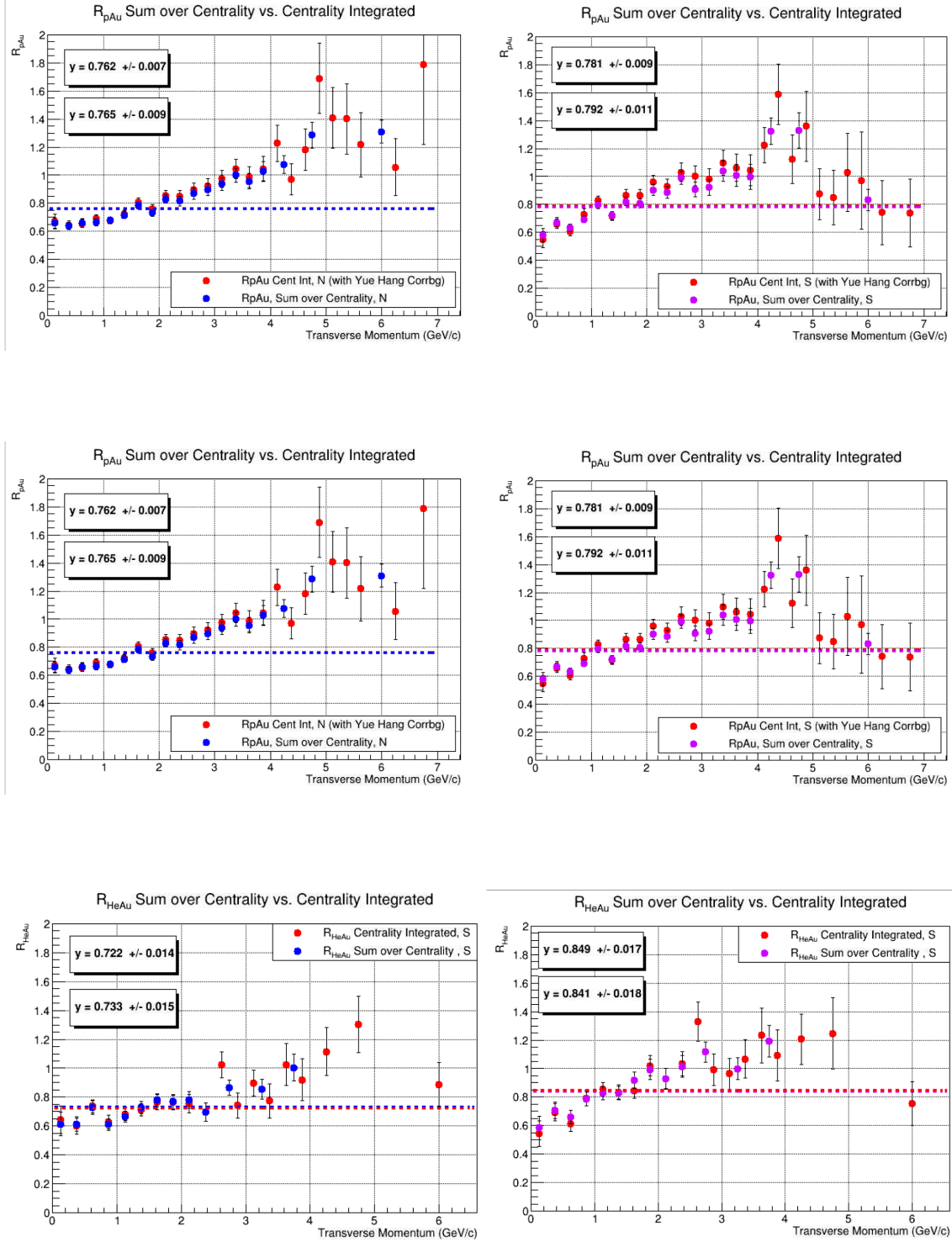


Figure 76: Top:  $R_{pAu}$  centrality integrated compared with the sum over all centralities in the North, left, and South arms. Middle:  $R_{pAl}$  centrality integrated compared with the sum over all centralities. Bottom:  $R_{HeAu}$  centrality integrated compared with the sum over all centralities. All measurements were made using Yue Hang's Correlated Background.



## 23 $R_{AB}$ vs. $y$

Preliminary was granted for Matt Durham and Sanghoon Lim for  $R_{AB}$  vs.  $y$  prior to the  $J/\psi$  transverse momentum analysis. Their results have been updated using Yue Hang's correlated background, and are shown below. Please see AN1354 for more details regarding these measurements.

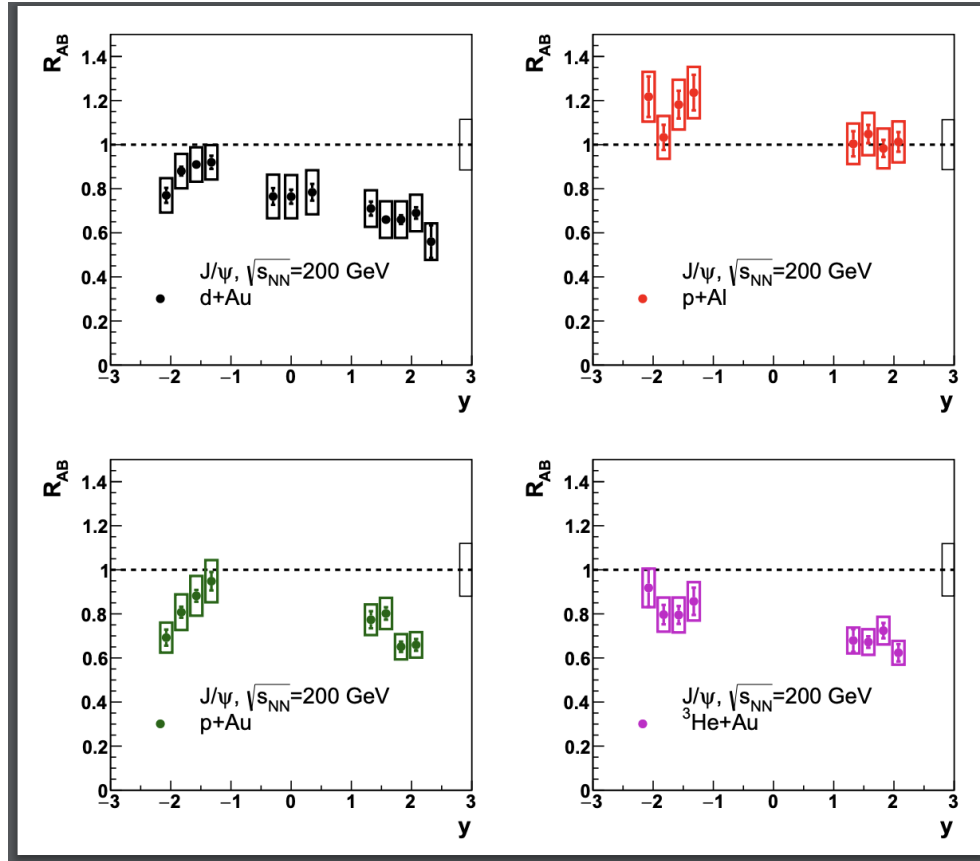


Figure 77:  $R_{AB}$  vs.  $y$  for Run15pAl, Run15pAu and Run14HeAu, compared with Run08dAu.

## 24 Rapidity with Centrality Dependence

Sanghoon Lim requested an additional measurement of  $R_{AB}$  vs.  $y$  with centrality dependence. All aspects of this measurement were carried out by Sanghoon aside from the yield extraction and systematic uncertainty due to the correlated background.

Yue Hang Leung's correlated background was used for all measurements. The Run15pp correlated background was used for Run15pAl, and the Run15pAu correlated background was used for both Run15pAu and Run14HeAu. This is the same approach that was used for  $J/\psi$  vs.  $p_T$ . Run15pAl Rapidity and Centrality binning matches the centrality and rapidity binning used for other measurements in this analysis. Run15pAl centrality: 0-20, 20-40, 40-72%. Run15pAu centrality: 0-5, 5-10, 10-20, 0-20, 20-40, 40-60, 60-88%. And Run14HeAu centrality: 0-20, 20-40, 40-88%.

There were enough statistics to complete these measurements in Run15pAu, Run15pAl and Run14HeAu. The rapidity binning is the same for all systems:  $1.2 < |y| < 1.45$ ,  $1.45 < |y| < 1.7$ ,  $1.7 < |y| < 1.95$ ,  $1.95 < |y| < 2.2$ . Example fits are shown in section 22.4.

### 24.1 Checks

Here we have also performed the same checks as with  $p_T$  and centrality dependence, comparing the sum over rapidity with the centrality integrated result. We also take the sum over centrality integrated fits and compare the result with the Minimum Bias fit. The results are shown for all systems.

0-20%					
Run15pAl	NORTH				
rap center	Case A	Ave FGH	Case F	Case G	Case H
1.325	355 +/- 22	351 +/- 22	348 +/- 25	354 +/- 21	352 +/- 21
1.575	1544 +/- 49	1473 +/- 58	1433 +/- 80	1432 +/- 46	1555 +/- 48
1.825	1657 +/- 54	1661 +/- 52	1620 +/- 55	1674 +/- 49	1689 +/- 53
2.075	993 +/- 37	1000 +/- 38	1006 +/- 39	983 +/- 38	1010 +/- 37
sum:	4549	4,485	4,407	4,443	4,606
cent Int	4496 +/- 86	4390 +/- 97	4300 +/- 117	4317 +/- 90	4552 +/- 85
sum/cent Int % diff	1.17%	2.14%	2.46%	2.88%	1.18%
sum Case A/Case FGH % diff		1.42%			
Case A/Case FGH cent Int % diff:		2.39%			
Run15pAl	SOUTH				
rap center	Case A	Ave Case FGH	Case F	Case G	Case H
-1.325	396 +/- 25	384 +/- 26	361 +/- 32	395 +/- 21	396 +/- 24
-1.575	1446 +/- 52	1427 +/- 50	1366 +/- 50	1457 +/- 50	1458 +/- 49
-1.825	1114 +/- 47	1156 +/- 42	1129 +/- 45	1155 +/- 47	1184 +/- 34
-2.075	348 +/- 35	364 +/- 29	357 +/- 31	363 +/- 32	373 +/- 24
sum:	3304	3,331	3213	3,370	3,411
cent Int	3286 +/- 82	3284 +/- 76	3133 +/- 80	3338 +/- 73	3382 +/- 74
sum/cent Int % diff	0.55%	1.42%	2.52%	0.95%	0.85%
sum Case A/Case FGH % diff		-0.81%			
Case A/Case FGH cent Int % diff:		0.06%			

20-40%					
Run15pAl	NORTH				
rap center	Case A	Ave FGH	Case F	Case G	Case H
1.325	227 +/- 17	218 +/- 17	204 +/- 17	225 +/- 16	226 +/- 17
1.575	1272 +/- 42	1240 +/- 52	1251 +/- 46	1193 +/- 68	1276 +/- 41
1.825	1388 +/- 44	1361 +/- 61	1363 +/- 51	1318 +/- 87	1403 +/- 44
2.075	747 +/- 34	770 +/- 47	782 +/- 37	738 +/- 68	791 +/- 35
sum:	3634	3,589	3,600	3,474	3,696
cent Int	3600 +/- 76	3495 +/- 85	3488 +/- 76	3363 +/- 100	3636 +/- 74
sum/cent Int % diff	0.94%	2.65%	3.16%	3.25%	1.64%
sum Case A/Case FGH % diff		1.25%			
Case A/Case FGH cent Int % diff:		2.96%			
Run15pAl	SOUTH				
rap center	Case A	Ave Case FGH	Case F	Case G	Case H
-1.325	302 +/- 19	295 +/- 20	281 +/- 22	302 +/- 19	302 +/- 19
-1.575	999 +/- 37	989 +/- 42	916 +/- 47	1025 +/- 39	1026 +/- 39
-1.825	715 +/- 36	748 +/- 35	738 +/- 39	753 +/- 33	754 +/- 34
-2.075	207 +/- 17	207 +/- 18	198 +/- 14	212 +/- 20	212 +/- 19
sum:	2223	2,239	2133	2,292	2,294
cent Int	2208 +/- 57	2188 +/- 57	2100 +/- 59	2231 +/- 56	2234 +/- 56
sum/cent Int % diff	0.68%	2.30%	1.56%	2.70%	2.65%
sum Case A/Case FGH % diff		0.72%			
Case A/Case FGH cent Int % diff:		0.91%			

40-72%					
Run15pAl	NORTH				
rap center	Case A	Ave FGH	Case F	Case G	Case H
1.325	292 +/- 19	281 +/- 22	258 +/- 27	293 +/- 20	291 +/- 19
1.575	1290 +/- 42	1262 +/- 45	1228 +/- 48	1262 +/- 44	1297 +/- 43
1.825	1450 +/- 48	1450 +/- 45	1435 +/- 40	1433 +/- 46	1481 +/- 48
2.075	929 +/- 39	935 +/- 40	956 +/- 41	914 +/- 43	934 +/- 36
sum:	3961	3,928	3,877	3,902	4,003
cent Int	3916 +/- 79	3843 +/- 81	3770 +/- 84	3799 +/- 85	3960 +/- 74
sum/cent Int % diff	1.14%	2.19%	2.79%	2.67%	1.08%
sum Case A/Case FGH % diff		0.84%			
Case A/Case FGH cent Int % diff:		1.88%			
Run15pAl	SOUTH				
rap center	Case A	Ave Case FGH	Case F	Case G	Case H
-1.325	250 +/- 18	244 +/- 19	241 +/- 22	245 +/- 18	245 +/- 18
-1.575	917 +/- 30	923 +/- 35	920 +/- 35	923 +/- 35	925 +/- 36
-1.825	714 +/- 31	740 +/- 31	738 +/- 32	733 +/- 31	750 +/- 31
-2.075	206 +/- 18	216 +/- 18	215 +/- 18	214 +/- 18	220 +/- 17
sum:	2087	2,123	2114	2,115	2,140
cent Int	2073 +/- 48	2109 +/- 50	2082 +/- 55	2107 +/- 43	2138 +/- 52
sum/cent Int % diff	0.67%	0.66%	1.52%	0.39%	0.09%
sum Case A/Case FGH % diff		-1.71%			
Case A/Case FGH cent Int % diff:		-1.72%			

0-5%							
Run15pAu	NORTH						
rap center	Fixed Case A	Case A	Ave FGH	Case F	Case G	Case H	AN 1354
1.325	155 +/- 14	149 +/- 14	149	150 +/- 15	145 +/- 14	151 +/- 19	-
1.575	643 +/- 28	624 +/- 29	604	610 +/- 34	603 +/- 30	600 +/- 36	-
1.825	562 +/- 28	561 +/- 30	548	555 +/- 31	547 +/- 37	543 +/- 41	-
2.075	277 +/- 20	274 +/- 22	272	282 +/- 25	267 +/- 27	267 +/- 24	-
sum:	1637	1608	1,573	1,597	1,562	1,561	-
rap Int	1632 +/- 47	1595 +/- 49	1557 +/- 63	1569 +/- 58	1556 +/- 60	1545 +/- 71	-
sum/rap Int % diff			0.81%	1.28%	1.77%	0.38%	1.03%
sum Case A/Case FGH % diff			2.20%				
Case A/Case FGH cent Int % diff:			2.54%				

Run15pAu	SOUTH						
rap center	Fixed Case A	Case A	Ave Case FGH	Case F	Case G	Case H	AN 1354
-1.325	247 +/- 25	240 +/- 21	241 +/- 20	240 +/- 20	241 +/- 20	241 +/- 20	-
-1.575	718 +/- 33	703 +/- 39	663 +/- 48	658 +/- 49	644 +/- 55	687 +/- 41	-
-1.825	474 +/- 29	487 +/- 33	513 +/- 29	525 +/- 29	507 +/- 30	507 +/- 27	-
-2.075	111 +/- 14	109 +/- 17	120 +/- 16	119 +/- 16	120 +/- 16	120 +/- 16	-
sum:	1550	1545	1,537	1542	1,499	1,555	-
rap Int	1537 +/- 50	1536 +/- 55	1576 +/- 53	1569 +/- 54	1579 +/- 52	1579 +/- 52	-
sum/rap Int % diff			0.58%	2.51%	1.74%	4.34%	1.23%
sum Case A/Case FGH % diff			0.52%				
Case A/Case FGH cent Int % diff:			-2.57%				

5-10%							
Run15pAu	NORTH						
rap center	Fixed Case A	Case A	Ave FGH	Case F	Case G	Case H	AN 1354
1.325	149 +/- 14	144 +/- 15	133 +/- 16	133 +/- 15	133 +/- 17	132 +/- 18	-
1.575	593 +/- 28	588 +/- 40	532 +/- 40	502 +/- 35	559 +/- 48	559 +/- 48	-
1.825	554 +/- 28	535 +/- 33	507 +/- 51	516 +/- 78	503 +/- 35	503 +/- 35	-
2.075	267 +/- 20	264 +/- 21	275 +/- 24	290 +/- 20	267 +/- 25	267 +/- 25	-
sum:	1563	1531	1,447	1,441	1,438	1,461	-
rap Int	1561 +/- 53	1539 +/- 54	1447 +/- 77	1441 +/- 71	1508 +/- 70	1447 +/- 77	-
sum/rap Int % diff			0.52%	0.00%	4.75%	5.85%	-
sum Case A/Case FGH % diff			6.51%				
Case A/Case FGH cent Int % diff:			6.16%				

Run15pAu	SOUTH						
rap center	Fixed Case A	Case A	Ave Case FGH	Case F	Case G	Case H	AN 1354
-1.325	194 +/- 16	189 +/- 17	175 +/- 23	168 +/- 26	170 +/- 21	187 +/- 23	-
-1.575	590 +/- 29	573 +/- 33	556 +/- 49	566 +/- 41	549 +/- 71	552 +/- 35	-
-1.825	424 +/- 29	420 +/- 26	427 +/- 34	438 +/- 26	421 +/- 39	422 +/- 37	-
-2.075	130 +/- 16	138 +/- 20	128 +/- 18	128 +/- 19	129 +/- 18	127 +/- 18	-
sum:	1338	1320	1,286	1300	1,269	1,288	-
rap Int	1328 +/- 44	1289 +/- 48	1279 +/- 71	1292 +/- 55	1278 +/- 59	1268 +/- 99	-
sum/rap Int % diff			2.38%	0.55%	-0.71%	1.56%	-
sum Case A/Case FGH % diff			2.61%				
Case A/Case FGH cent Int % diff:			0.79%				

10-20%							
Run15pAu	NORTH						
rap center	Fixed Case A	Case A	Ave FGH	Case F	Case G	Case H	AN 1354
1.325	220 +/- 18	224 +/- 18	222 +/- 18	222 +/- 18	222 +/- 18	219 +/- 17	-
1.575	1095 +/- 37	1074 +/- 38	1065 +/- 45	1061 +/- 41	1065 +/- 46	1069 +/- 48	-
1.825	1091 +/- 45	1082 +/- 59	1017 +/- 68	1057 +/- 78	1002 +/- 59	993 +/- 66	-
2.075	593 +/- 28	584 +/- 31	606 +/- 35	605 +/- 31	606 +/- 37	608 +/- 37	-
sum:	2999	2964	2,910	2,945	2,895	2,889	-
rap Int	2987 +/- 63	2931 +/- 66	2909 +/- 70	2891 +/- 66	2909 +/- 64	2927 +/- 81	-
sum/rap Int % diff			1.12%	0.03%	1.85%	0.48%	1.31%
sum Case A/Case FGH % diff			1.74%				
Case A/Case FGH cent Int % diff:			0.75%				

Run15pAu	SOUTH						
rap center	Fixed Case A	Case A	Ave Case FGH	Case F	Case G	Case H	AN 1354
-1.325	269 +/- 19	264 +/- 20	258 +/- 37	251 +/- 22	259 +/- 65	263 +/- 24	-
-1.575	937 +/- 37	921 +/- 42	878 +/- 58	889 +/- 48	855 +/- 78	890 +/- 47	-
-1.825	747 +/- 31	743 +/- 36	726 +/- 38	732 +/- 36	726 +/- 37	720 +/- 40	-
-2.075	181 +/- 17	186 +/- 20	186 +/- 22	187 +/- 21	186 +/- 23	185 +/- 22	-
sum:	2134	2114	2,048	2059	2,026	2,058	-
rap Int	2131 +/- 66	2124 +/- 65	2093 +/- 99	2096 +/- 66	2087 +/- 114	2096 +/- 116	-
sum/rap Int % diff			-0.47%	-2.17%	-1.78%	-2.97%	-1.83%
sum Case A/Case FGH % diff			3.17%				
Case A/Case FGH cent Int % diff:			1.47%				

0-20%							
Run15pAu	NORTH						
rap center	Fixed Case A	Case A	Ave FGH	Case F	Case G	Case H	AN 1354
1.325	520 +/- 26	513 +/- 27	514 +/- 26	513 +/- 26	514 +/- 26	514 +/- 26	-
1.575	2336 +/- 54	2288 +/- 57	2227 +/- 72	2223 +/- 72	2229 +/- 73	2229 +/- 70	-
1.825	2196 +/- 65	2178 +/- 64	2063 +/- 75	2124 +/- 66	2047 +/- 77	2018 +/- 81	-
2.075	1143 +/- 48	1125 +/- 60	1158 +/- 49	1169 +/- 46	1152 +/- 49	1154 +/- 52	-
sum:	6195	6104	5,962	6,029	5,942	5,915	-
rap Int	6191 +/- 91	6078 +/- 129	5960 +/- 126	5962 +/- 119	5965 +/- 124	5952 +/- 134	6026 +/- 138
sum/rap Int % diff		0.43%	0.03%	1.12%	-0.39%	-0.62%	
sum Case A/Case FGH % diff			2.35%				
Case A/Case FGH cent int % diff:			1.96%				

Run15pAu	SOUTH						
rap center	Fixed Case A	Case A	Ave Case FGH	Case F	Case G	Case H	AN 1354
-1.325	706 +/- 36	690 +/- 34	659 +/- 33	695 +/- 33	697 +/- 32	695 +/- 33	-
-1.575	2245 +/- 64	2207 +/- 80	2115 +/- 87	2148 +/- 82	2054 +/- 102	2143 +/- 76	-
-1.825	1674 +/- 74	1606 +/- 56	1592 +/- 75	1603 +/- 62	1586 +/- 80	1587 +/- 84	-
-2.075	410 +/- 25	416 +/- 28	442 +/- 28	440 +/- 29	443 +/- 27	443 +/- 27	-
sum:	5035	4919	4,808	4886	47,890	4,868	-
rap Int	4968 +/- 85	4916 +/- 105	4883 +/- 157	4876 +/- 153	4882 +/- 162	4890 +/- 155	5002 +/- 95
sum/rap Int % diff		0.06%	-1.55%	0.20%	2.11%	0.45%	
sum Case A/Case FGH % diff			2.28%				
Case A/Case FGH cent int % diff:			0.67%				

20-40%							
Run15pAu	NORTH						
rap center	Fixed Case A	Case A	Ave FGH	Case F	Case G	Case H	AN 1354
1.325	401 +/- 23	403 +/- 23	401 +/- 30	401 +/- 27	402 +/- 30	401 +/- 33	-
1.575	1893 +/- 54	1842 +/- 46	1688 +/- 83	1738 +/- 87	1662 +/- 84	1665 +/- 79	-
1.825	1922 +/- 55	1915 +/- 53	1908 +/- 57	1908 +/- 60	1909 +/- 59	1907 +/- 52	-
2.075	994 +/- 40	964 +/- 41	1015 +/- 54	1036 +/- 41	1005 +/- 59	1003 +/- 61	-
sum:	5210	5112	5052 +/- 119	5,083	4,978	4,976	-
rap Int	5162 +/- 89	5124	5012	5086 +/- 127	5049 +/- 77	5021 +/- 154	5077 +/- 120
sum/rap Int % diff		0.23%	0.79%	0.06%	1.42%	0.90%	
sum Case A/Case FGH % diff			2.21%				
Case A/Case FGH cent int % diff:			1.18%				

Run15pAu	SOUTH						
rap center	Fixed Case A	Case A	Ave Case FGH	Case F	Case G	Case H	AN 1354
-1.325	427 +/- 26	428 +/- 26	425 +/- 27	425 +/- 27	424 +/- 29	427 +/- 26	-
-1.575	1435 +/- 51	1427 +/- 46	1392 +/- 54	1396 +/- 53	1382 +/- 61	1399 +/- 49	-
-1.825	1112 +/- 46	1112 +/- 42	1065 +/- 48	1088 +/- 40	1057 +/- 58	1051 +/- 46	-
-2.075	256 +/- 22	235 +/- 22	256 +/- 22	255 +/- 19	256 +/- 23	258 +/- 23	-
sum:	3230	3202	3,138	3164	3,119	3,135	-
rap Int	3203 +/- 80	3173 +/- 79	3100 +/- 88	3087 +/- 82	3040 +/- 104	3173 +/- 79	3082 +/- 105
sum/rap Int % diff		0.91%	1.22%	4.12%	2.57%	1.20%	
sum Case A/Case FGH % diff			2.02%				
Case A/Case FGH cent int % diff:			2.33%				

40-60%							
Run15pAu	NORTH						
rap center	Fixed Case A	Case A	Ave FGH	Case F	Case G	Case H	AN 1354
1.325	295 +/- 19	290 +/- 20	265 +/- 27	268 +/- 26	265 +/- 25	262 +/- 30	-
1.575	1402 +/- 45	1400 +/- 44	1351 +/- 56	1370 +/- 48	1345 +/- 61	1337 +/- 58	-
1.825	1467 +/- 41	1454 +/- 68	1526 +/- 60	1515 +/- 93	1531 +/- 44	1531 +/- 44	-
2.075	849 +/- 39	832 +/- 35	880 +/- 34	876 +/- 34	882 +/- 34	882 +/- 34	-
sum:	4013	3976	4,022	4,029	4,023	4,012	-
rap Int	3944 +/- 80	3949 +/- 77	3948 +/- 108	3956 +/- 98	3961 +/- 98	3926 +/- 138	4022 +/- 152
sum/rap Int % diff		1.29%	1.86%	1.83%	1.55%	2.17%	
sum Case A/Case FGH % diff			-1.15%				
Case A/Case FGH cent int % diff:			0.03%				

Run15pAu	SOUTH						
rap center	Fixed Case A	Case A	Ave Case FGH	Case F	Case G	Case H	AN 1354
-1.325	271 +/- 20	269 +/- 19	262 +/- 21	262 +/- 20	262 +/- 23	262 +/- 19	-
-1.575	992 +/- 41	994 +/- 40	921 +/- 47	960 +/- 45	896 +/- 56	908 +/- 41	-
-1.825	653 +/- 29	654 +/- 28	687 +/- 34	685 +/- 32	687 +/- 35	689 +/- 34	-
-2.075	150 +/- 15	153 +/- 17	172 +/- 23	174 +/- 19	169 +/- 27	174 +/- 22	-
sum:	2066	2070	2,042	2081	2,014	2,033	-
rap Int	2063 +/- 51	2034 +/- 55	2030 +/- 69	2056 +/- 58	2020 +/- 74	2014 +/- 74	2026 +/- 98
sum/rap Int % diff		1.75%	0.59%	1.21%	0.30%	0.94%	
sum Case A/Case FGH % diff			1.36%				
Case A/Case FGH cent int % diff:			0.20%				

60-84%							
Run15pAu	NORTH						
rap center	Fixed Case A	Case A	Ave FGH	Case F	Case G	Case H	AN 1354
1.325	202 +/- 16	198 +/- 17	185 +/- 21	185 +/- 21	184 +/- 25	185 +/- 17	-
1.575	1004 +/- 35	1023 +/- 37	1021 +/- 39	1019 +/- 41	1024 +/- 36	1020 +/- 39	-
1.825	1160 +/- 43	1141 +/- 42	1127 +/- 54	1127 +/- 48	1127 +/- 58	1127 +/- 56	-
2.075	716 +/- 34	714 +/- 38	724 +/- 58	722 +/- 35	725 +/- 73	725 +/- 65	-
sum:	3081	3076	3,057	3,053	3,060	3,057	-
rap Int	3058 +/- 63	3031 +/- 65	3056 +/- 76	3052 +/- 75	3059 +/- 76	3058 +/- 77	3146 +/- 81
sum/rap Int % diff		1.47%	0.03%	0.03%	0.03%	0.03%	
sum Case A/Case FGH % diff			0.62%				
Case A/Case FGH cent Int % diff:			-0.82%				
Run15pAu	SOUTH						
rap center	Fixed Case A	Case A	Ave Case FGH	Case F	Case G	Case H	AN 1354
-1.325	183 +/- 14	181 +/- 15	182 +/- 15	182 +/- 15	182 +/- 15	182 +/- 15	-
-1.575	620 +/- 31	615 +/- 26	629 +/- 36	629 +/- 34	629 +/- 37	629 +/- 36	-
-1.825	474 +/- 25	474 +/- 25	500 +/- 25	498 +/- 26	500 +/- 25	500 +/- 25	-
-2.075	106 +/- 12	112 +/- 24	104 +/- 15	102 +/- 14	93 +/- 19	117 +/- 12	-
sum:	1383	1382	1,415	1411	1,404	1,428	-
rap Int	1363 +/- 42	1355 +/- 43	1398 +/- 50	1412 +/- 59	1356 +/- 48	1426 +/- 44	1438 +/- 43
sum/rap Int % diff		1.83%	1.21%	0.07%	3.48%	0.14%	
sum Case A/Case FGH % diff			-2.34%				
Case A/Case FGH cent Int % diff:			-3.12%				
SUMMARY	North Sum	MinBias, N	MB/Sum % diff	South Sum	MinBias, S	MB/Sum % diff	MB/Sum % diff
Sum cent Int	18229	18328 +/- 175	0.54%	11578	11661 +/- 152	0.71%	-0.55%
AN1354 sum cent Int	18371	18194 +/- 224	1.09%	11548	11602 +/- 193	0.47%	0.47%

0-20%							
Run14HeAu	NORTH						
rap center	Case A	Ave FGH	Case F	Case G	Case H	AN 1354	
1.325	122 +/- 14	116 +/- 15	116 +/- 14	116 +/- 15	116 +/- 16	-	
1.575	556 +/- 29	546 +/- 39	550 +/- 35	546 +/- 35	537 +/- 46	-	
1.825	560 +/- 34	533 +/- 37	529 +/- 32	532 +/- 35	539 +/- 44	-	
2.075	281 +/- 25	280 +/- 20	284 +/- 19	280 +/- 20	275 +/- 22	-	
sum:	1519	1,475	1,479	1,474	1,467	-	
rap Int	1509 +/- 51	1471 +/- 53	1486 +/- 48	1470 +/- 57	1476 +/- 55	1517 +/- 64	
sum/rap Int % diff	1.25%	0.27%	-0.47%	0.27%	-0.61%		
sum Case A/Case FGH % diff		2.94%					
Case A/Case FGH cent Int % diff:		-2.55%					
cent Int Case A/ prelim % diff:		-0.53%					
Run14HeAu	SOUTH						
rap center	Case A	Ave Case FGH	Case F	Case G	Case H	AN 1354	
-1.325	240 +/- 24	240 +/- 27	236 +/- 30	242 +/- 22	241 +/- 30	-	
-1.575	732 +/- 38	725 +/- 45	725 +/- 39	721 +/- 40	728 +/- 55	-	
-1.825	658 +/- 43	653 +/- 46	660 +/- 43	667 +/- 41	703 +/- 65	-	
-2.075	196 +/- 23	196 +/- 23	196 +/- 21	196 +/- 23	196 +/- 25	-	
sum:	1826	1,814	1,817	1,826	1,877	-	
rap Int	1814 +/- 79	1829 +/- 80	1778 +/- 66	1852 +/- 77	1857 +/- 97	1837 +/- 83	
sum/rap Int % diff	0.66%	-0.82%	2.17%	-1.41%	1.07%		
sum Case A/Case FGH % diff		0.38%					
Case A/Case FGH cent Int % diff:		0.66%					
cent Int Case A/ prelim % diff:		-0.82%					

20-40%						
Run14HeAu	NORTH					
rap center	Case A	Ave FGH	Case F	Case G	Case H	AN 1354
1.325	92 +/- 11	95 +/- 10	95 +/- 10	95 +/- 10	95 +/- 10	-
1.575	370 +/- 25	371 +/- 29	366 +/- 27	373 +/- 25	374 +/- 35	-
1.825	493 +/- 31	494 +/- 26	494 +/- 26	494 +/- 26	494 +/- 27	-
2.075	188 +/- 16	202 +/- 16	205 +/- 16	200 +/- 17	200 +/- 16	-
sum:	1143	1,162	1,160	1,162	1,163	-
rap Int	1154 +/- 47	1186 +/- 43	1183 +/- 41	1189 +/- 41	1185 +/- 47	1182 +/- 40
sum/rap Int % diff	-0.96%	-2.04%	-1.96%	-2.30%	-1.87%	
sum Case A/Case FGH % diff		-1.65%				
Case A/Case FGH cent Int % diff:		-2.74%				
cent Int Case A/ prelim % diff:		-2.40%				
Run14HeAu	SOUTH					
rap center	Case A	Ave Case FGH	Case F	Case G	Case H	AN 1354
-1.325	133 +/- 16	136 +/- 14	137 +/- 14	138 +/- 14	132 +/- 14	-
-1.575	450 +/- 30	406 +/- 34	392 +/- 34	412 +/- 37	413 +/- 31	-
-1.825	441 +/- 25	438 +/- 28	432 +/- 31	441 +/- 27	441 +/- 25	-
-2.075	150 +/- 17	146 +/- 18	150 +/- 15	138 +/- 24	150 +/- 15	-
sum:	1170	1,126	1111	1,129	1,136	-
rap Int	1158 +/- 45	1117 +/- 53	1122 +/- 56	1137 +/- 51	1093 +/- 56	1116 +/- 49
sum/rap Int % diff	1.09%	0.80%	-0.99%	-0.71%	3.86%	
sum Case A/Case FGH % diff		3.83%				
Case A/Case FGH cent Int % diff:		3.60%				
cent Int Case A/ prelim % diff:		3.69%				

40-88%						
Run14HeAu	NORTH					
rap center	Case A	Ave FGH	Case F	Case G	Case H	AN 1354
1.325	116 +/- 12	114 +/- 14	114 +/- 13	115 +/- 17	114 +/- 13	-
1.575	389 +/- 24	382 +/- 37	377 +/- 27	383 +/- 43	386 +/- 41	-
1.825	454 +/- 28	433 +/- 37	448 +/- 26	427 +/- 44	424 +/- 41	-
2.075	183 +/- 16	188 +/- 16	190 +/- 17	188 +/- 16	185 +/- 14	-
sum:	1151	1,117	1,129	1,113	1,109	-
rap Int	1123 +/- 46	1099 +/- 55	1105 +/- 46	1104 +/- 46	1087 +/- 74	1161 +/- 86
sum/rap Int % diff	2.46%	1.62%	2.15%	0.81%	2.00%	
sum Case A/Case FGH % diff		2.65%				
Case A/Case FGH cent Int % diff:		2.16%				
cent Int Case A/ prelim % diff:		-3.33%				
Run14HeAu	SOUTH					
rap center	Case A	Ave Case FGH	Case F	Case G	Case H	AN 1354
-1.325	140 +/- 15	139 +/- 20	135 +/- 29	144 +/- 14	138 +/- 16	-
-1.575	489 +/- 28	488 +/- 32	489 +/- 31	485 +/- 33	489 +/- 33	-
-1.825	393 +/- 31	404 +/- 25	403 +/- 25	405 +/- 25	405 +/- 25	-
-2.075	122 +/- 14	129 +/- 16	129 +/- 15	129 +/- 15	129 +/- 17	-
sum:	1144	1,160	1156	1,163	1,161	-
rap Int	1128 +/- 46	1153 +/- 41	1150 +/- 42	1155 +/- 41	1155 +/- 41	1126 +/- 112
sum/rap Int % diff	1.41%	0.61%	0.52%	0.69%	0.52%	
sum Case A/Case FGH % diff		1.29%				
Case A/Case FGH cent Int % diff:		-2.19%				
cent Int Case A/ prelim % diff:		0.18%				
SUMMARY	North Sum	MinBias, N	MB/Sum % diff	South Sum	MinBias, S	MB/Sum % diff
Sum cent Int	3786	3804 +/- 88	-0.47%	4100	4069 +/- 103	0.76%
AN1354 sum cent Int	3860	3825 +/- 91	0.91%	4079	3987 +/- 118	2.28%

## 24.2 Corrbg Systematic Uncertainty

To calculate the systematic uncertainty due to the correlated background, we used Sanghoon's Method (described in section 6.1). Here we have included the calculations for Run15pAl as an example.

0-20%						
NORTH						
Ave FGH	Case A	Case A err	$\text{delta }  \text{counts\_FGH} - \text{counts\_A}  / \text{counts\_A}$	$\text{sigma } (\text{err\_A} / \text{counts\_A})$	delta - sigma	
351	355	22	0.01126760563	0.06197183099	-0.05070422535	
1473	1544	49	0.04598445596	0.0317357513	0.01424870466	
1661	1657	54	0.002414001207	0.03258901629	-0.03017501509	
1000	993	37	0.007049345418	0.03726082578	-0.03021148036	
ave sigma_corrbg:			0.01667885205			

SOUTH						
Ave FGH	Case A	Case A err	$\text{delta }  \text{counts\_FGH} - \text{counts\_A}  / \text{counts\_A}$	$\text{sigma } (\text{err\_A} / \text{counts\_A})$	delta - sigma	
384	396	25	0.0303030303	0.06313131313	-0.03282828283	
1,427	1446	52	0.01313969571	0.03596127248	-0.02282157676	
1,156	1114	47	0.03770197487	0.04219030521	-0.004488330341	
364	348	35	0.04597701149	0.1005747126	-0.05459770115	
ave sigma_corrbg:			0.03178042809			

20-40%						
NORTH						
Ave FGH	Case A	Case A err	$\text{delta }  \text{counts\_FGH} - \text{counts\_A}  / \text{counts\_A}$	$\text{sigma } (\text{err\_A} / \text{counts\_A})$	delta - sigma	
218	227	17	0.03964757709	0.07488986784	-0.03524229075	
1240	1272	42	0.0251572327	0.03301886792	-0.00786163522	
1361	1388	44	0.01945244957	0.03170028818	-0.01224783862	
770	747	34	0.03078982597	0.04551539491	-0.01472556894	
ave sigma_corrbg:			0.02876177133			
SOUTH						
Ave FGH	Case A	Case A err	$\text{delta }  \text{counts\_FGH} - \text{counts\_A}  / \text{counts\_A}$	$\text{sigma } (\text{err\_A} / \text{counts\_A})$	delta - sigma	
295	302	19	0.02317880795	0.06291390728	-0.03973509934	
989	999	37	0.01001001001	0.03703703704	-0.02702702703	
748	715	36	0.04615384615	0.05034965035	-0.004195804196	
207	207	17	0	0.08212560386	-0.08212560386	
ave sigma_corrbg:			0.01983566603			

40-72%						
NORTH						
Ave FGH	Case A	Case A err	$\text{delta }  \text{counts\_FGH} - \text{counts\_A}  / \text{counts\_A}$	$\text{sigma } (\text{err\_A} / \text{counts\_A})$	delta - sigma	
281	292	19	0.03767123288	0.06506849315	-0.02739726027	
1262	1290	42	0.02170542636	0.03255813953	-0.01085271318	
1450	1450	48	0	0.03310344828	-0.03310344828	
935	929	39	0.006458557589	0.04198062433	-0.03552206674	
ave sigma_corrbg:			0.01645880421			
SOUTH						
Ave FGH	Case A	Case A err	$\text{delta }  \text{counts\_FGH} - \text{counts\_A}  / \text{counts\_A}$	$\text{sigma } (\text{err\_A} / \text{counts\_A})$	delta - sigma	
244	250	18	0.024	0.072	-0.048	
923	917	30	0.006543075245	0.03271537623	-0.02617230098	
740	714	31	0.03641456583	0.04341736695	-0.00700280112	
216	206	18	0.04854368932	0.08737864078	-0.03883495146	
ave sigma_corrbg:			0.0288753326			



## 24.3 Example Fits

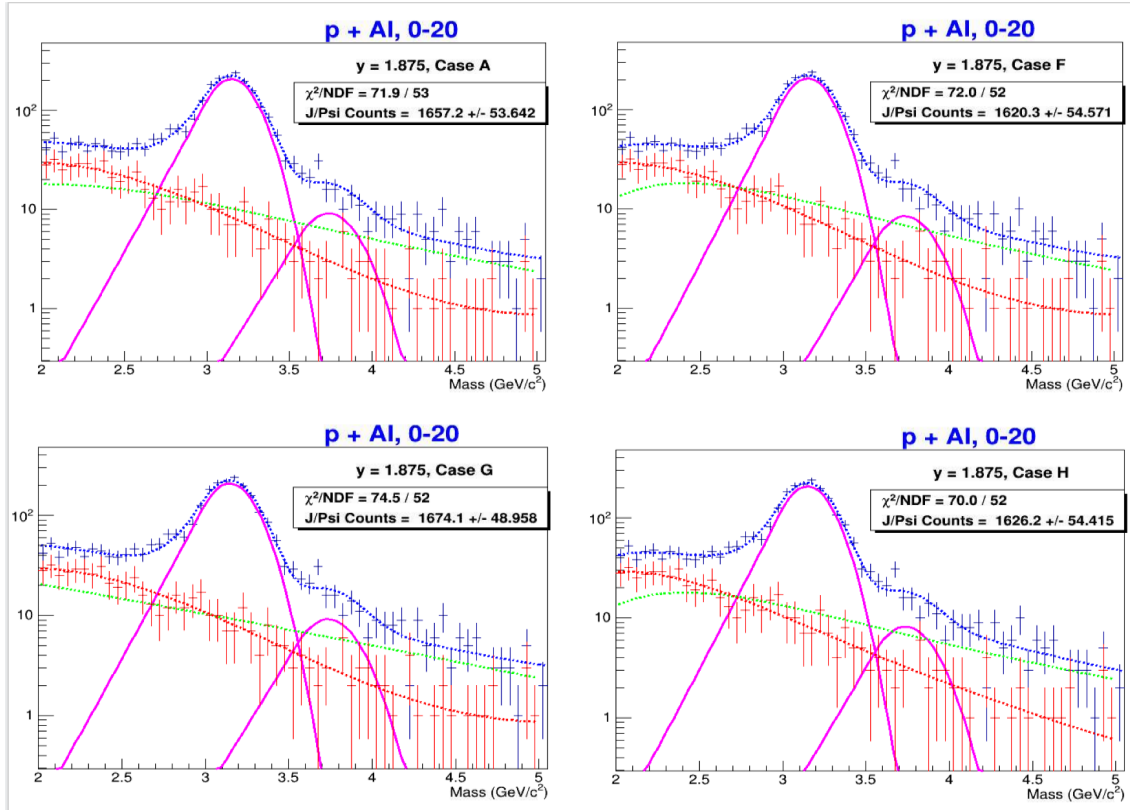
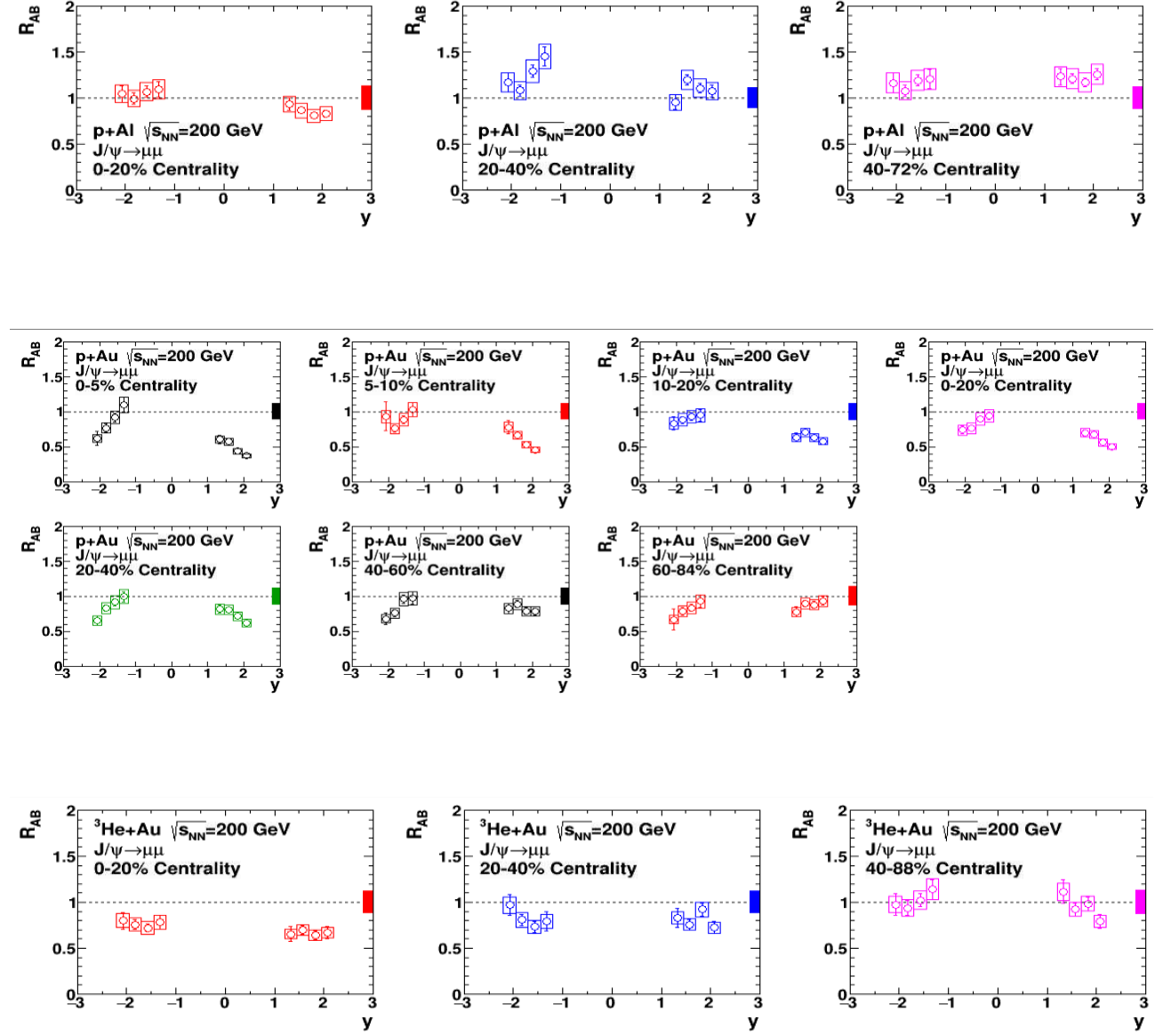


Figure 78: Top Left: pAl at forward rapidity  $1.7 < y < 1.95$  and 0-20% centrality for Case A compared with the corresponding Case F, G and H fits.

## 24.4 Results

The  $J/\psi$  lineshape in Run15pAl was not fixed for the rapidity with centrality dependence as was done for  $p_T$  with centrality dependence because the fits were stable having more statistics (larger binwidths).



## A Raw $J/\psi$ Counts: $p_T$ /Rapidity/Centrality Integrated

Table 8:  $p_T$ /rapidity integrated raw  $J/\psi$  counts for Run15pp.  $p_T$ /rapidity/centrality integrated (Minimum Bias) counts for Run15pAl, Run15pAu and Run14HeAu.

Arm	System	Raw $J/\psi$ Counts
North	Run15pp	$31,452 \pm 215$
	Run15pAl	$11,738 \pm 138$
	Run15pAu	$18,328 \pm 175$
	Run14HeAu	$3,804 \pm 88$
South	Run15pp	$28,511 \pm 205$
	Run15pAl	$7,455 \pm 115$
	Run15pAu	$11,661 \pm 152$
	Run14HeAu	$4,069 \pm 103$

## Raw $J/\psi$ Counts: Centrality Dependent ( $p_T$ /Rapidity Integrated)

[AN 1354 Section 4.7](#)

## Raw $J/\psi$ Counts: Rapidity Dependent ( $p_T$ /Centrality Integrated)

[AN 1354 Section 4.7](#)

## B Raw $J/\psi$ Counts:

### $p_T$ Dependent (Rapidity/Centrality Integrated)

Table 9: North arm raw  $J/\psi$  counts with statistical uncertainties obtained from the small systems study.

$p_T$ [GeV/c]	Run15pp, $N$	Run15pAu, $N$	Run15pAl, $N$	Run14HeAu, $N$
0.0 - 0.25	832 $\pm$ 51	421 $\pm$ 24	258 $\pm$ 22	78 $\pm$ 11
0.25 - 0.5	2246 $\pm$ 59	1074 $\pm$ 43	831 $\pm$ 38	196 $\pm$ 17
0.5 - 0.75	2848 $\pm$ 74	1393 $\pm$ 4	1056 $\pm$ 43	323 $\pm$ 21
0.75 - 1.0	3680 $\pm$ 78	1818 $\pm$ 56	1251 $\pm$ 45	347 $\pm$ 25
1.0 - 1.25	3687 $\pm$ 82	1873 $\pm$ 51	1231 $\pm$ 45	406 $\pm$ 25
1.25 - 1.5	3237 $\pm$ 71	1775 $\pm$ 51	1208 $\pm$ 42	381 $\pm$ 22
1.5 - 1.75	2877 $\pm$ 64	1732 $\pm$ 78	1050 $\pm$ 40	364 $\pm$ 24
1.75 - 2.0	2512 $\pm$ 59	1433 $\pm$ 49	934 $\pm$ 38	322 $\pm$ 21
2.0 - 2.25	1966 $\pm$ 54	1270 $\pm$ 37	783 $\pm$ 32	250 $\pm$ 20
2.25 - 2.5	1638 $\pm$ 48	1053 $\pm$ 36	597 $\pm$ 29	193 $\pm$ 17
2.5 - 2.75	1284 $\pm$ 42	875 $\pm$ 36	501 $\pm$ 28	214 $\pm$ 17
2.75 - 3.0	1086 $\pm$ 38	769 $\pm$ 45	466 $\pm$ 28	135 $\pm$ 15
3.0 - 3.25	868 $\pm$ 34	646 $\pm$ 30	392 $\pm$ 23	128 $\pm$ 12
3.25 - 3.5	704 $\pm$ 31	566 $\pm$ 28	284 $\pm$ 20	89 $\pm$ 13
3.5 - 3.75	520 $\pm$ 27	389 $\pm$ 22	240 $\pm$ 18	85 $\pm$ 11
3.75 - 4.0	378 $\pm$ 23	310 $\pm$ 20	146 $\pm$ 14	55 $\pm$ 8
4.0 - 4.25	275 $\pm$ 21	252 $\pm$ 18	-	-
4.25 - 4.5	231 $\pm$ 17	168 $\pm$ 14	-	-
4.0 - 4.5	-	-	226 $\pm$ 17	86 $\pm$ 12
4.5 - 4.75	180 $\pm$ 15	-	-	-
4.75 - 5.0	125 $\pm$ 13	161 $\pm$ 15	-	-
4.5 - 5.0	-	-	144 $\pm$ 13	60 $\pm$ 8
5.0 - 5.25	105 $\pm$ 12	107 $\pm$ 11	-	-
5.25 - 5.5	91 $\pm$ 12	86 $\pm$ 10	-	-
5.5 - 5.75	75 $\pm$ 10	68 $\pm$ 9	-	-
5.75 - 6.0	44 $\pm$ 9	57 $\pm$ 8	-	-
5.0 - 6.0	-	-	139 $\pm$ 13	-
5.0 - 7.0	-	-	-	55 $\pm$ 8
6.0 - 6.5	72 $\pm$ 9	55 $\pm$ 8	-	-
6.5 - 7.0	32 $\pm$ 7	41 $\pm$ 8	-	-
6.0 - 7.0	-	-	50 $\pm$ 8	-
$p_T$ Sum	31,593	18,535	11,780	3,769
Min Bias	31,452 $\pm$ 215	18,328 $\pm$ 175	11,738 $\pm$ 138	3,804 $\pm$ 88
% diff	0.45%	1.12%	0.36%	0.92%

Table 10: South arm raw  $J/\psi$  counts with statistical uncertainties obtained from the small systems study.

$p_T$ [GeV/c]	<i>Run15pp, S</i>	<i>Run15pAu, S</i>	<i>Run15pAl, S</i>	<i>Run14HeAu, S</i>
0.0 - 0.25	720 $\pm$ 33	218 $\pm$ 19	164 $\pm$ 19	68 $\pm$ 11
0.25 - 0.5	2048 $\pm$ 54	723 $\pm$ 33	523 $\pm$ 31	241 $\pm$ 20
0.5 - 0.75	2690 $\pm$ 60	841 $\pm$ 40	750 $\pm$ 40	273 $\pm$ 22
0.75 - 1.0	3299 $\pm$ 77	1196 $\pm$ 46	818 $\pm$ 38	433 $\pm$ 48
1.0 - 1.25	3528 $\pm$ 70	1439 $\pm$ 46	801 $\pm$ 37	501 $\pm$ 27
1.25 - 1.5	3066 $\pm$ 70	1118 $\pm$ 45	882 $\pm$ 36	447 $\pm$ 23
1.5 - 1.75	2796 $\pm$ 64	1195 $\pm$ 68	736 $\pm$ 35	391 $\pm$ 24
1.75 - 2.0	2185 $\pm$ 55	928 $\pm$ 40	560 $\pm$ 30	366 $\pm$ 24
2.0 - 2.25	1743 $\pm$ 44	819 $\pm$ 37	491 $\pm$ 28	265 $\pm$ 19
2.25 - 2.5	1424 $\pm$ 44	663 $\pm$ 31	367 $\pm$ 26	239 $\pm$ 18
2.5 - 2.75	1073 $\pm$ 38	552 $\pm$ 28	317 $\pm$ 24	238 $\pm$ 18
2.75 - 3.0	961 $\pm$ 35	464 $\pm$ 26	266 $\pm$ 22	151 $\pm$ 16
3.0 - 3.25	737 $\pm$ 31	357 $\pm$ 22	227 $\pm$ 18	113 $\pm$ 12
3.25 - 3.5	542 $\pm$ 27	304 $\pm$ 21	161 $\pm$ 15	93 $\pm$ 11
3.5 - 3.75	457 $\pm$ 24	245 $\pm$ 18	117 $\pm$ 12	89 $\pm$ 13
3.75 - 4.0	342 $\pm$ 21	179 $\pm$ 16	88 $\pm$ 11	59 $\pm$ 9
4.0 - 4.25	231 $\pm$ 17	142 $\pm$ 10	-	-
4.25 - 4.5	154 $\pm$ 15	125 $\pm$ 13	-	-
4.0 - 4.5	-	-	102 $\pm$ 13	73 $\pm$ 10
4.5 - 4.75	145 $\pm$ 13	82 $\pm$ 11	-	-
4.75 - 5.0	86 $\pm$ 10	61 $\pm$ 9	-	-
4.5 - 5.0	-	-	51 $\pm$ 8	45 $\pm$ 8
5.0 - 5.25	92 $\pm$ 11	41 $\pm$ 7	-	-
5.25 - 5.5	83 $\pm$ 11	36 $\pm$ 7	-	-
5.5 - 5.75	53 $\pm$ 9	28 $\pm$ 6	-	-
5.75 - 6.0	34 $\pm$ 7	17 $\pm$ 5	-	-
5.0 - 6.0	-	-	67 $\pm$ 9	-
5.0 - 7.0	-	-	-	52 $\pm$ 9
6.0 - 6.5	49 $\pm$ 8	19 $\pm$ 5	-	-
6.5 - 7.0	46 $\pm$ 8	18 $\pm$ 5	-	-
6.0 - 7.0	-	-	11 $\pm$ 4	-
$p_T$ Sum	28,583	11,810	7,500	4,138
Min Bias	28,511 $\pm$ 203	11,661 $\pm$ 152	7,455 $\pm$ 115	4,069 $\pm$ 103
% diff	0.25%	1.65%	0.61%	1.68%

## C Raw $J/\psi$ Counts: $p_T$ /Centrality Dependent (Rapidity Integrated)

0 - 20 Centrality, NORTH ARM				0 - 20 Centrality, SOUTH ARM			
pt [GeV/c]	Run15pAl	Run15pAu	Run14HeAu	pt [GeV/c]	Run15pAl	Run15pAu	Run14HeAu
0.125		139 +/- 15	29 +/- 6	0.125		88 +/- 13	23 +/- 5
0.375		334 +/- 24	78 +/- 10	0.375		300 +/- 24	105 +/- 14
0.625		452 +/- 48	115 +/- 12	0.625		368 +/- 26	120 +/- 14
0.875		579 +/- 41	136 +/- 13	0.875		511 +/- 28	198 +/- 19
1.125		655 +/- 31	162 +/- 14	1.125		617 +/- 33	215 +/- 19
1.375		595 +/- 33	148 +/- 14	1.375		475 +/- 30	184 +/- 16
1.625		557 +/- 28	159 +/- 14	1.625		519 +/- 30	188 +/- 17
1.875		506 +/- 29	119 +/- 13	1.875		415 +/- 26	184 +/- 16
2.125		438 +/- 24	100 +/- 12	2.125		370 +/- 28	124 +/- 14
2.375		337 +/- 29	82 +/- 10	2.375		301 +/- 22	126 +/- 13
2.625		300 +/- 24	-	2.625		259 +/- 19	-
2.75		-	131 +/- 13	2.75		-	154 +/- 15
2.875		276 +/- 21	-	2.875		182 +/- 17	-
3.125		221 +/- 18	-	3.125		155 +/- 14	-
3.25		-	105 +/- 11	3.25		-	90 +/- 10
3.375		216 +/- 15	-	3.375		124 +/- 14	-
3.625		133 +/- 13	-	3.625		117 +/- 13	-
3.75		-	60 +/- 8	3.75		-	73 +/- 10
3.825		119 +/- 12	-	3.825		75 +/- 10	-
4.25		141 +/- 13	-	4.25		106 +/- 12	-
4.75		120 +/- 12	-	4.75		68 +/- 9	-
6		147 +/- 14	-	6		72 +/- 9	-

20 - 40 Centrality, NORTH ARM				20 - 40 Centrality, SOUTH ARM			
pt [GeV/c]	Run15pAl	Run15pAu	Run14HeAu	pt [GeV/c]	Run15pAl	Run15pAu	Run14HeAu
0.125		103 +/- 12	24 +/- 6	0.125		61 +/- 9	23 +/- 6
0.375		294 +/- 24	83 +/- 10	0.375		201 +/- 17	81 +/- 11
0.625		383 +/- 24	102 +/- 11	0.625		227 +/- 21	92 +/- 12
0.875		479 +/- 37	88 +/- 11	0.875		342 +/- 21	121 +/- 15
1.125		571 +/- 27	133 +/- 13	1.125		448 +/- 23	149 +/- 14
1.375		499 +/- 25	114 +/- 12	1.375		330 +/- 23	118 +/- 13
1.625		504 +/- 26	99 +/- 11	1.625		325 +/- 22	122 +/- 15
1.875		428 +/- 25	105 +/- 12	1.875		225 +/- 19	97 +/- 16
2.125		358 +/- 21	74 +/- 10	2.125		214 +/- 18	78 +/- 10
2.375		318 +/- 20	64 +/- 10	2.375		155 +/- 16	68 +/- 10
2.625		252 +/- 18	-	2.625		143 +/- 14	-
2.75		-	120 +/- 12	2.75		-	115 +/- 12
2.875		212 +/- 17	-	2.875		126 +/- 14	-
3.125		176 +/- 15	-	3.125		108 +/- 12	-
3.25		-	53 +/- 8	3.25		-	60 +/- 8
3.375		135 +/- 13	-	3.375		99 +/- 11	-
3.625		113 +/- 11	-	3.625		64 +/- 10	-
3.75		-	41 +/- 7	3.75		-	40 +/- 7
3.825		91 +/- 10	-	3.825		45 +/- 8	-
4.25		134 +/- 13	-	4.25		90 +/- 10	-
4.75		68 +/- 10	-	4.75		48 +/- 7	-
6		129 +/- 12	-	6		50 +/- 7	-

40 - 88 Centralities, NORTH ARM					40 - 88 Centralities, SOUTH ARM				
pt [GeV/c]	40 - 72 Run15pAl	40 - 60 Run15pAu	60 - 84 Run15pAu	40 - 88 Run14HeAu	pt [GeV/c]	40 - 72 Run15pAl	40 - 60 Run15pAu	60 - 84 Run15pAu	40 - 88 Run14HeAu
0.125		97 +/- 11	83 +/- 10	30 +/- 5	0.125		47 +/- 8	30 +/- 7	19 +/- 5
0.375		254 +/- 19	198 +/- 17	53 +/- 8	0.375		136 +/- 16	99 +/- 11	58 +/- 9
0.625		286 +/- 23	283 +/- 20	83 +/- 10	0.625		172 +/- 15	119 +/- 13	72 +/- 10
0.875		402 +/- 25	351 +/- 24	85 +/- 10	0.875		209 +/- 17	159 +/- 14	70 +/- 9
1.125		431 +/- 26	295 +/- 20	87 +/- 11	1.125		281 +/- 19	135 +/- 13	70 +/- 9
1.375		407 +/- 25	302 +/- 22	101 +/- 11	1.375		224 +/- 19	131 +/- 13	87 +/- 11
1.625		409 +/- 24	267 +/- 19	96 +/- 10	1.625		222 +/- 18	143 +/- 13	94 +/- 12
1.875		262 +/- 20	233 +/- 17	79 +/- 10	1.875		178 +/- 15	111 +/- 12	44 +/- 8
2.125		273 +/- 18	198 +/- 16	73 +/- 9	2.125		155 +/- 15	93 +/- 11	48 +/- 8
2.375		210 +/- 15	183 +/- 15	37 +/- 9	2.375		126 +/- 12	83 +/- 10	39 +/- 6
2.625		182 +/- 16	145 +/- 14	-	2.625		99 +/- 11	63 +/- 8	-
2.75		-	-	63 +/- 9	2.75		-	-	80 +/- 10
2.875		168 +/- 14	116 +/- 12	-	2.875		85 +/- 10	60 +/- 10	-
3.125		142 +/- 13	104 +/- 12	-	3.125		53 +/- 8	44 +/- 7	-
3.25		-	-	34 +/- 6	3.25		-	-	31 +/- 6
3.375		101 +/- 11	110 +/- 11	-	3.375		53 +/- 8	27 +/- 6	-
3.625		103 +/- 11	44 +/- 7	-	3.625		35 +/- 7	29 +/- 5	-
3.75		-	-	31 +/- 6	3.75		-	-	29 +/- 5
3.825		62 +/- 9	38 +/- 6	-	3.825		37 +/- 7	22 +/- 5	-
4.25		87 +/- 10	63 +/- 9	-	4.25		43 +/- 7	28 +/- 6	-
4.75		71 +/- 10	45 +/- 8	-	4.75		22 +/- 5	20 +/- 4	-
6		76 +/- 10	56 +/- 9	-	6		26 +/- 7	18 +/- 4	-

## D Preliminary Plot Data Arrays

We have made some files that contain the data points and errors for the plots we are interested in requesting preliminary for. We have pasted these into Jupyter notebooks and attached the links here.

$R_{pAu}$  vs.  $p_T$

$R_{HeAu}$  vs.  $p_T$

## Corrected Preliminary Plot Data Arrays

We have updated the data arrays with the corrected number of events per centrality.

$R_{pAu}$  vs.  $p_T$  corrected

$R_{HeAu}$  vs.  $p_T$  corrected

$\langle p_T^2 \rangle$  vs.  $N_{coll}$  corrected